TRANSMISSION OF VECTOR QUANTIZATION OVER A FREQUENCY-SELECTIVE RAYLEIGH FADING CDMA CHANNEL

A Thesis Submitted
to the College of Graduate Studies and Research
in Partial Fulfillment of the Requirements
for the Degree of Master of Science
in the Department of Electrical Engineering
University of Saskatchewan

by

Son X. Nguyen

Saskatoon, Saskatchewan, Canada
December 2005

PERMISSION TO USE

In presenting this thesis in partial fulfillment of the requirements for a Postgraduate degree from the University of Saskatchewan, it is agreed that the Libraries of this University may make it freely available for inspection. Permission for copying of this thesis in any manner, in whole or in part, for scholarly purposes may be granted by the professors who supervised this thesis work or, in their absence, by the Head of the Department of Electrical Engineering or the Dean of the College of Graduate Studies and Research at the University of Saskatchewan. Any copying, publication, or use of this thesis, or parts thereof, for financial gain without the written permission of the author is strictly prohibited. Proper recognition shall be given to the author and to the University of Saskatchewan in any scholarly use which may be made of any material in this thesis.

Request for permission to copy or to make any other use of material in this thesis in whole or in part should be addressed to:

Head of the Department of Electrical Engineering
57 Campus Drive
University of Saskatchewan
Saskatoon, Saskatchewan, Canada
S7N 5A9

ACKNOWLEDGMENTS

I would like to gratefully acknowledge the enthusiastic supervision of my supervisor, Dr. Ha H. Nguyen who has brought me knowledge and energy to do this work. His patience, support and encouragement have been great sources that inspired me during my studies. This thesis would not have been done without his guidance and availability.

I would like to thank Telecommunication Research Laboratories (TRLabs) for the financial support.

Many thanks are extended to Nghi Tran and other friends in Communications Theories Research Group (CTRG), whose friendships and supports have made it more than a temporary place of study for people from around the world.

I am forever grateful to my parents and my sister whose love, foresight and values paved the way for a privileged education. To them, I dedicate this thesis.

UNIVERSITY OF SASKATCHEWAN

Electrical Engineering Abstract

TRANSMISSION OF VECTOR QUANTIZATION OVER A FREQUENCY-SELECTIVE RAYLEIGH FADING CDMA CHANNEL

Student: Son X. Nguyen

Supervisor: Prof. Ha H. Nguyen

M.Sc. Thesis Submitted to the

College of Graduate Studies and Research

December, 2005

ABSTRACT

Recently, the transmission of vector quantization (VQ) over a code-division multiple access (CDMA) channel has received a considerable attention in research community. The complexity of the optimal decoding for VQ in CDMA communications is prohibitive for implementation, especially for systems with a medium or large number of users. A suboptimal approach to VQ decoding over a CDMA channel, disturbed by additive white Gaussian noise (AWGN), was recently developed in [1], [2]. Such a suboptimal decoder is built from a soft-output multiuser detector (MUD), a soft bit estimator and the optimal soft VQ decoders of individual users. Due to its lower complexity and good performance, such a decoding scheme is an attractive alternative to the complicated optimal decoder. It is necessary to extend this decoding scheme for a frequency-selective Rayleigh fading CDMA channel, a channel model typically seen in mobile wireless communications. This is precisely the objective of this thesis.

A frequency-selective Rayleigh fading channel is typically modeled as a tapped-delay line [3]. In this channel model, the received amplitude over each path of each

user is a complex random variable. The delay between paths is an integer multiple of the chip duration. Therefore, the formulation of the suboptimal decoding proposed for an AWGN channel in [1], [2] needs to be carefully examined. In the suboptimal decoding under consideration, the received signal waveform is first correlated with delayed replicas of the users' signature waveforms to form the sufficient statistic. The sufficient statistic is then processed by the MUD and the VQ decoder in order to make the final decision for the source data. The soft-output MUD can be the jointly optimal MUD (OPT-MUD), the minimum mean-square error MUD (MMSE-MUD) or the decorrelating MUD (DC-MUD). For each type of MUD, the soft-bit estimates are calculated from the sufficient statistic and then fed into the soft VQ decoders [1]. Furthermore, the suboptimal decoders are obtained not only for binary phase shift keying (BPSK), but also for M-ary pulse amplitude modulation (M-PAM). This extension offers a flexible trade-off between spectrum efficiency and performance of the systems. In addition, two algorithms based on distance measure and reliability processing are introduced as other alternatives to the suboptimal decoder. Simulation results indicate that the suboptimal decoders studied in this thesis also performs very well over a frequency-selective Rayleigh fading CDMA channel.

Table of Contents

List of Tables

List of Figures

ABBREVIATIONS

ASK	Amplitude Shift Keying
AWGN	Additive White Gaussian Noise
BER	Bit Error Rate
BPSK	Binary Phase Shift Keying
BSC	Binary Symmetric Channel
CDMA	Code Division Multiuser Access
CSNR	Channel Signal-to-Noise Ratio
dB	Decibel
DC	Decorrelation
DC-MUD	Decorrelating Multiuser Detection
DS-CDMA	Direct-Sequence Code Division Multiuser Access
FDMA	Frequency Division Multiuser Access
FLSA	Full Linear Search Algorithm
Hz	Hertz
IA	Index Assignment
LGB	Linde-Buzo-Gray
LISA	Linear Increasing Swap Algorithm
LLR	Log Likelihood Ratio
M-PAM	M-ary Pulse Amplitude Modulation
M-PSK	M-ary Phase Shift Keying
M-QAM	M-ary Quadrature Amplitude Modulation
MAI	Multiuser Access Interference
MF	Matched Filter
ML	Maximum Likelihood
MMSE	Minimum Mean Square Error
MMSE-MUD	Minimum Mean Square Error Multiuser Detection

MUD	Multiuser Detection
OPT	Optimal
OPT-MUD	Optimal Multiuser Detection
PAM	Pulse Amplitude Modulation
PDF	Probability Density Function
PN	Pseudo-Noise
PSNR	Peak Signal-to-Noise Ratio
RVQ	Robust Vector Quantizer
SNR	Signal-to-Noise Ratio
TDMA	Time Division Multiuser Access
UL	Unified Linear
VQ	Vector Quantization

1. Introduction

Nowadays, digital communication systems play an important role in the daily activities of human being. In digital communications, the information in digital form is transmitted from a source to one or more destinations. Three basic elements of a digital communication system are the transmitter, the channel and the receiver. The transmitter uses proper signals to transmit information over the channel. The communication channel is the physical medium connecting the transmitter and the receiver. For example, the communication channel can be a pair of wires, a magnetic disk or the atmosphere. The receiver obtains the signal from the channel, then recovers the original information as correctly as possible.

The transmitter of a digital communication system is designed to transmit data in digital form. Consequently, the source outputs must be translated into digital format that can be transmitted digitally. The conversion of the source output to a digital form is performed by a source encoder. The output of a source encoder is a sequence of binary digits [3]. Vector quantization (VQ) was introduced in the late 1970's as a scheme for effectively mapping a sequence of vectors into a digital sequence of numbers. In source coding, vector quantization is an important technique which results in data compression. One of the most important advantages of VQ is that it can model any device that maps blocks of information source into a finite representation. VQ becomes common in many applications. It is also a major tool in many practical systems. For example, VQ is employed in most (low or medium rate) speech coding algorithms. Image and video coding that involves VQ are becoming hot topics for research [7]. This thesis also studies VQ as a source coding technique for a digital communication system.

In a communication system, a large number of users can share a common com-

munication channel to transmit information to a receiver. Multiaccess communication is referred to as *multipoint-to-point* communication. Point-to-multipoint and multipoint-to-point channels are sometimes distinguished as *downlink* and *uplink*, respectively. In general, there are several different ways in which multiple users can send information through the communication channel to the receiver. One simple method is to divide the available channel bandwidth into a number of frequency non-overlapping subchannels. Each subchannel is assigned to one user. This method is called *frequency-division multiple access* (FDMA). Another way for creating multiple subchannels is referred to as *time-division multiple access* (TDMA). In TDMA, time is partitioned into slots. Then, each user who wishes to transmit information is assigned to a particular time slot. Employing FDMA and TDMA is wasteful, especially when the number of users is large. In *code-division multiple access* (CDMA), one user is distinguished from another by superimposing a different pseudorandom pattern, also called a *code* or a *signature waveform*. Each transmitter sends its data stream by modulating its own signature waveform as in a single-user digital communication system. A particular receiver can recover the transmitted information intended for it by knowing the pseudorandom pattern. At the receiver, after correlating with signature waveforms, the received signal is processed by the multiuser detection (MUD) block to obtain the respective information for each user.

One advantage of CDMA technique is to combat the detrimental effects of interference due to jamming, interference arising from other users of the channel, and self-interference due to multipath propagation. The bandwidth of spread spectral signals used for the transmission is much greater than the information rate. The large redundancy inherent in spread spectral signals helps to overcome the severe levels of interference that are encountered in the transmission of digital information over radio channels. Another important feature in the design of spread spectral signals is pseudorandomness, which makes the signals appear similar to random noise and difficult to demodulate by receivers other than the intended ones. CDMA technique has been developed dramatically in recent years and become key in many current

commercial digital communication systems [3].

Transmission of VQ over a CDMA channel is therefore an important problem, which has received considerable attention in the research community. Figure 1.1 describes the general block diagram of such a system. The transmitter consists of

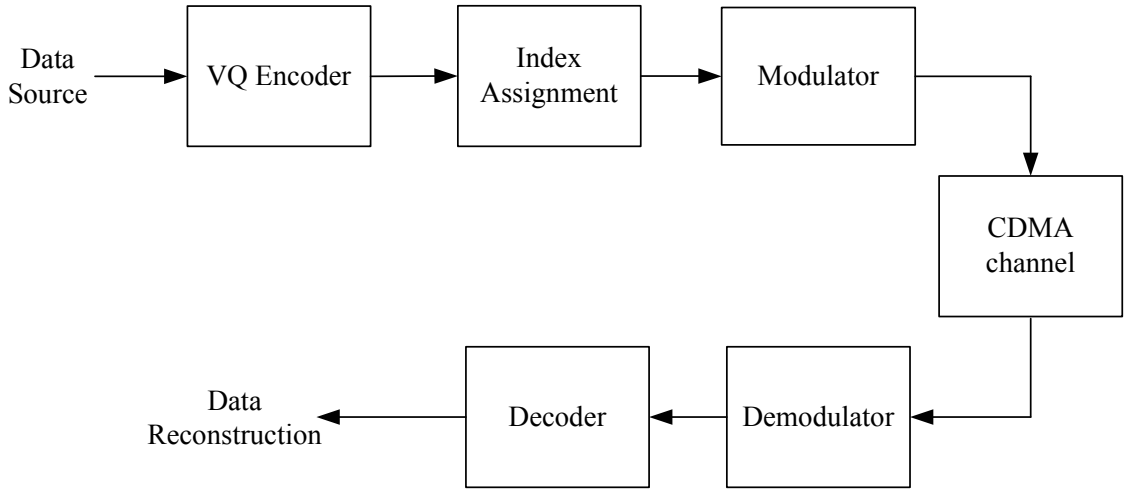

Figure 1.1 General block diagram of VQ transmission over a CDMA channel.

a VQ encoder, an index assignment (IA) operator and a modulator. The source information is encoded by the VQ encoder into index integers. Then, the index assignment block finds the best index assignment in terms of minimizing the channel distortion. The output of the index assignment block is a binary sequence that is then transmitted over the CDMA channel by the modulator. At the receiver, the opposite operations are performed accordingly. After demodulation, the decoder obtains the demodulated data in a proper sequence and then reconstructs the original information. The investigation of the optimal decoder for VQ over a CDMA channel appears in [7,8]. However, such an optimal decoder is too complicated to implement, especially when the number of users is medium or large. Recently, the author in [1], [2] derived a suboptimal decoder which is built from a soft-output multiuser detector (MUD), a soft bit estimator and the optimal soft VQ decoders of individual users. Due to its lower complexity and good performance, this decoding scheme is an attractive alternative to the complicated optimal decoder. It should be pointed out that the work in [1] only considers a CDMA channel disturbed by additive white Gaussian

noise (AWGN). Such a simple channel model is reasonable for communications over coaxial cables or optical links. When considering wireless communications, a unique and important phenomenon known as fading needs to be taken into account. In essence, fading refers to time-varying channel conditions, where the amplitude of the received signal changes due to constructive or destructive combination of the same transmitted signal that arrives to the receiver via different paths. These different paths are the consequence of reflections and/or diffractions of the electromagnetic wave. Moreover, if the bandwidth of the transmitted signal is large (which is typical of CDMA), the time-varying channel condition causes significantly different amplitude distortions over different ranges of frequency, a phenomenon known as frequency-selective fading. Due to the relevance of frequency-selective Rayleigh fading channel in wireless communications, it is necessary to extend and develop the technique in [1] for this type of channel.

1.1 Thesis Objectives

As mentioned earlier, the complexity of the decoder for VQ over a CDMA channel is a prominent problem. Different alternative suboptimal decoders to the complicated optimal decoder are studied in detail for a frequency-selective Rayleigh fading CDMA channel in this thesis. The first suboptimal decoder is essentially based on the approach presented in [1, 2]. Since the channel model considered in this thesis is completely different from the one in [1, 2], necesary and important modifications to the soft-output multiuser detector block in [1] need to be made. Additionally, two decoding algorithms that are based on distance measure and reliability processing [9] are investigated as other suboptimal decoding methods.

Since spectrum efficiency is an important consideration in a digital communication system, the suboptimal decoding of VQ over a frequency-selective Rayleigh fading CDMA channel is developed not only for binary phase shift keying (BPSK) modulation but also for M-ary pulse amplitude modulation (M-PAM). It is shown that the use of M-PAM offers a flexible trade-off between the bandwidth efficiency

and system performance.

1.2 Thesis Organization

The remaining of this thesis is organized as follows.

Chapter 2 provides background theories on the transmission of vector quantization (VQ) over a code-division multiple access (CDMA) channel. First, both scalar and vector quantization will be introduced. A well-known algorithm used to design VQ will also be presented. The description of VQ based on the Hadamard matrix representation is then discussed. Second, basic concepts and techniques of CDMA and multiuser detection are also presented in this chapter.

Chapter 3 presents and discusses the problem of transmitting VQ over a frequency-selective Rayleigh fading CDMA channel. The tapped-delayed line model for the channel is first introduced. Several common existing decoders for VQ over a such a channel are also summarized. An example will be presented to demonstrate how the overall system works.

Chapter 4 examines the suboptimal soft decoding scheme originally proposed in [1,2] for VQ transmitted over a frequency-selective Rayleigh fading CDMA channel. Such a decoder is built from a soft-output multiuser detector (MUD), a soft bit estimator and the optimal soft VQ decoding of an individual user. The main contribution of this chapter is the development of three soft-output multiuser detectors (MUD) for a frequency-selective Rayleigh fading CDMA channel. These MUDs includes the maximum likelihood (optimal) multiuser detector (OPT-MUD), the minimum mean-square error multiuser detector (MMSE-MUD) and the decorrelating multiuser detector (DC-MUD). Furthermore, two algorithms that are based on distance measure and reliability processing are also proposed to simplify the complexity of the soft-output OPT-MUD.

Chapter 5 extends the proposed decoding schemes to systems employing M-PAM. Instead of binary phase shift keying (BPSK), using M-PAM can transmit more than

one information bit during a symbol duration. This allows a faster transmission rate without requiring a larger transmission bandwidth. Therefore, a higher spectrum efficiency is obtained. However, the performance of the systems is degraded compared to that of systems with BPSK. This is because there are more signal points in the signal constellation of M-PAM and the minimum distance between signals decreases for the same average energy. With this extension, this chapter offers a trade-off between bandwidth efficiency and performance of the system.

Finally, Chapter 6 draws conclusions and provides some suggestions for further studies.

2. Background

Since this thesis deals with vector quantization and CDMA, this chapter first provides necessary background theories on these two techniques.

2.1 Vector Quantization

In a digital communication system, whether a source is analog or discrete, it must be converted to a format that can be transmitted digitally. This conversion of the source output to a digital form is performed by the source encoder, whose output may be assumed to be a sequence of binary digits [3]. Mathematical models and quantitative measures are provided to treat the information emitted by a source and quantization is a very powerful tool in source coding. When transmitting data, the sender wants to send his/her information as much as possible in a limited duration of time. By applying the sampling theorem, the output of an analog source is converted to an equivalent sequence of discrete-time samples. The samples are then quantized, in amplitude, from a infinite number of values to some fixed values of quantization categories. The quantization categories are then encoded. One type of simple encoding is to represent each discrete amplitude level by a sequence of binary digits. Therefore, quantization of the amplitudes of the sampled signal results in data compression, but it also introduces some distortion of the waveform and a loss of signal fidelity. The minimization of this distortion should be considered in any quantization schemes.

The simplest type of quantization, performed on sample-by-sample basis, is called scalar quantization. Figure 2.1 illustrates the process of scalar quantization. Here $x(t)$ is a message waveform. By applying the sampling theorem with sampling rate $\frac{1}{T_s}$, where T_s is the sampling duration, the output of an analog signal $x(t)$ is converted to

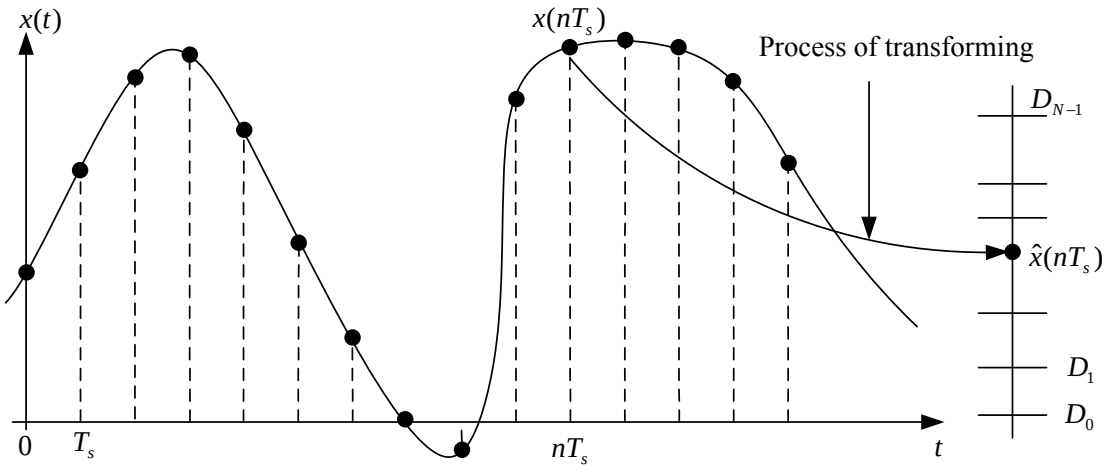

Figure 2.1 The process of scalar quantization.

an equivalent sequence of discrete-time samples $\{x(nT_s)\}_{n=0}^{\infty}$. In scalar quantization, each sample value[1] $x(nT_s) = x_n$ is transformed to a quantized value. The term *distortion* means some measure of the difference between the actual source samples $\{x_n\}$ and the corresponding quantized values $\{\hat{x}_n\}$.

The design of a quantizer depends on the properties of the message signal. Assume that the uniform quantizer has N levels and the maximum amplitude of the message signal is $x_{\max}$. Then the quantization step-size is given by [6],

$$\nabla = \frac{2x_{\max}}{N} \tag{2.1}$$

Let ϑ be the error introduced by the quantizer, then $-\nabla/2 \leq \vartheta \leq \nabla/2$. If the step-size ∇ can be made sufficiently small (i.e., the number of quantization intervals N is sufficiently large), then it is reasonable to assume that the quantization error ϑ is a *uniform* random variable over the range $[-\nabla/2, \nabla/2]$. The probability density function (pdf) of the random variable $\boldsymbol{\vartheta}$ is therefore given by,

$$f_{\boldsymbol{\vartheta}}(\vartheta) = \begin{cases} \frac{1}{\nabla}, & -\frac{\nabla}{2} \leq \vartheta \leq \frac{\nabla}{2} \\ 0, & \text{otherwise} \end{cases} \tag{2.2}$$

In *uniform quantizers*, all the quantization regions are of equal size and the target (quantized) levels are at the midpoint of the quantization regions. Though simple,

[1]The sample value $x(nT_s)$ is written as x_n for simplicity.

uniform quantizers are not optimal in terms of minimizing the signal-to-quantization noise ratio. The optimal quantizer is designed to maximize the signal-to-quantization noise. Necessary and sufficient conditions for a memoryless quantizer to be optimal are known as the *Lloyd-Max conditions* which will be represented later in this section. Based on the *Lloyd-Max conditions*, it can be easily verified that for the special case where the message signal is uniformly distributed, the optimal quantizer is a uniform quantizer. Thus, as long as the distribution of the message signal is close to uniform, the uniform quantizer works fine. However, for certain signals such as voice, the input distribution is far from being uniform. For a voice signal in particular, there exists a higher probability for small amplitudes (corresponding to silent periods and soft speech) and a lower probability for large amplitudes (corresponding to loud speech). Therefore it is more efficient to design a quantizer with more quantization regions at lower amplitudes and less quantizations regions at larger amplitudes. The resulting quantizer will be a *nonuniform quantizer* having quantization regions of various sizes [6].

Instead of performing quantization on sample-by-sample basis, vector quantization (VQ) is the joint quantization of a block of signal samples or a block of signal parameters. It can be seen that scalar quantization is a special case of VQ when the number of samples in a block is one. The VQ transforming process is illustrated in Figure 2.2. Here, every d-dimensional source vector $\mathbf{X} = [x_1, x_2, \ldots, x_d]$ with real-valued, continuous-amplitude components $\{x_k, 1 \leq k \leq d\}$ is quantized into another d-dimensional vector $\hat{\mathbf{X}}$ with components $\{\hat{x}_k, 1 \leq k \leq d\}$. For convenience, express the quantization operation as $Q(\cdot)$, so that $\hat{\mathbf{X}} = Q(\mathbf{X})$ [6].

A fundamental result of rate-distortion theory (due to C. Shannon) is that better performance can be achieved by quantizing vectors instead of scalars, *even if the continuous source is memoryless* [6]. If, in addition, the signal samples or signal parameters are statistically dependent, the redundancy can be exploited by jointly quantizing blocks of samples or parameters and an even greater efficiency can be achieved (i.e., lower bit rate) compared with what can be achieved by scalar quanti-

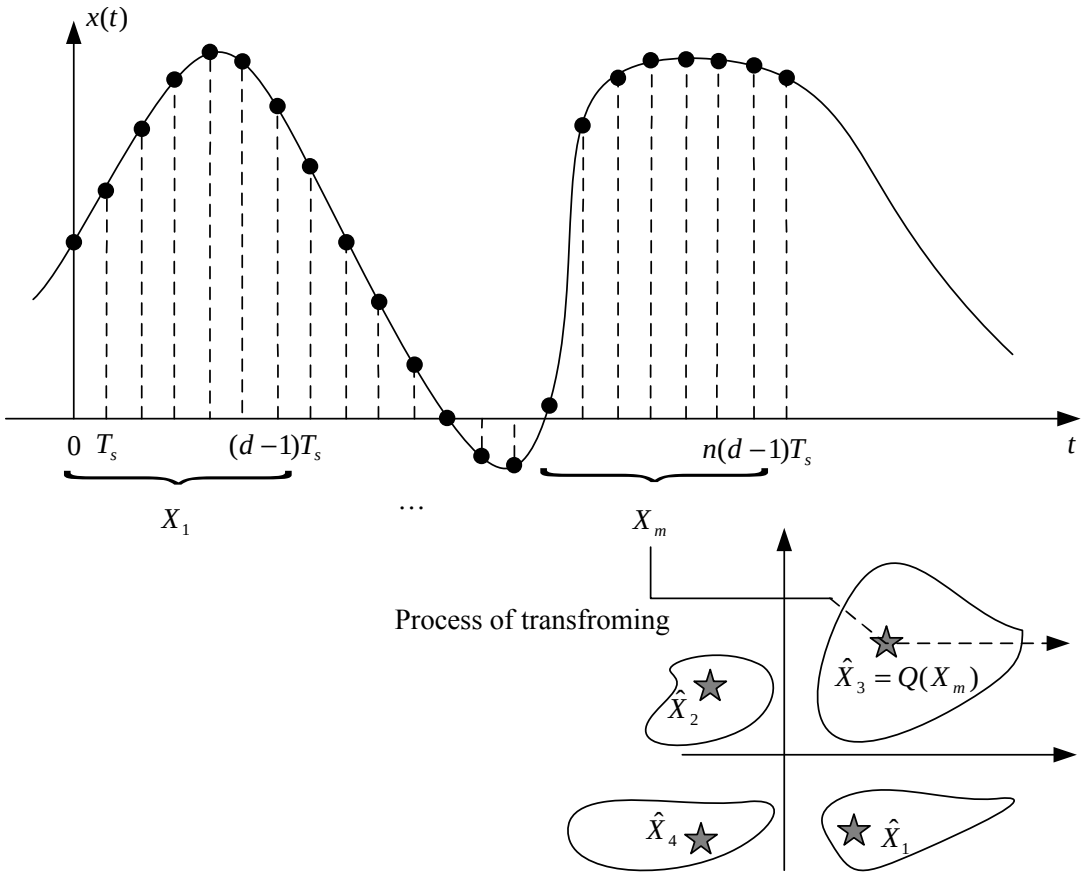

Figure 2.2 Illustration of vector quantization process [4].

zation [3].

As an example, consider the quantization of two-dimensional vectors $\mathbf{X} = [x_1, x_2]$. The two-dimensional space is partitioned into cells as illustrated in Figure 2.3. Here, every pair of numbers falling in a particular cell is approximated by a star associated with that cell. Note that there are $16 = 2^4$ cells (regions) and 16 stars–each of which can be uniquely represented by 4 bits[2]. Thus, this is a 2-dimensional, 4-bit VQ. Its rate is 2 bits/source dimension. In this example, the stars are called codevectors and the regions defined by the borders are called encoding regions. The set of all codevectors is called the codebook and the set of all encoding regions is called the partition of the source space.

Basically, vector quantization can be viewed as a pattern recognition problem

[2]Each bit presents a binary value, 0 or 1.

involving the classification of blocks of data into a discrete number of categories or *cells* (or regions) in a way that optimizes some fidelity criterion such as the mean-square error distortion.

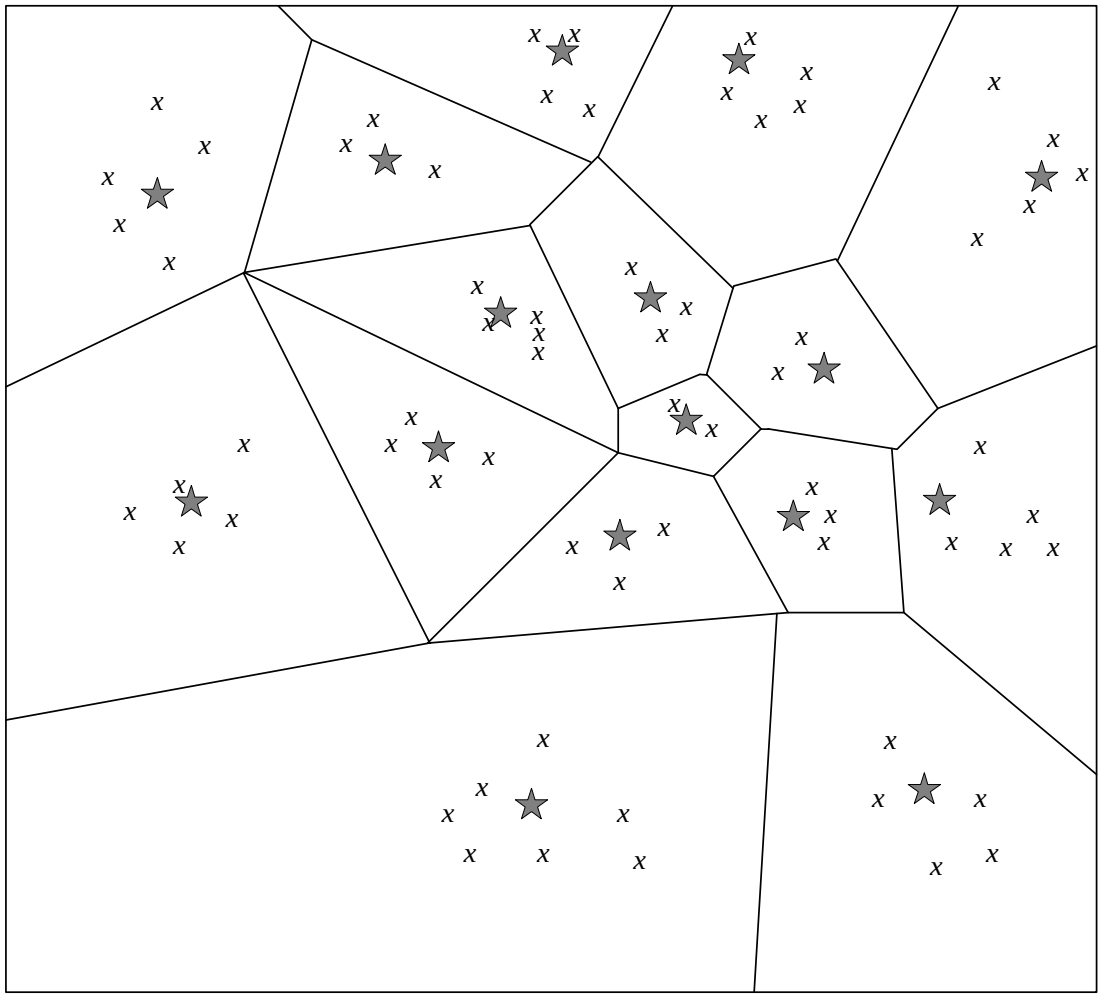

Figure 2.3 An example of two-dimensional vector quantization: Input vectors are marked with x, codewords are marked with stars, and regions are separated with boundary lines.

In the general case, denote the set of possible codevectors as $\{\hat{\mathbf{X}}_n, 1 \leq n \leq N\}$ and the set of encoding regions by $\mathcal{P} = \{S_1, S_2, \ldots, S_N\}$. The quantization of the d-dimensional source vector $\mathbf{X}$ into an d-dimensional vector $\hat{\mathbf{X}}$ introduces a quantization error or a distortion $d(\mathbf{X}, \hat{\mathbf{X}})$, defined as

$$d(\mathbf{X}, \hat{\mathbf{X}}) = \frac{1}{d} \sum_{k=1}^{d} |x_k - \hat{x}_k|^p, \tag{2.3}$$

where p takes values from the set of positive integers. Then, the average distortion over the set of input vectors $\mathbf{X}$ is:

$$\begin{aligned}\Phi &= \sum_{n=1}^{N} \Pr(\mathbf{X} \in S_n) E\{d(\mathbf{X}, \hat{\mathbf{X}}_n) | \mathbf{X} \in S_n\} \\ &= \sum_{n=1}^{N} \Pr(\mathbf{X} \in S_n) \int_{\mathbf{X} \in S_n} d(\mathbf{X}, \hat{\mathbf{X}}_n) p(\mathbf{X}) d\mathbf{X} \end{aligned} \tag{2.4}$$

where $\Pr(\mathbf{X} \in S_n)$ is the probability that the vector $\mathbf{X}$ falls into cell S_n and $p(\mathbf{X})$ is the joint PDF of the d random variables which is determined by the source statistics. If the mean-square error (l_2 norm) is used for distortion measure, then

$$d(\mathbf{X}, \hat{\mathbf{X}}) = \frac{1}{d} \sum_{k=1}^{d} (x_k - \hat{x}_k)^2 \tag{2.5}$$

Thus the main problem in designing the optimal VQ is to partition the d-dimensional source space into N cells $\{S_n, 1 \leq n \leq N\}$ and to choose the codevectors $\{\hat{\mathbf{X}}_n, 1 \leq n \leq N\}$ so that the average distortion is minimized. It can be shown [3] that there are two necessary and sufficient conditions for the optimal vector quantizer. The first is that the optimal quantizer must employ the nearest-neighbor rule, which can be expressed as:

$$Q(\mathbf{X}) = \hat{\mathbf{X}}_n \text{ if and only if } d(\mathbf{X}, \hat{\mathbf{X}}_n) \leq d(\mathbf{X}, \hat{\mathbf{X}}_m), \quad n \neq m, \quad 1 \leq m, n \leq N \tag{2.6}$$

The second condition necessary for optimality is that each codevector $\hat{\mathbf{X}}_n$ must be chosen to minimize the average distortion in cell S_n. This means that $\hat{\mathbf{X}}_n$ is the vector in S_n that minimizes:

$$\Phi_n = E\{d(\mathbf{X}, \hat{\mathbf{X}}) | \mathbf{X} \in S_n\} = \int_{\mathbf{X} \in S_n} d(\mathbf{X}, \hat{\mathbf{X}}) p(\mathbf{X}) d\mathbf{X} \tag{2.7}$$

The vector $\hat{\mathbf{X}}_n$ that minimizes Φ_n is called the *centroid* of cell S_n.

The above two conditions can be applied to design the optimal VQ when the joint PDF $p(\mathbf{X})$ is known. However, in practice, the joint PDF $p(\mathbf{X})$ of the data vector may not be known. Because of this, the design of a vector quantizer was considered a challenging problem in the earlier days. In 1980, Linde, Buzo, and Gray

proposed a VQ design algorithm (known as the LBG algorithm[3]) based on a training sequence [10]. The use of a training sequence bypasses the need for multi-dimensional integration. A VQ that is designed using this algorithm is referred to in the literature as an LBG-VQ.

2.1.1 The LBG Algorithm

It is assumed that there is a training sequence consisting of M source vectors:

$$\mathcal{T} = \{\mathbf{X}_1, \mathbf{X}_2, \ldots, \mathbf{X}_M\}. \tag{2.8}$$

This training sequence can be obtained from some large database. For example, if the source is a speech signal, then the training sequence can be obtained by recording several long telephone conversations. Here M is assumed to be sufficiently large so that all the statistical properties of the source are captured by the training sequence. It is assumed that the source vectors are d-dimensional, i.e.,

$$\mathbf{X}_m = [x_{m,1}, x_{m,2}, \ldots, x_{m,d}], \quad m = 1, 2, \ldots, M \tag{2.9}$$

Let N be the number of codevectors and let

$$\mathcal{C} = \{\hat{\mathbf{X}}_1, \hat{\mathbf{X}}_2, \ldots, \hat{\mathbf{X}}_N\} \tag{2.10}$$

represent the codebook. Similarly, each codevector is represented by

$$\hat{\mathbf{X}}_n = [\hat{x}_{n,1}, \hat{x}_{n,2}, \ldots, \hat{x}_{n,d}], \quad n = 1, 2, \ldots, N \tag{2.11}$$

The quantization for this training sequence is as follows

$$Q(\mathbf{X}_m) = \hat{\mathbf{X}}_n, \quad \text{if } \mathbf{X}_m \in S_n \tag{2.12}$$

Assuming a squared-error distortion measure, the average distortion is given by:

$$\Phi_{ave} = \frac{1}{Md} \sum_{m=1}^{M} ||\mathbf{X}_m - Q(\mathbf{X}_m)||^2 \tag{2.13}$$

[3]The LBG algorithm is also known as the K-means algorithm.

where $||\mathbf{e}||^2 = e_1^2 + e_2^2 + \ldots + e_d^2$. The design problem can be succinctly stated as follows: Given $\mathcal{T}$ and N, find $\mathcal{C}$ and the partition $\mathcal{P}$ such that Φ_{ave} is minimized [6].

Optimality Criteria. Similar to the previous discussion, it can be shown [3] that if $\mathcal{C}$ and $\mathcal{P}$ form a solution to the above minimization problem, then they must satisfy the following two criteria.

1) Nearest Neighbor Condition:

$$S_n = \{\mathbf{X} : ||\mathbf{X} - \hat{\mathbf{X}}_n||^2 \leq ||\mathbf{X} - \hat{\mathbf{X}}_{n'}||^2, \quad \forall n, n^{'} = 1, 2, \ldots, N\} \tag{2.14}$$

This condition says that the encoding region S_n should consist of all vectors that are closer to $\hat{\mathbf{X}}_n$ than any of the other codevectors. For those vectors lying on the boundary, any tie-breaking procedure will do.

2) Centroid Condition:

$$\hat{\mathbf{X}}_n = \frac{\sum_{\mathbf{X}_m \in S_n} \mathbf{X}_m}{\sum_{\mathbf{X}_m \in S_n} 1}, \quad m, n = 1, 2, \ldots, N. \tag{2.15}$$

This condition says that the codevector $\hat{\mathbf{X}}_n$ should be average of all those training vectors that are in encoding region S_n. In implementation, one should ensure that at least one training vector belongs to each encoding region (so that the denominator in the above equation is never 0).

The LBG Algorithm. The LBG-VQ design algorithm is an iterative algorithm which alternatively solves the above two optimality criteria. The algorithm requires an initial codebook $\mathcal{C}^{(0)}$. This initial codebook is obtained by the splitting method. In this method, an initial codevector is set as the average of the entire training sequence. This codevector is then split into two. The iterative algorithm is run with these two vectors as the initial codebook. The final two codevectors are splitted into four and the process is repeated until the desired number of codevectors is obtained. The algorithm is summarized below [6].

1. Given $\mathcal{T}$ and the number of codevectors $\mathcal{N}$. Let ϵ be a "small" number.

2. Let $N = 1$ and

$$\hat{\mathbf{X}}_1^* = \frac{1}{M}\sum_{m=1}^{M}\mathbf{X}_m \tag{2.16}$$

Calculate

$$\Phi_{ave}^* = \frac{1}{Md}\sum_{m=1}^{M}||\mathbf{X}_m - \hat{\mathbf{X}}_1^*||^2 \tag{2.17}$$

3. **Splitting**: For $i = 1, 2, \ldots, N$, set

$$\hat{\mathbf{X}}_i^{(0)} = (1+\epsilon)\hat{\mathbf{X}}_i^* \tag{2.18}$$

$$\hat{\mathbf{X}}_{N+i}^{(0)} = (1-\epsilon)\hat{\mathbf{X}}_i^*. \tag{2.19}$$

Set $N = 2N$.

4. **Iteration**: Let $\Phi_{ave}^{(0)} = \Phi_{ave}^*$. Set the iteration index $i = 0$.

   i. For $m = 1, 2, \ldots, M$, find the minimum value of

   $$||\mathbf{X}_m - \hat{\mathbf{X}}_n^{(i)}||^2,$$

   over all $n = 1, 2, \ldots, N$. Let n^* be the index which achieves the minimum. Set $Q(\mathbf{X}_m) = \hat{\mathbf{X}}_{n^*}^{(i)}$.

   ii. For $n = 1, 2, \ldots, N$, update the codevector

   $$\hat{\mathbf{X}}_n^{(i+1)} = \frac{\sum\limits_{\mathbf{X}_m : Q(\mathbf{X}_m) = \hat{\mathbf{X}}_n^{(i)}} \mathbf{X}_m}{\sum\limits_{\mathbf{X}_m : Q(\mathbf{X}_m) = \hat{\mathbf{X}}_n^{(i)}} 1} \tag{2.20}$$

   iii. Set $i = i + 1$.

   iv. Calculate

   $$\Phi_{ave}^{(i)} = \frac{1}{Md}\sum_{m=1}^{M}||\mathbf{X}_m - Q(\mathbf{X}_m)||^2 \tag{2.21}$$

   v. If $(\Phi_{ave}^{(i-1)} - \Phi_{ave}^{(i)})/\Phi_{ave}^{(i-1)} > \epsilon$, go back to Step (i).

   vi. Set $\Phi_{ave}^* = \Phi_{ave}^{(i)}$. For $n = 1, 2, \ldots, N$, set $\hat{\mathbf{X}}_n^* = \hat{\mathbf{X}}_n^{(i)}$ as the final codevectors.

5. Repeat Steps 3 and 4 until the desired number of codevectors is obtained.

Figure 2.4 shows, in a flow diagram, the detailed steps of the LBG algorithm.

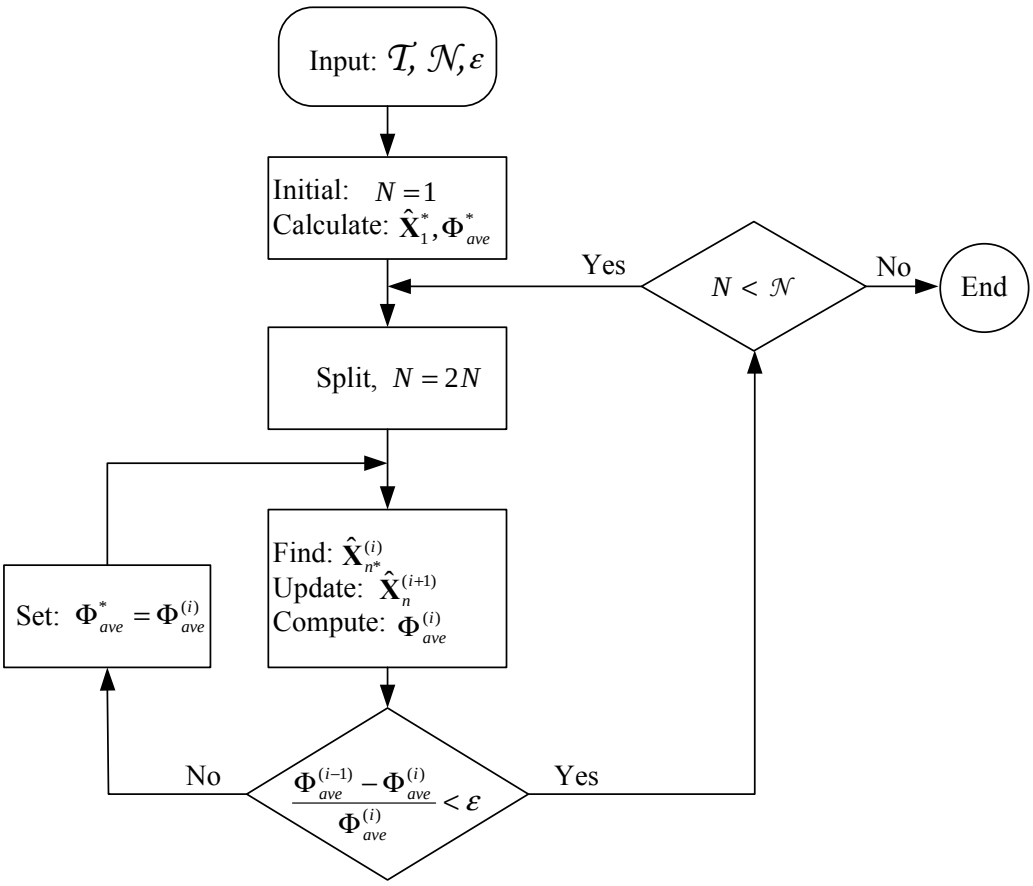

Figure 2.4 Flow diagram of the LBG algorithm, modified from [5].

2.1.2 Description of VQ Based on Hadamard Matrix

Vector quantization (VQ) is an important technique for block-based source coding. In the derivation of decoder expression, the *Hadamard representation* for VQ can be employed conveniently and effectively [7]. A more thorough presentation of this representation can be found in [11]. Previous works have shown that the *Hadamard transform* is a powerful tool in the analysis of VQ over the binary-symmetric channel [11], [12], [13], and [14]. In what follows, the Hadamard representation for the centroids of VQ will be discussed.

A (Sylvester-type) Hadamard matrix, $\mathbf{H}^{(2^L)}$, of size $N = 2^L$, is a symmetric square matrix with elements from $\{\pm 1\}$. It is defined recursively as

$$\mathbf{H}^{(1)} = \begin{bmatrix} +1 & +1 \\ +1 & -1 \end{bmatrix}; \quad \mathbf{H}^{(2^L)} = \mathbf{H}^{(1)} \otimes \mathbf{H}^{(2^{L-1})}, \quad L > 1, \tag{2.22}$$

where the symbol $\otimes$ denotes the Kronecker product. As a definition, the Kronecker product of two matrices $\mathbf{A}$ and $\mathbf{B}$ is given as follows [14]:

$$\mathbf{A} \otimes \mathbf{B} = \begin{bmatrix} \{\mathbf{A}\}_{0,0}\mathbf{B} & \dots & \{\mathbf{A}\}_{0,m-1}\mathbf{B} \\ \vdots & \ddots & \vdots \\ \{\mathbf{A}\}_{n-1,0}\mathbf{B} & \dots & \{\mathbf{A}\}_{n-1,m-1}\mathbf{B} \end{bmatrix} \tag{2.23}$$

where $\mathbf{A}$ is of size n rows and m columns. The recursive nature of the Hadamard matrix gives the following useful property. If the natural binary representation of integer i is $(b_L, b_{L-1}, \dots, b_1)$, with logical "zero" represented by $+1$ and logical "one" by -1, the ith column of $\mathbf{H}^{(2^L)}$ can be computed as

$$\mathbf{h}_i^{(2^L)} = \begin{bmatrix} 1 \\ b_L \end{bmatrix} \otimes \begin{bmatrix} 1 \\ b_{L-1} \end{bmatrix} \otimes \dots \otimes \begin{bmatrix} 1 \\ b_1 \end{bmatrix}. \tag{2.24}$$

Another useful property of Hadamard matrix is that, for any size $N = 2^L$, the multiplication of the Hadamard matrix by itself is $\mathbf{H}^{(2^L)} \times \mathbf{H}^{(2^L)} = N \times \mathbf{I}$, where $\mathbf{I}$ is the identity matrix of size N. Therefore $\left(\mathbf{H}^{(2^L)}\right)^{-1} = N^{-1} \times \mathbf{H}^{(2^L)}$. This latter property is often employed to define Hadamard matrices of general sizes [15]. The *Hadamard transform* $\{\tilde{a}_m\}_{m=1}^{N-1}$ of a sequence $\{a_m\}_{m=1}^{N-1}$, where $N = 2^L$, is defined as [14]

$$[\tilde{a}_0, \tilde{a}_1, \dots, \tilde{a}_{N-1}]^\top = \mathbf{H}^{(2^L)} \times [a_0, a_1, \dots, a_{N-1}]^\top. \tag{2.25}$$

The question is that how the Hadamard matrix and Hadamard transform can be useful for VQ description. To answer this question, consider a general vector-valued function $\mathbf{f} : \{0, 1, \dots, N-1\} \rightarrow \mathbb{R}^d$ where the domain is an integer set. Such a function can always be presented as $\mathbf{f}(n) = \mathbf{T} \cdot \mathbf{h}_n^{(N)}, n = 0, 1, \dots, N-1$, where $\mathbf{h}_n^{(N)}$ is the nth column of an $N \times N$ Hadamard matrix $\mathbf{H}^{(N)}$, and $\mathbf{T}$ is a real transform matrix. The matrix $\mathbf{T}$ is obtained as $\mathbf{T} = N^{-1}[\mathbf{f}(0), \mathbf{f}(1), \dots, \mathbf{f}(N-1)] \cdot \mathbf{H}^{(N)}$. In the special case where $\mathbf{f}$ represents the encoder centroids, $\mathbf{c}_i = E[\mathbf{X}|\mathbf{I} = i]$, one can simply represent the encoder centroids as

$$\mathbf{c}_i = \mathbf{T} \cdot \mathbf{h}_i^{(N)} \tag{2.26}$$

In essence, the above representation gives an efficient way of describing the mapping from the individual bits of index i to the corresponding encoder centroid [14]. This

VQ representation has turned out to be very useful, especially in the analysis of the channel robustness of VQ's [7], [11], [16] and [14]. This representation for the encoder centroids is also the key to many of the results in this thesis.

2.2 Code-Division Multiple-Access (CDMA)

In communication systems, users can send data from one place to many other places or data can be transmitted from many points to another point. Multiaccess communication is sometimes referred to as *multipoint-to-point* communication. The engineering issues in the dual *point-to-multipoint* channel depend on the commonality of the information transmitted to each destination [17]. As mentioned earlier, there are three common multiple access techniques in digital communications. *Frequency-Division Multiple Access* (FDMA) assigns a different carrier frequency band to each user so that the resulting spectra do not overlap. *Time-Division Multiple Access* assigns each user to a time slot. Channel or receiver nonideal effects may require the insertion of guard times in TDMA and spectral guard bands in FDMA to avoid *cochannel interference*. In *Code-Division Multiple Access* (CDMA), more than one user are allowed to share a channel or subchannel by the use of direct-sequence spread spectrum signals. In this method, each user is assigned a unique code sequence or *signature sequence* that allows the user to spread the information signal across the whole frequency band. Signals from various users are then separated at the receiver by cross correlating the received signal with each of the possible user signature sequences [3]. In CDMA, the channel introduces cross correlation among users' signals. Therefore, statistical knowledge about all users' signals can be utilized in order to enhance the performance in decoding one particular user [7].

Multiuser detection (MUD) is an important technique in the receiver of a CDMA system. Four important multiuser detectors, namely the optimal MUD, the conventional matched-filter detector, the minimum mean-square error MUD and the decorrelating MUD will be presented in this section. Each of them has its own properties. The selection of which type of MUD depends on the required complexity and

performance.

2.2.1 System Model

Consider a CDMA channel shared by K simultaneous users. Each user is assigned a signature waveform $s_k(t)$ of duration T, where T is the symbol interval. A signature waveform is generally constructed as [3]

$$s_k(t) = \sum_{n=0}^{\mathcal{L}-1} g_k(n)p(t - n\tau_c), \qquad 0 \le t \le T \tag{2.27}$$

where $\{g_k(n), 0 \le n \le \mathcal{L} - 1\}$ is a pseudonoise (PN) code sequence consisting of $\mathcal{L}$ chips that take values $\{\pm 1\}$, $p(t)$ is a chip pulse of duration τ_c, and τ_c is the chip interval. Thus, each symbol has $\mathcal{L}$ chips and $T = \mathcal{L}\tau_c$. Without loss of generality, it is assumed that all K signature waveforms have unit energy, i.e.,

$$\int_0^T s_k^2(t)\mathrm{d}t = 1, \quad k = 1, 2, \ldots, K \tag{2.28}$$

The cross correlations between pairs of signature waveforms play an important role in the metrics for signal detector and on its performance. The cross correlations between two signature waveforms are defined as follows:

$$\rho_{kl}(\tau) = \int_\tau^T s_k(t)s_l(t - \tau)\mathrm{d}t \tag{2.29}$$

$$\rho_{lk}(\tau) = \int_0^\tau s_k(t)s_l(t + T - \tau)\mathrm{d}t \tag{2.30}$$

where $0 \le \tau \le T$ and $k < l$. Equations (2.29) and (2.30) are applied to asynchronous transmission of the K users. For synchronous transmission, the time epochs of users are aligned at the receiver, thus $\tau = 0$, and only $\rho_{kl}(0)$ is needed [3]. This requires closed-loop timing control or providing the transmitters with access to a common clock (such as the Global Positioning System) [17]. The system is synchronous in the sense that the transmission rate is the same for all the K users.

For simplicity, it is assumed that binary antipodal signals are used to transmit the information from each user (i.e., binary phase shift keying (BPSK) modulation). The information sequence of the kth user is denoted by $\{b_k(i)\}$, where the value of

each information bit is ± 1. It is convenient to consider the transmission of a block of bits of some arbitrary length, say $\mathbb{N}$. Then, the data block from the kth user is

$$\mathbf{b}_k = [b_k(1), \ldots, b_k(\mathbb{N})]^\top \tag{2.31}$$

and the corresponding equivalent low-pass, transmitted waveform can be expressed as

$$s_k(t) = \sqrt{E_k} \sum_{i=1}^{\mathbb{N}} b_k(i) s_k(t - iT) \tag{2.32}$$

where E_k is the signal energy per bit for user k. The composite transmitted signal for the K users can be written as

$$\begin{aligned} s(t) &= \sum_{k=1}^{K} s_k(t - \tau_k) \\ &= \sum_{k=1}^{K} \sqrt{E_k} \sum_{i=1}^{\mathbb{N}} b_k(i) s_k(t - iT - \tau_k), \end{aligned} \tag{2.33}$$

where $\{\tau_k\}$ are the delays, which satisfy $0 \leq \tau_k \leq T$ for $1 \leq k \leq K$. Without loss of generality, one can assume that $0 \leq \tau_1 \leq \ldots \leq \tau_K < T$, when considering the asynchronous transmission mode. In the special case of synchronous transmission, $\tau_k = 0$ for $1 \leq k \leq K$.

For simplicity in presenting the main principles of different MUDs, the transmitted signal is assumed to be corrupted by only additive white Gaussian noise (AWGN). Hence, the received signal can be expressed as

$$y(t) = s(t) + u(t) \tag{2.34}$$

where $s(t)$ is given as in (2.33) and $u(t)$ is zero-mean white Gaussian noise with two sided power spectral density $\frac{N_0}{2}$ [3].

2.2.2 Multiuser Detection in CDMA

The receiver in a CDMA system tries to recover the transmitted information from the received signal $y(t)$ as correctly as possible. For simplicity, the K-user synchronous CDMA channel is considered. For synchronous transmission, it is sufficient to consider

the signal received in one symbol interval, e.g., the first interval. Therefore, the received signal can be written as

$$y(t) = \sum_{k=1}^{K} \sqrt{E_k} b_k s_k(t) + u(t), \qquad 0 \le t \le T. \tag{2.35}$$

where the time index i has been dropped for simplicity.

The received continuous-time signal waveform is converted into a discrete-time process by passing through a bank of matched filters, each matched to the signature waveform of a different user. In the synchronous case, the outputs of the bank of matched filter are

$$\begin{aligned} z_1 &= \int_0^T y(t) s_1(t) \mathrm{d}t \\ &\vdots \\ z_K &= \int_0^T y(t) s_K(t) \mathrm{d}t. \end{aligned} \tag{2.36}$$

This process is illustrated in the Fig. 2.5. The output of the kth matched filter can

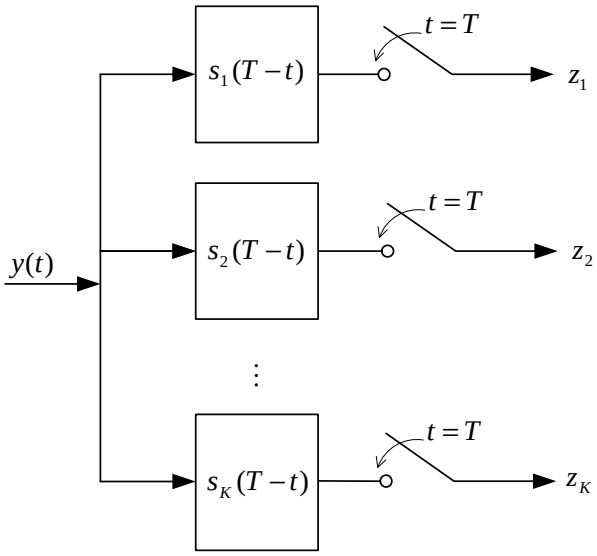

Figure 2.5 Discrete-time K-dimensional vector of matched filter outputs.

be further written as:

$$\begin{aligned} z_k &= \int_0^T y(t)s_k(t)\mathrm{d}t \\ &= \sqrt{E_k}b_k + \sum_{\substack{l=1 \\ l\neq k}}^{K} \sqrt{E_l}b_l \int_0^T s_k(t)s_l(t)\mathrm{d}t + u_k \end{aligned} \tag{2.37}$$

where the noise component

$$u_k = \int_0^T u(t)s_k(t)\mathrm{d}t \tag{2.38}$$

is a Gaussian random variable with zero mean and variance computed as follows:

$$\begin{aligned} \sigma^2 &= E[u_k^2] \\ &= \int_0^T \int_0^T E[u(t_1)u(t_2)]s_k(t_1)s_k(t_2)\mathrm{d}t_1\mathrm{d}t_2 \\ &= \frac{1}{2}N_0 \int_0^T \int_0^T \delta(t_1 - t_2)s_k(t_1)s_k(t_2)\mathrm{d}t_1\mathrm{d}t_2 \\ &= \frac{1}{2}N_0 \int_0^T s_k^2(t)\mathrm{d}t = \frac{N_0}{2}. \end{aligned} \tag{2.39}$$

The $\mathbf{z} = [z_1, \ldots, z_K]^\top$ vector of the matched filter outputs is known as a *sufficient statistic* that contains all the information in the original observation [17]. The output vector of the bank of K matched filters' outputs can also be written using matrix notation as follows

$$\mathbf{z} = \mathbf{RWb} + \mathbf{u}, \tag{2.40}$$

where the $K \times K$ diagonal matrix of the received amplitudes is $\mathbf{W} = \mathrm{diag}\{\sqrt{E_1}, \ldots, \sqrt{E_K}\}$, $\mathbf{R} = \{\rho_{k,l}\}_{k,l=1}^K$ is the normalized cross-correlation matrix whose component is computed by $\rho_{lk} = \int_0^T s_k(t)s_l(t)\mathrm{d}t$ and $\mathbf{u}$ is a Gaussian random vector with zero mean and covariance matrix equal to $E[\mathbf{uu}^\top] = \sigma^2\mathbf{R}$. Based on the sufficient statistic $\mathbf{z}$, the transmitted bit sequence $\mathbf{b}$ can be detected by one of the following multiuser detectors.

The optimum multiuser detector. The optimum maximum-likelihood receiver selects the most probable sequence of bits $\{b_k, 1 \leq k \leq K\}$ given the received signal $y(t)$ in (2.35). Obviously, there are 2^K different possibilities for $\mathbf{b} = [b_1, b_2, \ldots, b_K]^\top$.

The solution of the optimal receiver chooses the most likely $\mathbf{b}$ that maximizes the likelihood function [17]:

$$\exp\left\{-\frac{1}{2\sigma^2}\int_0^T\left[y(t)-\sum_{k=1}^{K}\sqrt{E_k}b_k s_k(t)\right]^2\mathrm{d}t\right\}. \tag{2.41}$$

It is easy to see that maximizing (2.41) is minimizing the following log likelihood function:

$$\Lambda_{OPT}(\mathbf{b})=\int_0^T\left[y(t)-\sum_{k=1}^{K}\sqrt{E_k}b_k s_k(t)\right]^2\mathrm{d}t \tag{2.42}$$

The above log likelihood function is expanded as follows:

$$\begin{aligned}\Lambda_{OPT}(\mathbf{b}) &= \int_0^T y^2(t)\mathrm{d}t-2\sum_{k=1}^{K}\sqrt{E_k}b_k\int_0^T y(t)s_k(t)\mathrm{d}t\\ &+ \sum_{l=1}^{K}\sum_{k=1}^{K}\sqrt{E_lE_k}b_k b_l\int_0^T s_k(t)s_l(t)\mathrm{d}t\end{aligned} \tag{2.43}$$

It is observed that the selection of $\mathbf{b}$ does not depend on the first term of (2.43). Therefore, $\mathbf{b}$ can be chosen to minimize:

$$-2\sum_{k=1}^{K}\sqrt{E_k}b_k\int_0^T y(t)s_k(t)\mathrm{d}t+\sum_{l=1}^{K}\sum_{k=1}^{K}\sqrt{E_lE_k}b_k b_l\int_0^T s_k(t)s_l(t)\mathrm{d}t \tag{2.44}$$

Define and compute the correlation metric as follows:

$$\begin{aligned}\Omega(\mathbf{b}) &= 2\sum_{k=1}^{K}\sqrt{E_k}b_k\int_0^T y(t)s_k(t)\mathrm{d}t-\sum_{l=1}^{K}\sum_{k=1}^{K}\sqrt{E_lE_k}b_k b_l\int_0^T s_k(t)s_l(t)\mathrm{d}t\\ &= 2\mathbf{b}^\top\mathbf{W}\mathbf{z}-\mathbf{b}^\top\mathbf{W}\mathbf{R}\mathbf{W}\mathbf{b}.\end{aligned} \tag{2.45}$$

Then the demodulated information sequence of the K users can be found as:

$$\mathbf{b} = \arg\max_{\mathbf{b}=\{\pm1\}^K}\left\{2\mathbf{b}^\top\mathbf{W}\mathbf{z}-\mathbf{b}^\top\mathbf{W}\mathbf{R}\mathbf{W}\mathbf{b}\right\}. \tag{2.46}$$

Observe from (2.45) that the optimum detector must have knowledge of the received signal energies and all the signature waveforms of K users in order to compute the correlation metrics. There are 2^K possible choices of the information sequence of the K users. The optimum detector computes the correlation metrics $\Omega(\mathbf{b})$ for

each sequence and selects the sequence that yields the largest correlation metric. Obviously, the optimum detector has a complexity that grows exponentially with the number of users, K.

Since it is too complicated to implement an optimum detector for a CDMA system with a medium or large number of users, three types of suboptimum detectors whose computational complexities grow linearly with the number of users will be introduced next. The simplest suboptimum detector is the conventional matched-filter detector.

Conventional matched-filter (MF) detector. In the conventional matched-filter detector, the received signal is first correlated with the signature waveform of the desired user. The correlator output is then simply compared with a zero threshold to make the decision on the transmitted bit. That is,

$$\hat{b}_k = \text{sgn}(z_k), \tag{2.47}$$

where z_k is calculated from (2.37). Thus, this detecting scheme neglects the presence of the other users in CDMA channel. This is equivalent to assume that the aggregate noise plus interference is white and Gaussian [3]. Fig. 2.6 shows the structure of the MF detector.

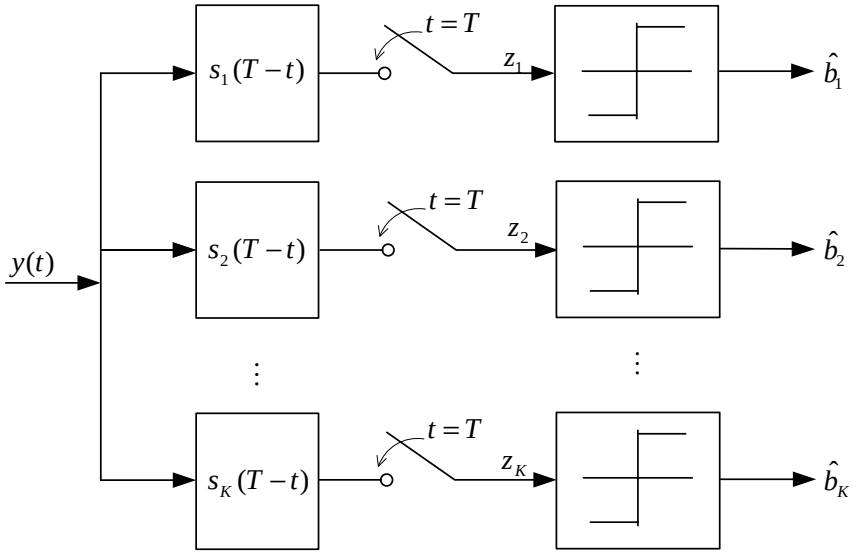

Figure 2.6 Structure of the matched-filter detector.

In Equation (2.37), the first component contains the desired signal of user k, the

second component is due to multiple-access interference (MAI) from all other $(K-1)$ users and the last component is due to the background noise. Clearly, if the signature sequences are orthogonal, the interference from the other users vanishes and this conventional detector is optimum. On the other hand, if one or more signature waveforms are not orthogonal to the desired user's signature waveform, the interference from the other users can become excessive if the power levels of the signals of one or more of the other users is sufficiently larger than the power level of the kth user. This situation is generally called the *near-far problem* in multiuser communications, and necessitates some type of power control for conventional detection [3].

Decorrelating detector. The large gaps in performance and complexity between the conventional single-user matched filter and the optimum multiuser detector encourage the search for other multiuser detectors. The decorrelating detector is not only a simple and natural strategy but it is optimal according to three different criteria: least-squares, near-far resistance, and maximum-likelihood when the received amplitudes are unknown [17].

The vector of the bank of K matched filters' outputs is computed in (2.40). It is observed that $\mathbf{z}$ is described by a K-dimensional Gaussian PDF with mean $\mathbf{RWb}$ and covariance matrix $\sigma^2\mathbf{R}$. That is,

$$f(\mathbf{z}) = \frac{1}{\sqrt{(2\pi\sigma^2)^K|\mathbf{R}|}} \exp\left\{-\frac{1}{2\sigma^2}(\mathbf{z}-\mathbf{RWb})^\top \mathbf{R}^{-1}(\mathbf{z}-\mathbf{RWb})\right\} \tag{2.48}$$

The best linear estimate of $\mathbf{b}' = \mathbf{Wb}$ is the value that maximizes $f(\mathbf{z})$ or equivalently minimizes the following log likelihood function

$$\begin{aligned} \Lambda_{DC}(\mathbf{b}') &= (\mathbf{z}-\mathbf{RWb})^\top \mathbf{R}^{-1}(\mathbf{z}-\mathbf{RWb}) \\ &= (\mathbf{z}-\mathbf{Rb}')^\top \mathbf{R}^{-1}(\mathbf{z}-\mathbf{Rb}') \end{aligned} \tag{2.49}$$

The result of this minimization yields [3]

$$\tilde{\mathbf{b}} = \mathbf{R}^{-1}\mathbf{z} \tag{2.50}$$

Then, the estimation of the transmitted binary sequence is obtained by taking the

sign of each element of $\tilde{\mathbf{b}}$, i.e.,

$$\hat{\mathbf{b}} = \text{sgn}(\tilde{\mathbf{b}}) = \text{sgn}(\mathbf{W}\mathbf{b} + \mathbf{R}^{-1}\mathbf{u}) \tag{2.51}$$

Observe that multiuser interference is completely removed by the decorrelator and the only source of interference remained is the background noise. It should be noted, however, that the price to pay for removing the multiuser interference is the enhancement of the background noise. Fig. 2.7 illustrates the receiver structure. Since

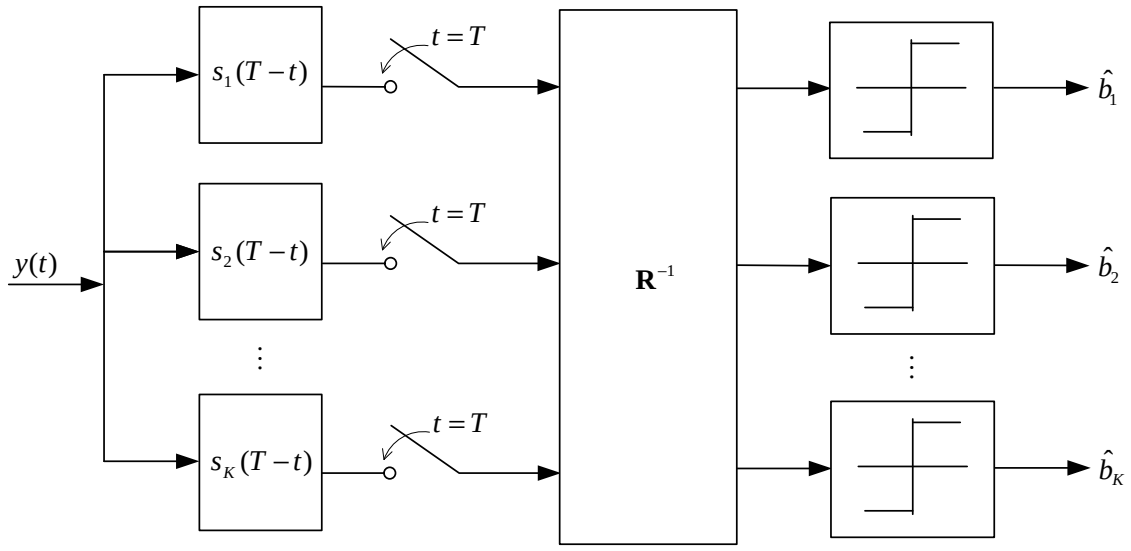

Figure 2.7 Structure of the decorrelating detector.

the estimate $\hat{\mathbf{b}}$ is obtained by performing a linear transformation on the vector of correlator outputs, the computational complexity is linear in K.

Minimum mean-square error detector. A common approach in estimation theory to the problem of estimating a random variable Ψ on the basis of observations $\mathbf{z}$ is to choose the function $\hat{\Psi}(\mathbf{z})$ that minimizes the mean-square error (MSE):

$$E\{[\Psi - \hat{\Psi}(\mathbf{z})]^2\} \tag{2.52}$$

Under very general conditions, it can be shown that the solution is the conditional-mean estimator [17]:

$$\hat{\Psi}(\mathbf{z}) = E[\Psi|\mathbf{z}]. \tag{2.53}$$

In most problems, it is challenging to derive the conditional-mean estimator from the joint distribution of Ψ and $\mathbf{z}$. For that reason, it is common to minimize the MSE within a restricted set of linear transformations of $\mathbf{z}$. The linear minimum mean-square error (MMSE) estimator is, in general, easy to compute and it depends on the joint distribution of Ψ and $\mathbf{z}$ only through their variances and covariance. This problem of linear estimation can be applied to the problem of linear multiuser detection by requiring that the MSE between the kth user bit b_k and the output of the kth linear transformation $\mathbf{m}_k^\top \mathbf{z}$ be minimized. Although this approach does not lead to the minimization of the bit-error-rate, it is a sensible criterion, particularly when the multiuser receiver, rather than demodulating the data, supplies soft decisions to an error-control decoder.

The MMSE linear detector for the kth user chooses the K-vector $\mathbf{m}_k$ that minimizes

$$E\left[\left(b_k - \mathbf{m}_k^\top \mathbf{z}\right)^2\right]. \tag{2.54}$$

The total number of users is K in the system. Therefore, there are K uncoupled optimization problems (one for each user), which can be solved simultaneously by choosing the $K \times K$ matrix $\mathbf{M}$ (whose kth column is equal to $\mathbf{m}_k$) that achieves

$$\min_{\mathbf{M} \in R^{K \times K}} E\left[\|\mathbf{b} - \mathbf{M}\mathbf{z}\|^2\right], \tag{2.55}$$

where $\mathbf{z}$ is given in (2.40). The solution to this optimization problem is given in [17], as

$$\mathbf{M} = \mathbf{W}^{-1}\left(\mathbf{R} + \sigma^2 \mathbf{W}^{-2}\right)^{-1} \tag{2.56}$$

The decision outputs of the MMSE linear detector can then be expressed as

$$\hat{b}_k = \operatorname{sgn}\left\{\left[\left(\mathbf{R} + \sigma^2 \mathbf{W}^{-2}\right)^{-1} \mathbf{z}\right]_k\right\}. \tag{2.57}$$

Therefore, the MMSE linear detector replaces the transformation $\mathbf{R}^{-1}$ of the decorrelating detector by $(\mathbf{R} + \sigma^2 \mathbf{W}^{-2})^{-1}$, where $\mathbf{W}^{-2} = \operatorname{diag}\left\{\frac{1}{E_1}, \ldots, \frac{1}{E_K}\right\}$. The structure of the MMSE detector is shown in Fig. 2.8.

Similarly to the DC detector, the complexity of the MMSE detector increases linearly with the number of users K. The MMSE receiver requires knowledge of

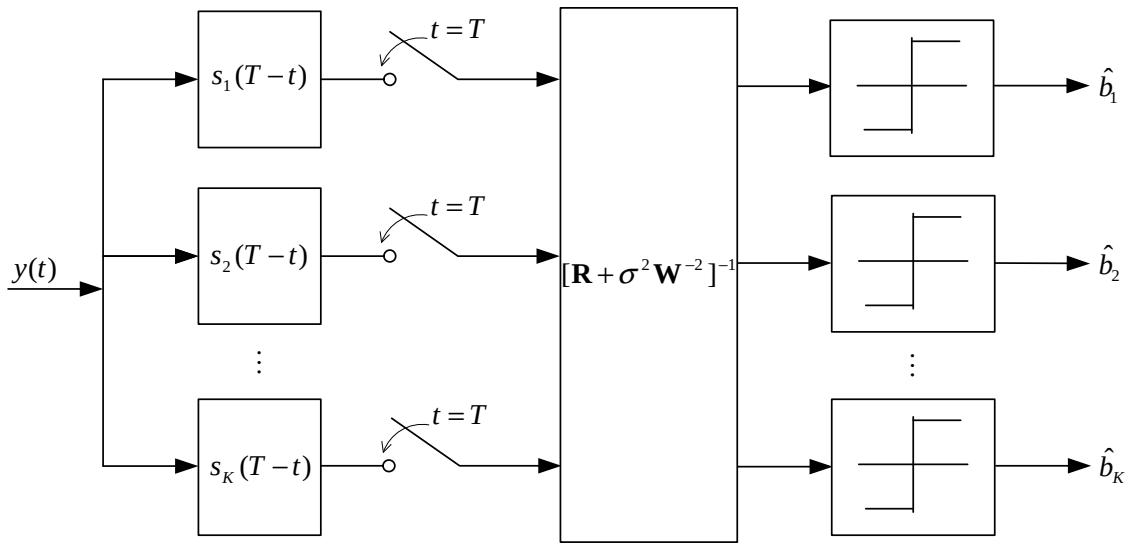

Figure 2.8 The MMSE linear detector for the synchronous channel.

all users' signature waveforms, as well as knowledge of the signal-to-noise ratios of all users [6]. The benefit obtained from the requirement of more information for the receiver implementation is the superiority in bit-error-rate performance of the corresponding receiver [18].

The trade-off between the error performance and the complexity of various MUDs needs to be carefully examined when a CDMA communications system is designed. As an example, Fig. 2.9 plots the bit-error-rates (BERs) achieved by various linear multiuser detectors discussed earlier in this chapter (the solid lines). The results are presented for a system having eight (K=8) users with identical crosscorrelation (equal to 0.1) and perfect power control. Also shown in the figure are the BERs computed based on Gaussian approximation. Note that for the decorrelating receiver, the exact BER is exactly the same as Gaussian approximation. For the MF, the approximation is only accurate for very low signa-to-noise ratios. For this system, the performances of the DC and the MMSE receiver are indistinguishable [6].

Based on numerical and some analytical results, Poor and Verdú conjectured that the BER of the MMSE detector is better than that of the decorrelator for all levels of background Gaussian noise, number of users, and crosscorrelation matrices [18].

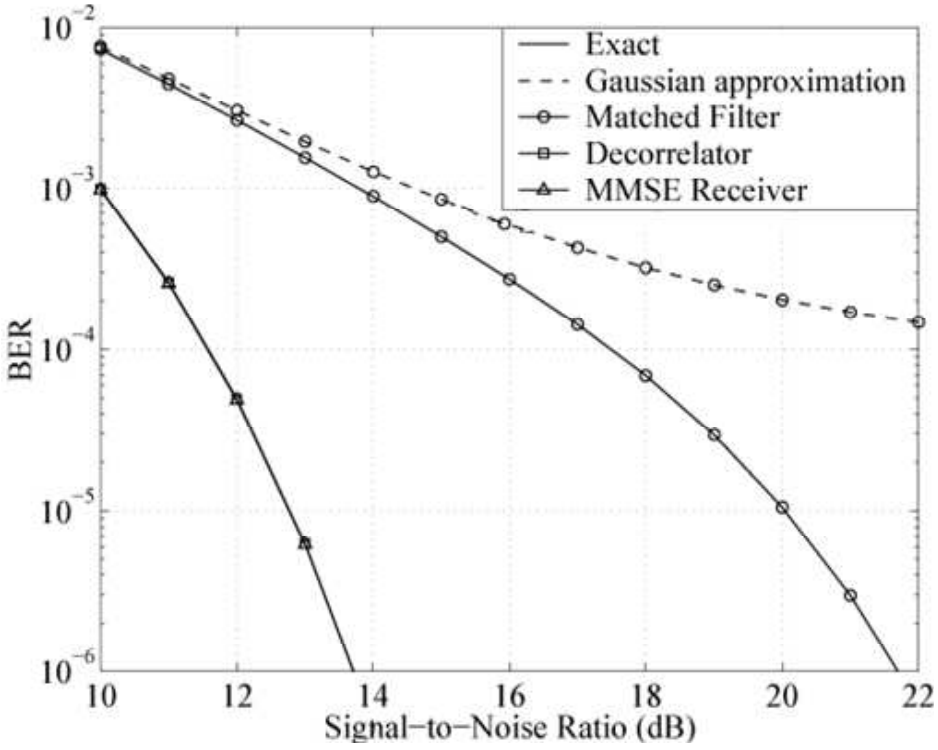

Figure 2.9 BERs of different MUDs for a system with $K = 8$, $\rho_{k,l} = 0.1$ [6].

However, is it recently shown in [19] that this relative performance is not always true [6].

Finally, a unified linear (UL) receiver was recently introduced in [20, 21]. The strategy for the UL receiver is to minimize the weighted sum of the MAI and the background noise where the weighting factor is adjusted according to the relative levels of the MAI and the background noise in order to improve the bit-error-rate performance. By tunning the weighting factor, it is possible to improve the performance of the UL receiver over that of any of the above mentioned linear receivers [6].

3. Transmission of VQ Over A Frequency-Selective Rayleigh Fading CDMA Channel

Chapter 2 presents basic concepts and theories of vector quantization (VQ) and CDMA techniques. As mentioned before, transmission of VQ over a CDMA channel is an important and interesting problem, both from theoretical and practical perspectives. This chapter describes this research problem in details. Previous solutions to the problem are also presented and their limitations are discussed.

3.1 System Description

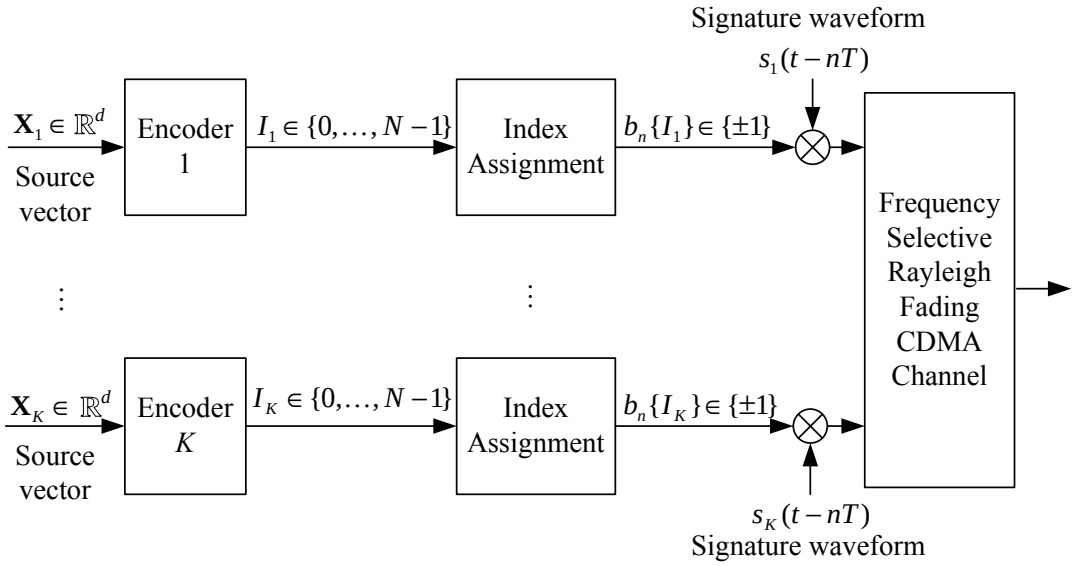

Figure 3.1 Structure of the transmitter.

The general structure of the transmitter is shown in Figure 3.1. There are K users in a CDMA system where the kth user transmits his/her d-dimensional source vector $\mathbf{X}_k \in \mathbb{R}^d$. The encoder of the kth user then encodes $\mathbf{X}_k$ into an index $I_k \in$

$\{0, 1, \ldots, N-1\}$, where $N = 2^L$ for some integer L. The kth encoder is described by a partition $\{S_i^{(k)}\}_{i=0}^{N-1}$ of the Euclidean source space $\mathbb{R}^d$ such that if $\mathbf{X}_k \in S_i^{(k)}$, then $I_k = i$ and $P_i^{(k)} = \Pr(I_k = i) = \Pr(X_k \in S_i^{(k)})$. The *encoder entropy* of the kth user is defined as $H_k = -\sum_{j=0}^{N-1} P_j^{(k)} \log_2 P_j^{(k)}$. Also, let the ith encoder centroid of user k be defined as $\mathbf{c}_i^{(k)} = E[\mathbf{X}_k | I_k = i]$. The codebook of the VQ is arranged with good index assignments based on LISA-algorithm [13]. The detail of this algorithm is provided in Appendix A. For transmission, the index I_k is converted into a binary sequence of L bits, denoted as $(b_1(I_k), \ldots, b_L(I_k))$ where $b_n(I_k) \in \{\pm 1\}$. These bits are transmitted over a frequency selective Rayleigh fading CDMA channel. The channel model in the system under consideration is similar to the one in [8]. Here, the frequency-selective Rayleigh fading channel is also modeled as a tapped-delay line [3] where the received amplitude over each path of each user is a complex Gaussian random variable and the delay between paths is an integer multiple of the chip duration.

More precisely, assuming BPSK modulation, the transmitted signal of user k at time $n \in \{1, \ldots, L\}$ is $\sqrt{E_k} b_n(I_k) s_k(t - (n-1)T)$, where E_k and $s_k(t)$ are the bit energy and the real-valued signature waveform of the kth user. The users' signature waveforms all have a duration of T seconds and are normalized to have unit energy. Let P be the number of multipaths, τ_c be the chip duration, and $a_{k,i}(n)$ be the received amplitude of user k over path i and at bit duration n. The fading amplitudes are assumed to be constant over one bit interval T (slow fading) and independent in n (perfect interleaving).

Figure 3.2 illustrates the tapped-delay line model of this channel. The received signal component, stemming from the transmission of the L bits of user k, is given by:

$$y_k(t) = \sqrt{E_k} \sum_{n=1}^{L} b_n(I_k) \mathbf{s}_k^\top (t - (n-1)T) \mathbf{a}_k(n), \quad 0 \le t \le LT \tag{3.1}$$

where $\mathbf{s}_k(t) = [s_k(t), s_k(t-\tau_c), \ldots, s_k(t-(P-1)\tau_c)]^\top$, and $\mathbf{a}_k(n) = [a_{k,0}(n), a_{k,1}(n), \ldots, a_{k,P-1}(n)]^\top$ is the vector of independent complex Gaussian random variables.

At the receiver, the received signal waveform $y(t)$, stemming from the transmitted

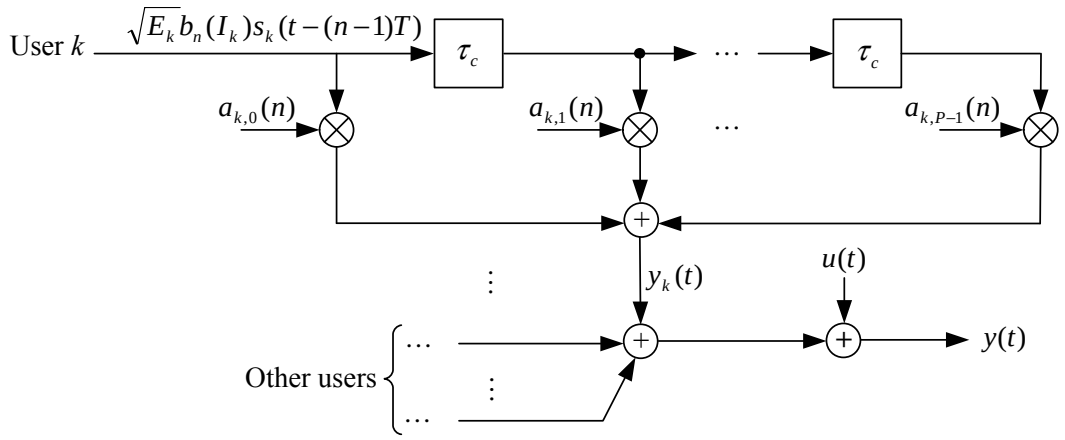

Figure 3.2 Tapped-delay line model of a frequency-selective fading channel.

signals of all the K users plus the additive white Gaussian noise, is then given as

$$y(t) = \sum_{k=1}^{K} y_k(t) + u(t), \tag{3.2}$$

where $u(t)$ is complex AWGN with covariance equal to $E[u(t)u^*(s)] = \sigma^2\delta(t-s)$.

Let $\mathbf{z}_k(n)$ be a vector formed by correlating the received waveform $y(t)$ with the delayed replicas of the signature waveform of user k, that is:

$$\mathbf{z}_k(n) = \int_{(n-1)T}^{nT} y(t)\mathbf{s}_k(t-(n-1)T)\mathrm{d}t. \tag{3.3}$$

This operation defines the continuous-time to discrete-time front-end processing of the receiver and is illustrated in Fig. 3.3. When the symbol period is much greater than the delay spread of the channel, it is reasonable to assume that no intersymbol interference occurs. Using (3.1) and substituting (3.2) into (3.3), $\mathbf{z}_k(n)$ can be expressed as

$$\begin{aligned}\mathbf{z}_k(n) &= \sqrt{E_k}b_n(I_k)\mathbf{R}_{kk}\mathbf{a}_k(n) + \sum_{\substack{l=1\\l\neq k}}^{K}\sqrt{E_l}b_n(I_l)\mathbf{R}_{kl}\mathbf{a}_l(n)\\ &+ \int_{(n-1)T}^{nT}\mathbf{s}_k(t-(n-1)T)u(t)\mathrm{d}t\end{aligned} \tag{3.4}$$

where $\mathbf{R}_{kl}$ is $P\times P$ cross correlation matrix of all the delayed replicas of the signature waveforms of users k and l. It can be computed as

$$\mathbf{R}_{kl} = \int_0^T \mathbf{s}_k(t)\mathbf{s}_l^\top(t)\mathrm{d}t \tag{3.5}$$

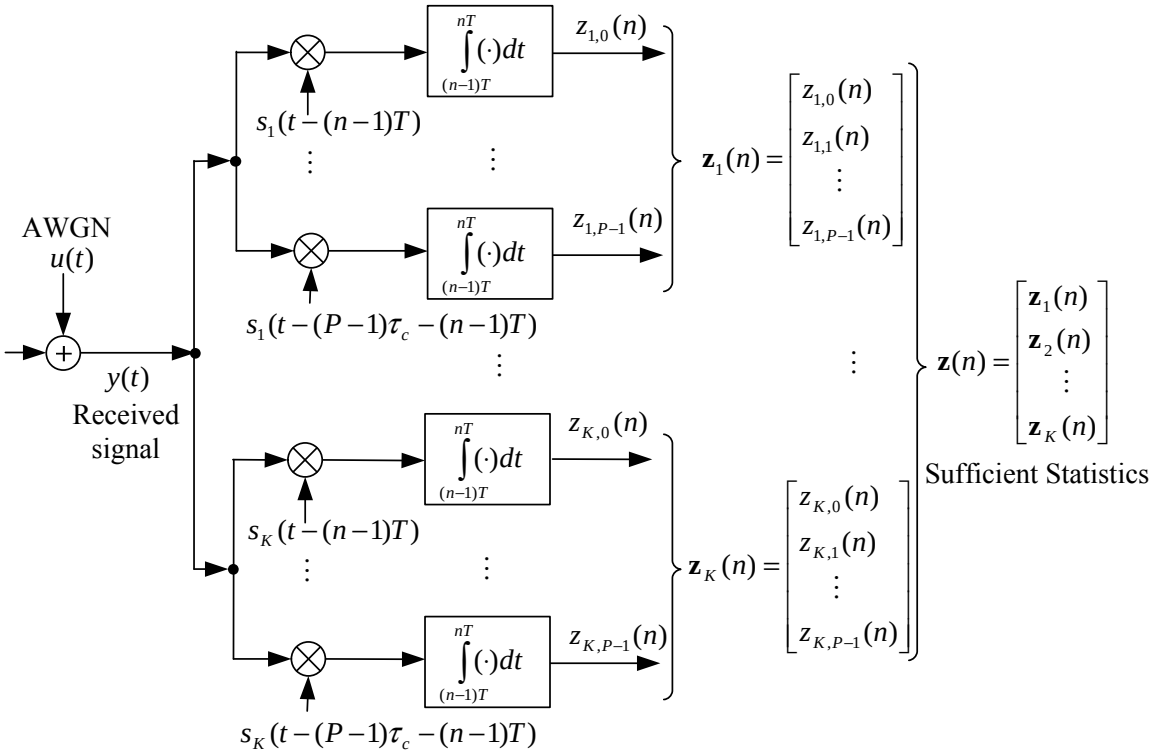

Figure 3.3 Front-end processing of the receiver.

During the nth bit duration, the received vectors of all users can be merged into a KP-vector $\mathbf{z}(n) = [\mathbf{z}_1^\top(n), \ldots, \mathbf{z}_K^\top(n)]^\top$. Using matrix notations, $\mathbf{z}(n)$ can be written as:

$$\mathbf{z}(n) = \mathbf{RWA}(n)\mathbf{b}(n) + \mathbf{u}(n) \tag{3.6}$$

where the $KP \times KP$ matrix $\mathbf{R}$ is built up by stacking all the submatrices $\{\mathbf{R}_{kl}\}_{k,l=1}^{K}$, $\mathbf{W} = \mathrm{diag}(\mathbf{W}_1, \ldots, \mathbf{W}_K)$ is the $KP \times KP$ real matrix with $\mathbf{W}_k = \sqrt{E_k}\mathbf{I}_P$ (where $\mathbf{I}_P$ denotes the $P \times P$ identity matrix). Moreover, $\mathbf{A}(n) = \mathrm{diag}(\mathbf{a}_1(n), \ldots, \mathbf{a}_K(n))$ is a $KP \times K$ block diagonal matrix. The vector $\mathbf{b}(n) = [b_n(I_1), \ldots, b_n(I_k)]^\top$ contains the transmitted bits of all users at time n. The noise vector $\mathbf{u}(n)$ is a complex zero-mean Gaussian vector of size KP and covariance matrix $E[\mathbf{u}(n)\mathbf{u}^H(n)] = \sigma^2\mathbf{R}$. It is well-known that $\mathbf{z}(n)$ contains sufficient statistics for the decoding of the source vectors.

3.2 Known Decoders

At the receiver, the decoder tries to make the decision for the source vectors based on the sufficient statistics and the source statistics as correctly as possible. In what follows, previously proposed decoding schemes are reviewed.

3.2.1 The Optimal Decoder

The jointly optimal multiuser decoder takes the source statistics of all users into account. Such a decoder measures the *sufficient statistic* $\mathbf{Z} = [\mathbf{z}^\top(1), \ldots, \mathbf{z}^\top(L)]^\top$ and forms the optimal estimate $\hat{\mathbf{X}}^K(\mathbf{Z}) = [\hat{\mathbf{X}}_1^\top(\mathbf{Z}), \ldots, \hat{\mathbf{X}}_K^\top(\mathbf{Z})]^\top$ that minimizes the distortion $E\{\|\mathbf{X}_k - \hat{\mathbf{X}}_k(\mathbf{Z})\|^2\}$ for every user k. An implementation of such optimal decoder based on Hadamard matrix description of the VQ's (hence it is referred to as the *Hadamard-based* multiuser decoder (HMD)) is presented in [7] and [8]. In HMD, the ith centroid of user k is represented as $\mathbf{c}_i^{(k)} = \mathbf{T}_k \mathbf{h}_i^{(N)}$. This presentation was previously discussed in Section 2. Hence, the optimal estimate $\hat{\mathbf{X}}^K(\mathbf{Z})$ is the conditional mean $\hat{\mathbf{X}}^K(\mathbf{Z}) = E[\mathbf{X}^K|\mathbf{Z}] = E[\mathbf{c}^K|\mathbf{Z}]$, where $\mathbf{X}^K$ and $\mathbf{c}^K$ are the augmented source vector and the augmented centroid vector, respectively [7]. This implies that the soft estimate $\hat{\mathbf{X}}^K(\mathbf{Z})$ is formed as a weighted sum over the encoder centroids $\mathbf{c}^K = \mathbb{T}\mathbf{h}_{i^K}^{(M)}$, where $\mathbb{T}$ is the corresponding augmented transform matrix, i^K is the sampled value of the index vector $I^K = [I_1, \ldots, I^K]^\top$ and $\mathbf{h}_{i^K}^{(M)}$ is a size $M = N^K$ Hadamard matrix column, obtained as $\mathbf{h}_{i^K}^{(M)} = \mathbf{h}_{i_K}^{(N)} \otimes \ldots \otimes \mathbf{h}_{i_1}^{(N)}$. $\hat{\mathbf{X}}^K(\mathbf{Z})$ can be therefore expressed as follows [8]

$$\begin{aligned} \hat{\mathbf{X}}^K(\mathbf{Z}) &= \mathbb{T}E[\mathbf{h}_{I^K}^{(M)}|\mathbf{Z} = \mathbf{z}] \\ &= \mathbb{T}\frac{\sum_{i^K} \mathbf{h}_{i^K}^{(M)} p_{\mathbf{Z}}(\mathbf{z}|i^K) P_{i^K}}{\sum_{i^K} p_{\mathbf{Z}}(\mathbf{z}|i^K) P_{i^K}}, \end{aligned} \tag{3.7}$$

where

$$p_{\mathbf{Z}}(\mathbf{z}|i^K) = \frac{\exp\left\{-\frac{1}{\sigma^2}\sum_{n=1}^{L}[\mathbf{z}(n) - \mathbf{RWA}(n)\mathbf{b}(n)]^H \mathbf{R}^{-1}[\mathbf{z}(n) - \mathbf{RWA}(n)\mathbf{b}(n)]\right\}}{(\pi\sigma^2)^{KPL}|\mathbf{R}|^L}, \tag{3.8}$$

and

$$P_{i^K} = P_{i_1}^{(1)} P_{i_2}^{(2)} \ldots P_{i_K}^{(K)}. \tag{3.9}$$

The structure of the optimal decoder is illustrated in Fig. 3.4. As can be seen from (3.7), this approach is too complicated for a CDMA system with a medium or large number of users. This is because its total decoding complexity is about $\mathcal{O}(PKL \cdot 2^{KL})$ operations.

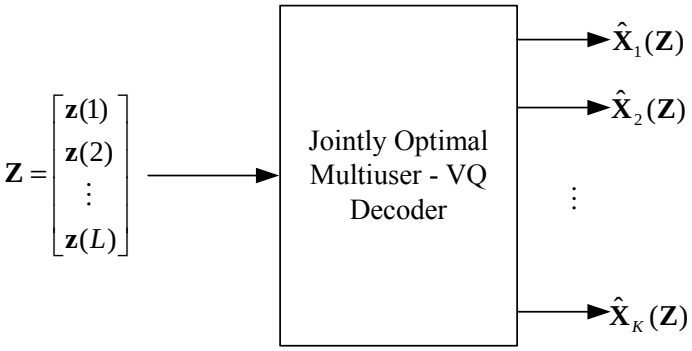

Figure 3.4 Model of the jointly optimal multiuser-VQ decoder.

3.2.2 The Suboptimal Decoder Based on Table Look-up

Figure 3.5 shows the structure of an alternative decoding approach that is based on a combination of separate multiuser detection (MUD) and table-lookup (or hard) VQ decoding. Let $\hat{b}_n(I_k)$ be the hard decision produced by the MUD for user k at

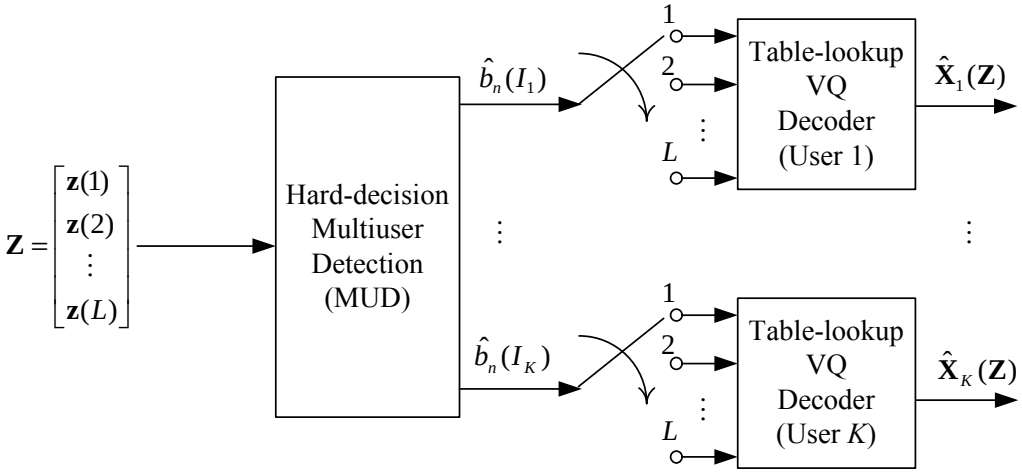

Figure 3.5 Model of the suboptimal decoder based on table-lookup.

time n and let $\hat{\mathbf{b}}(n) = [\hat{b}_n(I_1), \ldots, \hat{b}_n(I_K)]^\top$. If the optimal MUD is used, the hard bit decisions are based on the maximum likelihood (ML) decision rule [1]. Instead

of the ML rule, the decorrelating MUD (DC-MUD) makes the hard bit decisions at time n based on $\mathbf{R}^{-1}\mathbf{z}(n)$. On the other hand, the MMSE-MUD provides the hard bit decisions based on a linear filtering $\mathbf{m}_k^H(n)\mathbf{z}(n)$ of $\mathbf{z}(n)$ that minimizes the mean-square error $E\left[\left\|b_n(I_k) - \mathbf{m}_k^H(n)\mathbf{z}(n)\right\|^2\right]$ [17].

Next, the VQ decoder of the kth user converts L consecutive bits $\{\hat{b}_n(I_k)\}_{n=1}^{L}$ to the estimated index $\hat{i}_k$ and outputs the centroid $\mathbf{c}_{\hat{i}_k}^{(k)}$ for VQ decoding (table-lookup decoding). The complexity of such a suboptimal hard-decision decoder largely depends on the type of MUD employed. It is about $\mathcal{O}(PL \cdot 2^K)$ operations for the OPT-MUD. On the other hand, the decoding complexity is about $\mathcal{O}(PL \cdot K^2)$ if either DC-MUD or MMSE-MUD is used.

3.3 An Example

To illustrate how the system works in general, an example is presented in this subsection. Consider a simple CDMA system with 2 users whose signature sequences of length 7 are [1100101] and [0110110], respectively [22]. One user transmits a 512×512 monochrome image of "Lena" and the other user transmits a 512×512 monochrome image of "Barbara". For transmission, these two images are sampled and quantized with the LBG-VQ. The VQ codebook is designed from 20 different 512×512 monochrome images. Common images such as "baboon", "bridge", "pepper", and "f16" are used as the training data. The pixels of all images are presented by 8 bits. The VQ is trained for image sources in a noiseless channel with the codevector dimension $d = 8$ and the number of codevectors $N = 2^L = 64$. The compression ratio is thus $L/d = 6/8 = 0.75$ bits/pixel [2]. The output of VQ is then arranged with a good index assignments based on the LISA algorithm [13] (see Appendix A). For simplicity, it is assumed that two users have the same average received energy per bit, i.e., $E_1 = E_2 = E_b$. The simulation is run for a frequency-selective Rayleigh fading CDMA channel with $P = 3$ paths . The transmission system is illustrated in Fig. 3.6.

The decoding schemes used in simulation are the Hadamard-based multiuser

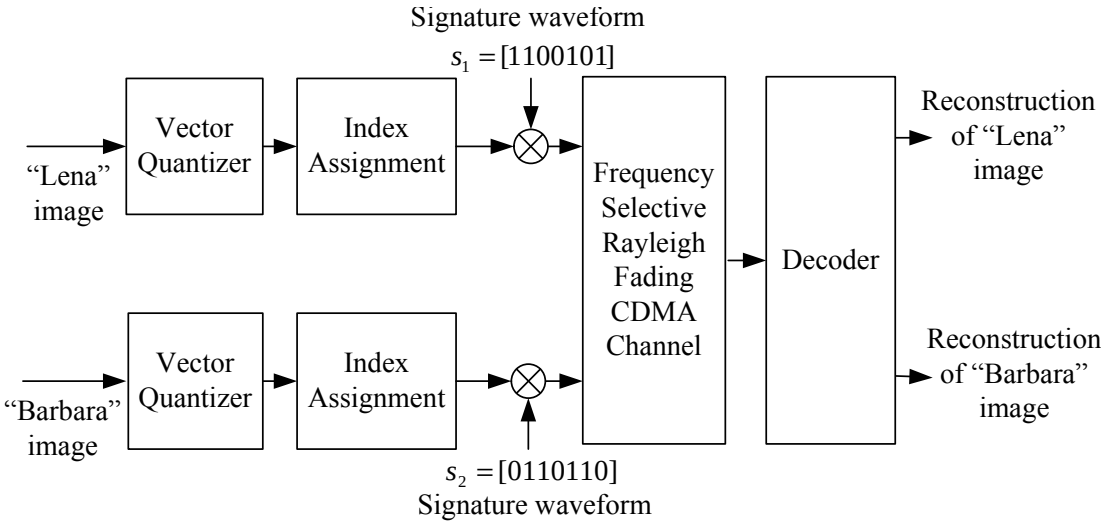

Figure 3.6 Image transmission using VQ over a CDMA channel.

decoder (HMD) and the suboptimal hard-decision decoders employing the OPT-MUD, the MMSE-MUD and the DC-MUD. Two original images are shown in Figures 3.7 and 3.8. The performances of various decoders are illustrated by displaying the reconstructed images for both users in Figures 3.9 to 3.16. The simulations were run at the channel signal-to-noise ratio (CSNR) $E_b/N_0 = 8$ (dB). The performance of VQ decoders can also be measured in terms of either the output signal-to-noise ratio, $\text{SNR}_k = E\{\|\mathbf{X}_k\|^2\}/E\{\|\mathbf{X}_k - \hat{\mathbf{X}}_k\|^2\}$, or the peak signal-to-noise ratio (PSNR) of the reconstructed image for each user k, which is defined as $\text{PSNR}_k = \|\max(\mathbf{X}_k)\|^2/E\{\|\mathbf{X}_k - \hat{\mathbf{X}}_k\|^2\}$. Table 3.1 tabulates the SNRs and PSNRs offered by different decoding schemes. It can be observed clearly from Figures 3.9-3.16 and Table 3.1 that a better quality of reconstructed images is obtained by using a more-complicated decoding scheme.

Table 3.1 SNRs and PSNRs for CSNR = 8 (dB).

	HMD		OPT-MUD		MMSE-MUD		DC-MUD	
	SNR	PSNR	SNR	PSNR	SNR	PSNR	SNR	PSNR
User 1	12.11	25.41	10.71	25.25	9.56	24.09	4.83	19.36
User 2	9.87	23.26	9.88	23.26	9.09	22.47	5.45	18.84

Figure 3.7 Original image of "Lena".

Figure 3.8 Original image of "Barbara".

Figure 3.9 Reconstructed image of "Lena" with the HMD decoder.

Figure 3.10 Reconstructed image of "Barbara" with the HMD decoder.

Figure 3.11 Reconstructed image of "Lena" using the suboptimal hard decoder with OPT-MUD.

Figure 3.12 Reconstructed image of "Barbara" using the suboptimal hard decoder with OPT-MUD.

Figure 3.13 Reconstructed image of "Lena" using the suboptimal hard decoder with MMSE-MUD.

Figure 3.14 Reconstructed image of "Barbara" using the suboptimal hard decoder with MMSE-MUD.

Figure 3.15 Reconstructed image of "Lena" using the suboptimal hard decoder with DC-MUD.

Figure 3.16 Reconstructed image of "Barbara" using the suboptimal hard decoder with DC-MUD.

4. The Suboptimal Soft-Decision Decoders

Chapter 3 presented several options for decoding VQ over a CDMA channel. The suboptimal hard-decision decoders have a low computational complexity with respect to the number of users K. They, however, perform poorly at low and medium ranges of the channel signal-to-noise ratio (CSNR) [1, 2]. On the other hand, the optimal HMD is too complicated for systems with a medium to large number of users. Recently, the author in [1, 2] proposed a low complexity, suboptimal decoder for VQ over a CDMA channel. This decoder has the same complexity as that of the suboptimal hard decoder but its performance is much improved. The structure of this suboptimal soft-decision decoder is shown in Fig. 4.1. It should be pointed out that the work in [1, 2], however, only considers the AWGN and frequency-flat Rayleigh fading channels, where the transmitted signal is affected only in amplitude and not by multipath effects. An important contribution of this chapter is to extend the scheme in [1, 2] to a frequency-selective fading channel, where the received signal is affected in both strength and shape due to multipath effects. Note that such an extension is not simple as it might first appear. The complication is due to the fact that one has to modify both the soft-output MUD and the soft bit estimator shown in Fig. 4.1.

Observe that the suboptimal decoder in [1, 2] is also based on separate multiuser detection and VQ decoding. However, instead of using the table-lookup (or hard) VQ decoding, the individual soft VQ decoders are employed to make the decision for the source vectors based on the soft bit estimates that are calculated from the soft bit estimator. As in [1, 2], to see what are the soft bit estimates needed for individual soft VQ decoders, it is appropriate to consider the optimal decoding of VQ over a single-user frequency-selective Rayleigh fading channel first.

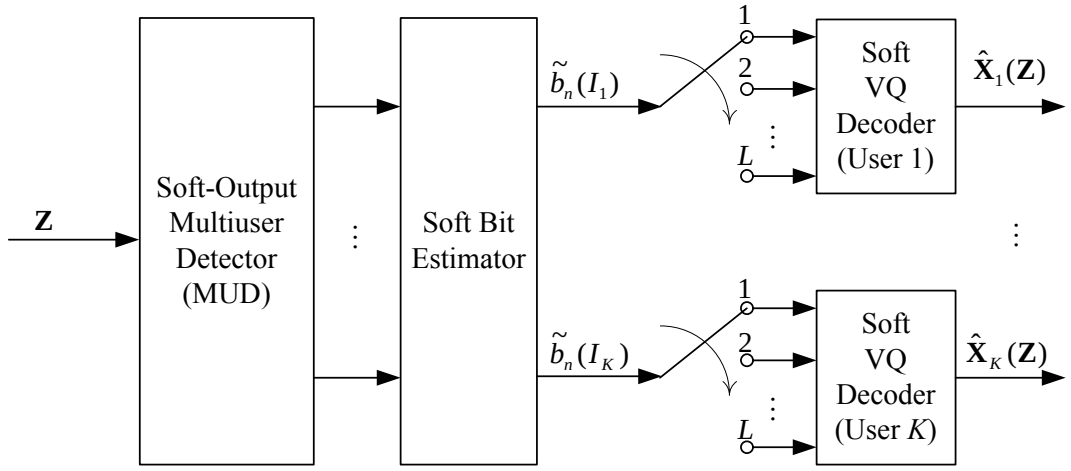

Figure 4.1 Structure of the suboptimal soft decoder [1, 2].

Without loss of generality, assume that only one user, namely user k, transmits a d-dimensional source vector $\mathbf{X}_k$ over a frequency-selective fading channel. Similar to (3.4), the discrete channel output is simply

$$\mathbf{z}_k(n) = \sqrt{E_k} b_n(I_k)\mathbf{a}_k(n) + \mathbf{u}_k(n), \qquad n = 1, 2 \ldots, L \tag{4.1}$$

where the noise $\mathbf{u}_k(n)$ is a complex Gaussian random vector of size P with zero-mean and covariance matrix equal to $\sigma^2\mathbf{R}_{kk}$. The optimal decoder that minimizes the mean-square error computes the following conditional expectation:

$$\hat{\mathbf{X}}_k(\mathbf{z}^{(k)}) = \sum_{i_k=0}^{N-1} \Pr(I_k = i_k | \mathbf{Z}^{(k)} = \mathbf{z}^{(k)}) \cdot \mathbf{c}_{i_k}^{(k)} \tag{4.2}$$

where $\mathbf{z}^{(k)}$ is the sample value of $\mathbf{Z}^{(k)} = [\mathbf{z}_k^\top(1), \mathbf{z}_k^\top(2), \ldots, \mathbf{z}_k^\top(L)]^\top$ and, recall that, $\mathbf{c}_{i_k}^{(k)}$ is the i_kth centroid of the kth user's codebook.

A detailed treatment of the above decoder based on Hadamard matrix and the related Hadamard transform is given in [7] for an AWGN channel. Such a decoder provides a description of the optimal decoding scheme in terms of the estimates of the individual bits of the transmitted index. The main operation of the Hadamard-based representation was summarized in Subsection 2.1.2 of Chapter 2. More specifically, the encoder centroids can be represented as

$$\mathbf{c}_{i_k}^{(k)} = \mathbf{T}\mathbf{h}_{i_k} \tag{4.3}$$

where $\mathbf{T}$ is the encoder's transform matrix and $\mathbf{h}_{i_k}$ is the i_kth column of an $N \times N$ Sylvester-type Hadamard matrix $\mathbf{H}$. Following the same derivations in [1, 2] and [7], it can be shown that Equation (4.2) can be computed as

$$\hat{\mathbf{X}}_k(\mathbf{z}^{(k)}) = \mathbf{T}\frac{\left(\sum_{i=0}^{N-1} P_i^{(k)}\mathbf{h}_{i_k}\mathbf{h}_{i_k}^{\top}\right)\cdot\hat{\mathbf{p}}(\mathbf{z}^{(k)})}{\left(\sum_{i=0}^{N-1} P_i^{(k)}\mathbf{h}_{i_k}\right)^{\top}\cdot\hat{\mathbf{p}}(\mathbf{z}^{(k)})} \tag{4.4}$$

where

$$\hat{\mathbf{p}}(\mathbf{z}^{(k)}) = [1, \tilde{b}_L(I_k)]^{\top} \otimes \cdots \otimes [1, \tilde{b}_1(I_k)]^{\top} \tag{4.5}$$

and the symbol $\otimes$ denotes Kronecker matrix product as defined in (2.23). The MMSE soft estimate $\tilde{b}_n(I_k)$ of the bit $b_n(I_k)$ is computed from the channel output in (4.1) as

$$\begin{aligned}\tilde{b}_n(I_k) &= E\left\{b_n(I_k)|\mathbf{z}_k(n); \Pr(b_n(I_k) = +1) = \frac{1}{2}\right\} \\ &= \tanh\left[\sigma^{-2}\sqrt{E_k}\breve{z}_k(n)\right]\end{aligned} \tag{4.6}$$

where $\breve{z}_k(n) = 2\Re\{\mathbf{a}_k^H(n)\mathbf{z}_k(n)\}$ is equivalent to the output of a RAKE receiver. Here RAKE receiver refers to a popular diversity combining technique. In essence, the RAKE receiver uses multi correlators to process several received signal arrived over multipaths. Each correlator in a RAKE receiver is called finger. The correlators' outputs are coherently combined to achieve improved reliability of the decision variable, hence improved performance. Since the action of the RAKE receiver is similar to that of a garden rake, hence the name and mnemonic of the receiver. Note that for the case of an AWGN channel, the corresponding statistic is shown in [1, 2] to be simply the first component of $\mathbf{z}_k(n)$. Observe that, in the case of a multipath fading channel, the statistic is extended to the "RAKE statistic", giving the extension of the AWGN result to multipath fading an intuitively satisfying interpretation.

In the suboptimal soft decoder proposed in [1, 2], it is observed that the optimal Hadamard-based soft VQ decoder for a single-user channel can also be employed for an individual user in a CDMA channel if the soft bit estimates can be generated from the soft-output MUD in Fig. 4.1. The soft bit estimates for a given MUD can be

defined as follows [1, 2]

$$\tilde{b}_n(I_k) = \sum_{b_n(I_k)\in\{\pm 1\}} b_n(I_k)\Pr(b_n(I_k)|\text{ MUD}). \tag{4.7}$$

Let $q = \Pr(b_n(I_k) = +1|\text{ MUD})$ in (4.7), then $\Pr(b_n(I_k) = -1|\text{ MUD}) = 1 - q$. Equation (4.7) is written as:

$$\begin{aligned}
\tilde{b}_n(I_k) &= q - (1-q) = \frac{q-(1-q)}{q+(1-q)} \\
&= \frac{\frac{q}{1-q}-1}{\frac{q}{1-q}+1} = \frac{\left[\frac{q}{1-q}\right]^{\frac{1}{2}} - \left[\frac{q}{1-q}\right]^{-\frac{1}{2}}}{\left[\frac{q}{1-q}\right]^{\frac{1}{2}} + \left[\frac{q}{1-q}\right]^{-\frac{1}{2}}} \\
&= \frac{e^{\frac{\frac{1}{2}\log\left[\frac{q}{1-q}\right]}{2}} - e^{\frac{-\frac{1}{2}\log\left[\frac{q}{1-q}\right]}{2}}}{e^{\frac{\frac{1}{2}\log\left[\frac{q}{1-q}\right]}{2}} + e^{\frac{-\frac{1}{2}\log\left[\frac{q}{1-q}\right]}{2}}} \\
&= \tanh\left(\frac{1}{2}\log\left[\frac{q}{1-q}\right]\right).
\end{aligned} \tag{4.8}$$

Moreover, the *a posteriori* log-likelihood ratio (LLR) of the bit $b_n(I_k)$ at the output of an MUD is defined as

$$\begin{aligned}
\lambda(b_n(I_k)) &\triangleq \log\frac{\Pr[b_n(I_k)=+1|\text{MUD}]}{\Pr[b_n(I_k)=-1|\text{MUD}]} \\
&= \log\left[\frac{q}{1-q}\right]
\end{aligned} \tag{4.9}$$

It then follows from (4.8) and (4.9) that the soft bit estimate $\tilde{b}_n(I_k)$ of the bit $b_n(I_k)$ can be computed from the LLR at the output of MUD as follows:

$$\tilde{b}_n(I_k) = \tanh\left[\frac{1}{2}\lambda(b_n(I_k))\right] \tag{4.10}$$

If the transmitted bits $b_n(I_k)$ are equally likely, the *a posteriori* LLR can be explicitly computed for each type of multiuser detection. The use of different types of MUD requires different levels of computational complexity for the suboptimal soft decoding scheme considered in this chapter. In what follows, the optimal multiuser detector (OPT-MUD), the minimum mean-square error multiuser detector (MMSE-MUD), and the decorrelating detector (DC-MUD) are analyzed in order to obtain the *a posteriori* LLR that is used to compute the soft bit estimates.

4.1 Suboptimal Soft Decoding with OPT-MUD

The soft-output MUD obtains the sufficient statistic from the bank of correlators and then provides the LLR for computing the soft bit estimates. Over the duration n, the received vector $\mathbf{z}(n)$ and its properties are presented in (3.6). The probability density function of $\mathbf{z}(n)$ is completely specified by the mean and the covariance matrix, and given by

$$f(\mathbf{z}(n)) = \frac{\exp\left\{-\sigma^{-2}\left[\mathbf{z}(n) - \mathbf{RWA}(n)\mathbf{b}(n)\right]^H \mathbf{R}^{-1}\left[\mathbf{z}(n) - \mathbf{RWA}(n)\mathbf{b}(n)\right]\right\}}{(\pi\sigma^2)^{KP}|\mathbf{R}|} \quad (4.11)$$

Substitute (4.11) into (4.9), the LLR can be computed for the optimal multiuser detector (OPT-MUD) with the assumption of equally likely transmitted bits $b_n(I_k)$ as follows:

$$\begin{aligned}
\lambda^{\mathrm{OPT}}[b_n(I_k)] &= \log\frac{\Pr[b_n(I_k)=+1|\mathbf{z}(n)]}{\Pr[b_n(I_k)=-1|\mathbf{z}(n)]} \\
&= \log\frac{\{f[\mathbf{z}(n)|b_n(I_k)=+1]f[b_n(I_k)=+1]\}/f[\mathbf{z}(n)]}{\{f[\mathbf{z}(n)|b_n(I_k)=-1]f[b_n(I_k)=-1]\}/f[\mathbf{z}(n)]} \\
&= \log\frac{f[\mathbf{z}(n)|b_n(I_k)=+1]}{f[\mathbf{z}(n)|b_n(I_k)=+1]} \\
&= \log\frac{\sum\limits_{\mathbf{b}(n)\in\mathcal{B}_k^+}\exp\left\{-\frac{1}{\sigma^2}[\mathbf{z}(n) - \mathbf{RWA}(n)\mathbf{b}(n)]^H \mathbf{R}^{-1}\left[\mathbf{z}(n) - \mathbf{RWA}(n)\mathbf{b}(n)\right]\right\}}{\sum\limits_{\mathbf{b}(n)\in\mathcal{B}_k^-}\exp\left\{-\frac{1}{\sigma^2}[\mathbf{z}(n) - \mathbf{RWA}(n)\mathbf{b}(n)]^H \mathbf{R}^{-1}\left[\mathbf{z}(n) - \mathbf{RWA}(n)\mathbf{b}(n)\right]\right\}}
\end{aligned} \quad (4.12)$$

where

$$\mathcal{B}_k^+ \triangleq \{(b_n(I_1),\ldots,b_n(I_{k-1}),+1,b_n(I_{k+1}),\ldots,b_n(I_K)) : b_n(I_j)\in\{\pm1\}, j\neq k\} \quad (4.13)$$

$$\mathcal{B}_k^- \triangleq \{(b_n(I_1),\ldots,b_n(I_{k-1}),-1,b_n(I_{k+1}),\ldots,b_n(I_K)) : b_n(I_j)\in\{\pm1\}, j\neq k\} \quad (4.14)$$

The soft bit estimates generated from the optimal MUD can be computed by substituting (4.12) into (4.10). The soft individual VQ encoders then use these soft bit estimates to make the decision for source vectors.

Simulation results provided in the next section show that the suboptimal soft decoder using the OPT-MUD has a good error performance that is very close to the

performance of the optimal decoder. However, it should be pointed out that with the use of the OPT-MUD, the complexity of the decoder is about $\mathcal{O}(KP \cdot 2^{KP})$, which is still exponential in number of users K. To further reduce the computational complexity of the suboptimal soft decoder using the OPT-MUD, the MMSE-MUD and the DC-MUD can be employed.

4.2 Suboptimal Soft Decoding with MMSE-MUD

Instead of employing the OPT-MUD, here the decoder uses the MMSE-MUD to compute the LLR for the soft bit estimator. In this suboptimal soft decoding, the soft MMSE-MUD applies the linear filter $\mathbf{m}_k^H(n)$ for the user k at time n to minimize the following mean-square error:

$$\mathrm{MSE}_k = E\left[\left\|b_n(I_k) - \mathbf{m}_k^H(n)\mathbf{z}(n)\right\|^2\right] \tag{4.15}$$

The MSE_k in the above equation is expanded as follows:

$$\begin{aligned}\mathrm{MSE}_k &= E\left[\left(b_n(I_k) - \mathbf{m}_k^H(n)\mathbf{z}(n)\right)\left(b_n(I_k) - \mathbf{m}_k^H(n)\mathbf{z}(n)\right)^H\right] \\ &= E\left[1 - b_n(I_k)\mathbf{m}_k^H(n)\mathbf{z}(n) - b_n(I_k)\mathbf{z}^H(n)\mathbf{m}_k(n) + \mathbf{m}_k^H(n)\mathbf{z}(n)\mathbf{z}^H(n)\mathbf{m}_k(n)\right]\end{aligned} \tag{4.16}$$

Substitute (3.6) into (4.16) and note that $E[\mathbf{u}(n)\mathbf{u}^H(n)] = \sigma^2\mathbf{R}$, $E[\mathbf{b}(n)\mathbf{b}^\top(n)] = \mathbf{I}$, and $E[\mathbf{u}(n)] = 0$, then MSE_k is given as

$$\begin{aligned}\mathrm{MSE}_k &= 1 - \mathbf{e}_k^\top\mathbf{A}^H(n)\mathbf{W}\mathbf{R}\mathbf{m}_k(n) - \mathbf{m}_k^H(n)\mathbf{R}\mathbf{W}\mathbf{A}(n)\mathbf{e}_k \\ &+ \mathbf{m}_k^H(n)\mathbf{R}\mathbf{W}\mathbf{A}(n)\mathbf{A}^H(n)\mathbf{W}\mathbf{R}\mathbf{m}_k(n) + \sigma^2\mathbf{m}_k^H(n)\mathbf{R}\mathbf{m}_k(n)\end{aligned} \tag{4.17}$$

where $\mathbf{e}_k$ is a K-vector of all zeros, except for the kth element, which is one. The mean-square error MSE_k is now a function of $\mathbf{m}_k(n)$. Therefore, the filter solution of $\mathbf{m}_k(n)$ is obtained by setting the derivative of MSE_k (with respect to $\mathbf{m}_k(n)$) to zero:

$$\frac{\partial \mathrm{MSE}_k}{\partial \mathbf{m}_k(n)} = 0 \tag{4.18}$$

Solving the above equation yields

$$\mathbf{m}_k^H(n) = \mathbf{e}_k^\top\mathbf{A}^H(n)\mathbf{W}\mathbf{R}\left[\mathbf{R}\mathbf{W}\mathbf{A}(n)\mathbf{A}^H(n)\mathbf{W}\mathbf{R} + \sigma^2\mathbf{R}\right]^{-1} \tag{4.19}$$

Now, the output of the MMSE-MUD corresponding to the kth user can be computed as follows:

$$\begin{aligned} u_n^{(k)} &= \mathbf{m}_k^H(n)\mathbf{z}(n) \\ &= \mathbf{e}_k^\top \mathbf{A}^H(n)\mathbf{W}\mathbf{R}\left[\mathbf{R}\mathbf{W}\mathbf{A}(n)\mathbf{A}^H(n)\mathbf{W}\mathbf{R} + \sigma^2\mathbf{R}\right]^{-1} \\ &\times \left[\mathbf{R}\mathbf{W}\mathbf{A}(n)\mathbf{b}(n) + \mathbf{u}(n)\right]. \end{aligned} \tag{4.20}$$

It is shown in [18] that the distribution of the residual interference-plus-noise at the output of the linear MMSE-MUD is well approximated by a Gaussian distribution. Thus, it can be assumed that the output $u_n^{(k)}$ in (4.20) represents the output of an equivalent AWGN channel as follows:

$$u_n^{(k)} = \mu_n^{(k)} b_n(I_k) + \eta_n^{(k)} \tag{4.21}$$

where $\mu_n^{(k)}$ is the equivalent amplitude of the kth user's signal and $\eta_n^{(k)}$ is a zero-mean complex Gaussian noise sample with variance $(\nu_n^{(k)})^2$. From (4.20) and (4.21), the parameters $\mu_n^{(k)}$ and $(\nu_n^{(k)})^2$ are given as follows:

$$\begin{aligned} \mu_n^{(k)} &= E\left\{b_n(I_k)u_n^{(k)}\right\} \\ &= \mathbf{e}_k^\top \mathbf{A}^H(n)\mathbf{W}\mathbf{R}\left(\mathbf{R}\mathbf{W}\mathbf{A}(n)\mathbf{A}^H(n)\mathbf{W}\mathbf{R} + \sigma^2\mathbf{R}\right)^{-1} \times \mathbf{R}\mathbf{W}\mathbf{A}(n)\mathbf{e}_k \end{aligned} \tag{4.22}$$

and

$$(\nu_n^{(k)})^2 = \mathrm{var}\{u_n^{(k)}\} = E\left\{\left(u_n^{(k)}\right)^2\right\} - \left(\mu_n^{(k)}\right)^2 \tag{4.23}$$

From (4.20), it follows that

$$\begin{aligned} E\left\{\left(u_n^{(k)}\right)^2\right\} &= E\left\{\left(u_n^{(k)}\right)\left(u_n^{(k)}\right)^H\right\} \\ &= \mathbf{e}_k^\top \mathbf{A}^H(n)\mathbf{W}\mathbf{R}\left[\mathbf{R}\mathbf{W}\mathbf{A}(n)\mathbf{A}^H(n)\mathbf{W}\mathbf{R} + \sigma^2\mathbf{R}\right]^{-1}\mathbf{R}\mathbf{W}\mathbf{A}(n)\mathbf{e}_k \\ &= \mu_n^{(k)} \end{aligned} \tag{4.24}$$

Substitute (4.24) into (4.23), the variance of $u_n^{(k)}$ can be expressed as

$$(\nu_n^{(k)})^2 = \mu_n^{(k)} - \left(\mu_n^{(k)}\right)^2 = \mu_n^{(k)}[1 - \mu_n^{(k)}]. \tag{4.25}$$

Note that, both $\mu_n^{(k)}$ and $\nu_n^{(k)}$ are real-valued quantities. The approximated Gaussian probability density function of the output $u_n^{(k)}$ is now written as

$$f(u_n^{(k)}) = \frac{1}{2\pi\nu_n^{(k)}} \exp\left\{ \frac{-\left\|u_n^{(k)} - b_n(I_k)\mu_n^{(k)}\right\|^2}{\left(\nu_n^{(k)}\right)^2} \right\} \tag{4.26}$$

Based on the above approximation for the PDF of $u_n^{(k)}$, the *a posteriori* LLR of the soft MMSE-MUD is given by

$$\begin{aligned} \lambda^{\text{MMSE}}[b_n(I_k)] &= \log \frac{f[u_n^{(k)}|b_n(I_k)=+1]}{f[u_n^{(k)}|b_n(I_k)=-1]} \\ &= -\frac{1}{\left(\nu_n^{(k)}\right)^2} \left\{ \left\|u_n^{(k)} - \mu_n^{(k)}\right\|^2 - \left\|u_n^{(k)} + \mu_n^{(k)}\right\|^2 \right\} \\ &= \frac{\mu_n^{(k)} \left[u_n^{(k)} + \left(u_n^{(k)}\right)^* \right]}{\mu_n^{(k)}[1-\mu_n^{(k)}]} \\ &= \frac{2\Re\{u_n^{(k)}\}}{1-\mu_n^{(k)}} \end{aligned} \tag{4.27}$$

Similarly to the OPT-MUD, the LLR computed from the MMSE-MUD in (4.27) is fed into the soft bit estimator. The computational complexity of the MMSE-MUD is about $\mathcal{O}(PL \cdot K^2)$ which is clearly much lower than that of the optimal decoder and the soft-decision decoder based on the soft OPT-MUD.

4.3 Suboptimal Soft Decoding with DC-MUD

As discussed in Subsection 2.2.2, for the soft DC-MUD, the sufficient statistic $\mathbf{z}(n)$ is multiplied with $\mathbf{R}^{-1}$ to give $\mathbf{v}(n) = \mathbf{R}^{-1}\mathbf{z}(n)$. That is

$$\begin{aligned} \mathbf{v}(n) &= \mathbf{R}^{-1}[\mathbf{RWA}(n)\mathbf{b}(n) + \mathbf{u}(n)] \\ &= \mathbf{WA}(n)\mathbf{b}(n) + \mathbf{R}^{-1}\mathbf{u}(n). \end{aligned} \tag{4.28}$$

The vector $\mathbf{v}(n)$ can also be represented as $\mathbf{v}(n) = [\mathbf{v}_1^\top(n), \ldots, \mathbf{v}_K^\top(n)]^\top$, where $\mathbf{v}_k(n)$ is the P-vector corresponding to the kth user and can be written as follows:

$$\mathbf{v}_k(n) = b_n(I_k)\sqrt{E_k}\mathbf{a}_k(n) + \tilde{\mathbf{u}}_k(n). \tag{4.29}$$

If the matrix $\mathbf{R}^{-1}$ of size $KP \times KP$ is partitioned into K^2 submatrices, each of size $P \times P$, as

$$\mathbf{R}^{-1} = \begin{bmatrix} \mathbf{R}_{11}^{+} & \dots & \mathbf{R}_{1K}^{+} \\ \vdots & \ddots & \vdots \\ \mathbf{R}_{K1}^{+} & \dots & \mathbf{R}_{KK}^{+} \end{bmatrix} \tag{4.30}$$

Then, $\tilde{\mathbf{u}}_k(n)$ in (4.29) is a complex Gaussian random vector of length P, with zero-mean and covariance matrix $\sigma^2\mathbf{R}_{kk}^{+}$. Given the channel fading amplitudes, the probability density function of $\mathbf{v}_k(n)$ is completely specified by the mean vector $b_n(I_k)\sqrt{E_k}$ $\mathbf{a}_k(n)$ and the covariance matrix $\sigma^2\mathbf{R}_{kk}^{+}$, written as

$$f(\mathbf{v}_k(n)) = \frac{\exp\left\{-\frac{1}{\sigma^2}[\mathbf{v}_k(n) - b_n(I_k)\sqrt{E_k}\mathbf{a}_k(n)]^H(\mathbf{R}_{kk}^{+})^{-1}[\mathbf{v}_k(n) - b_n(I_k)\sqrt{E_k}\mathbf{a}_k(n)]\right\}}{(\pi\sigma^2)^P|\mathbf{R}_{kk}^{+}|} \tag{4.31}$$

It then follows that the *a posteriori* LLR provided by the DC-MUD can be computed as:

$$\lambda^{\mathrm{DC}}[b_n(I_k)] = \log\frac{f[\mathbf{v}_k(n)|b_n(I_k) = +1]}{f[\mathbf{v}_k(n)|b_n(I_k) = -1]} \tag{4.32}$$

Equation (4.32) can be expressed using (4.31) as

$$\begin{aligned} \lambda^{\mathrm{DC}}[b_n(I_k)] &= \left\{-\frac{1}{\sigma^2}[\mathbf{v}_k(n) - \sqrt{E_k}\mathbf{a}_k(n)]^H(\mathbf{R}_{kk}^{+})^{-1}[\mathbf{v}_k(n) - \sqrt{E_k}\mathbf{a}_k(n)]\right\} \\ &- \left\{-\frac{1}{\sigma^2}[\mathbf{v}_k(n) + \sqrt{E_k}\mathbf{a}_k(n)]^H(\mathbf{R}_{kk}^{+})^{-1}[\mathbf{v}_k(n) + \sqrt{E_k}\mathbf{a}_k(n)]\right\} \\ &= \frac{4\sqrt{E_k}}{\sigma^2}\Re\left[\mathbf{a}_k^H(n)(\mathbf{R}_{kk}^{+})^{-1}\mathbf{v}_k(n)\right] \end{aligned} \tag{4.33}$$

The soft output of the DC-MUD from the above equation is passed to the soft bit estimator. The soft bit estimator in turn calculates the soft bits $\tilde{b}_n(I_k)$ of the transmitted bits $b_n(I_k)$ and then feeds them to the individual VQ decoders. Simulation results in Section 4.4 show that the suboptimal soft decoder using the DC-MUD as described above has a good performance at practical range of the channel signal-to-noise ratio (CSNR). More importantly, the complexity of the overall decoder is only about $\mathcal{O}(PL \cdot K^2)$.

4.4 Illustrative Simulation Results

First, the transmission of two images (for 2 users) over a frequency-selective Rayleigh fading CDMA channel is once again considered. The reconstructions of "Lena" and "Barbara" images are performed for the suboptimal soft decoding schemes in order to compare the performance between the hard and the soft decoders. All the system parameters used in simulations are the same as that specified in Section 3.3 for the simulations of hard-decoding schemes. The PSNRs of both users employing different types of MUD in the soft decoding scheme are tabulated in Table 4.1. Comparing the quality of reconstructed images shown in Figures 4.2 to 4.7 and those displayed in 3.11 to 3.16 clearly demonstrates that a better performance is achieved by the proposed soft-decoding schemes over their hard-decoding counterparts.

Table 4.1 PSNRs for the soft-decoding schemes at CSNR = 8 (dB).

	OPT-MUD		MMSE-MUD		DC-MUD	
	SNR	PSNR	SNR	PSNR	SNR	PSNR
User 1	10.92	25.45	8.67	23.20	5.56	20.09
User 2	9.89	23.28	7.96	21.35	5.87	19.25

To provide quantitative performance comparison between the hard-decision and soft-decision decoding schemes, simulations with synthetic data sources are considered next. Here the source of an individual user is modeled as a zero-mean, unit-variance, stationary and first order Gauss-Markov random process with correlation coefficient ϱ. Mathematically,

$$X_n = \varrho X_{n-1} + \zeta_n, \tag{4.34}$$

where $\{\zeta_n\}$ is an independent and identically distributed zero-mean Gaussian process with variance $1 - \varrho^2$. The performance of VQ decoders is measured by the output signal-to-noise ratio (SNR) versus the CSNR, i.e., E_b/N_0. Each curve represents for one decoder's performance over the specified range of channel quality. As usual, at low CSNR, all decoders perform poorly, because the background noise dominates the signal. On the contrary, the value of output SNR increases at higher CSNR, where

the channel has a better quality. The parameters of the VQ used in the simulations are $d = 3$ and $L = 3$. The VQ was trained for the Gauss-Markov source having $\varrho = 0.9$ in a noiseless channel. The codebook of the VQ is arranged with good index assignments based on the LISA-algorithm [13]. For this VQ the entropy is $H_k = 2.93$ (bits) and the highest achievable value of the SNR for this VQ is 9.35 (dB). The frequency-selective Rayleigh fading channel is simulated with three paths where the path delay between the two adjacent paths equals to the chip duration and the relative average amplitudes over the three paths are 0.52, 0.39 and 0.29 [8].

Figure 4.8 compares the performance of three different hard-decision decoders, while a similar comparison is shown in Fig. 4.9 for the corresponding suboptimal soft-decision decoding schemes. Also displayed in Figs. 4.8 and 4.9 is the performance of the optimal HMD to serve as the upper bound. Two common observations from these two figures are (i) The use of a more complicated MUD results in a better SNR performance, especially over the range of medium CSNR; and (ii) The performance of all the decoders (hard or soft) can asymptotically approach the highest achievable value of SNR at the high CSNR region (more than about 18 dB). More importantly, the superiority of a soft decoding scheme over its hard decoding counterpart is evident from these two figures, especially over the range of small CSNR. Finally, it can be seen from Fig. 4.9 that the SNR performances of the optimal HMD decoding and the soft decoder based on the OPT-MUD are indistinguishable.

Simulations for CDMA systems with a larger number of users are also carried out. Figures 4.10 and 4.11 show the performance of both hard and soft suboptimal decoders for a three-path Rayleigh fading CDMA systems with $K = 4$ and $K = 8$ users, respectively. For both systems, the VQ is trained with the same parameters as for the case of two-user system except that $L = 5$. The entropy of VQ in this case is $H_k = 4.92$ (bits) and the signal-to-distortion ratio, which is the highest achievable value of SNR, is 13.2 (dB). For the system with $K = 4$, four users employ random signature sequences of length 31. On the other hand, for the eight-user system, individual users are assigned Gold sequences of length 31 [23] in order to reduce the

cross-correlation. Table 4.2 tabulates random signature sequences and Gold sequences used in the simulations.

As can be predicted, the performance curves of the soft decoding schemes are always higher than that of the hard decoding schemes with the same type of MUD. The advantage of the proposed decoder with soft-output MUD and soft-VQ decoding over the table-lookup decoder can be clearly observed from figures 4.10 and 4.11 for each type of MUD, especially at low to medium CSNR [2]. Such performance improvement is obtained with no extra computational complexity. Another observation is that there seems to be a little performance improvement by the user of MMSE-MUD over DC-MUD when the number of user is small. This is due to the fact that the level of multiple-access-interference (MAI) is small and the two MMSE-MUD and DC-MUD perform fairly close in this case. The advantage of using MMSE-MUD over DC-MUD becomes more evident when a system with a larger number of users, $K = 8$, (i.e., a higher level of MAI) is shown in Fig. 4.11.

Table 4.2 Signature sequences used in simulations.

$K = 4$ (Random sequences)	s_1	1 1 1 0 1 0 1 0 1 0 1 0 1 1 1 1 1 1 0 1 1 1 0 0 1 1 0 1 1 0 0
	s_2	0 0 0 0 1 1 0 0 1 0 1 0 0 1 0 1 0 1 0 1 0 0 0 1 1 1 1 1 0 1 1
	s_3	1 0 1 0 1 0 1 0 1 0 1 0 1 0 1 0 1 1 1 1 1 1 1 1 1 1 0 1 0 0 1 0
	s_4	0 0 0 1 1 1 1 0 1 0 1 0 1 0 1 0 1 0 1 0 1 0 1 0 1 0 1 1 1 1 1
$K = 8$ (Gold sequences)	s_1	0 0 0 0 1 0 0 1 0 1 1 0 0 1 1 1 1 1 0 0 0 1 1 0 1 1 1 0 1 0 1
	s_2	0 1 0 0 0 1 0 0 1 0 1 0 1 1 0 0 0 0 1 1 1 0 0 1 1 0 1 1 1 1 1
	s_3	1 0 1 0 1 0 1 1 0 0 1 1 0 0 0 1 1 1 0 1 1 0 1 0 0 0 1 1 0 1 0
	s_4	1 1 0 1 1 0 0 0 0 1 0 0 1 1 0 0 1 1 0 0 1 0 0 0 1 0 0 0 0 0 1 0
	s_5	1 1 1 0 0 0 0 1 1 1 1 1 0 0 1 0 0 1 0 0 0 0 0 1 1 1 0 1 1 1 0
	s_6	1 1 1 1 1 1 0 1 0 0 1 0 1 1 0 1 0 0 0 0 0 1 0 1 0 1 1 1 0 0 0
	s_7	1 1 1 1 0 0 1 1 0 1 0 0 0 0 1 0 1 0 1 0 0 1 1 1 0 0 1 0 0 1 1
	s_8	0 1 1 1 0 1 0 0 0 1 1 1 0 1 0 1 0 1 1 1 0 1 1 0 0 0 0 0 1 1 0

Figure 4.2 Reconstructed image of "Lena" using the suboptimal soft decoder with OPT-MUD.

Figure 4.3 Reconstructed image of "Barbara" using the suboptimal soft decoder with OPT-MUD.

Figure 4.4 Reconstructed image of "Lena" using the suboptimal soft decoder with MMSE-MUD.

Figure 4.5 Reconstructed image of "Barbara" using the suboptimal soft decoder with MMSE-MUD.

Figure 4.6 Reconstructed image of "Lena" using the suboptimal soft decoder with DC-MUD.

Figure 4.7 Reconstructed image of "Barbara" using the suboptimal soft decoder with DC-MUD.

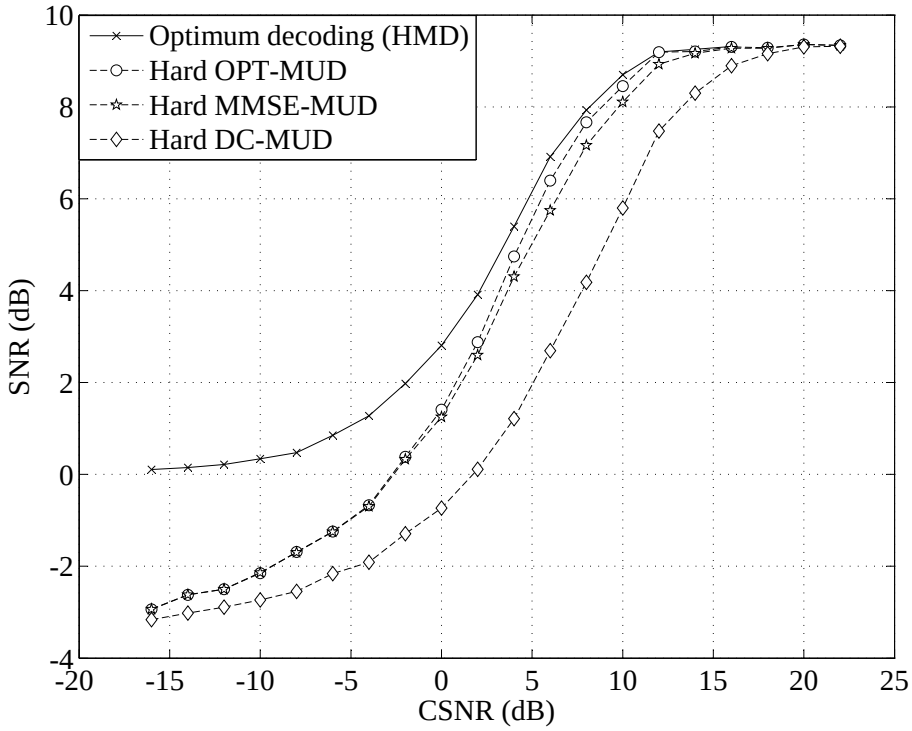

Figure 4.8 Performance comparison of different hard decoding schemes over a 3-path Rayleigh fading CDMA system with two users.

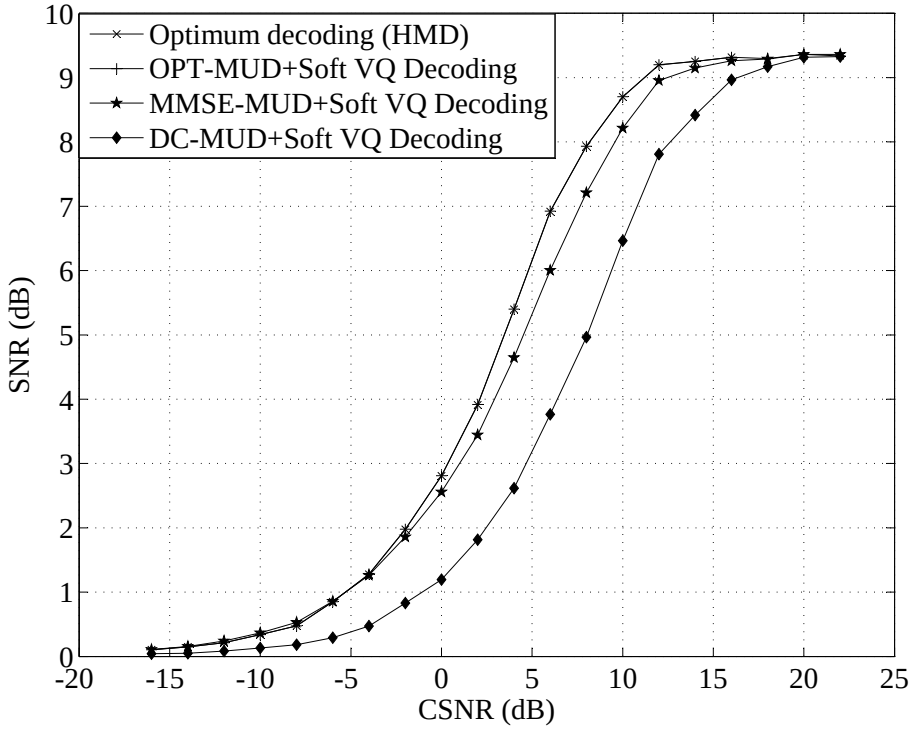

Figure 4.9 Performance comparison of different soft decoding schemes over a 3-path Rayleigh fading CDMA system with two users.

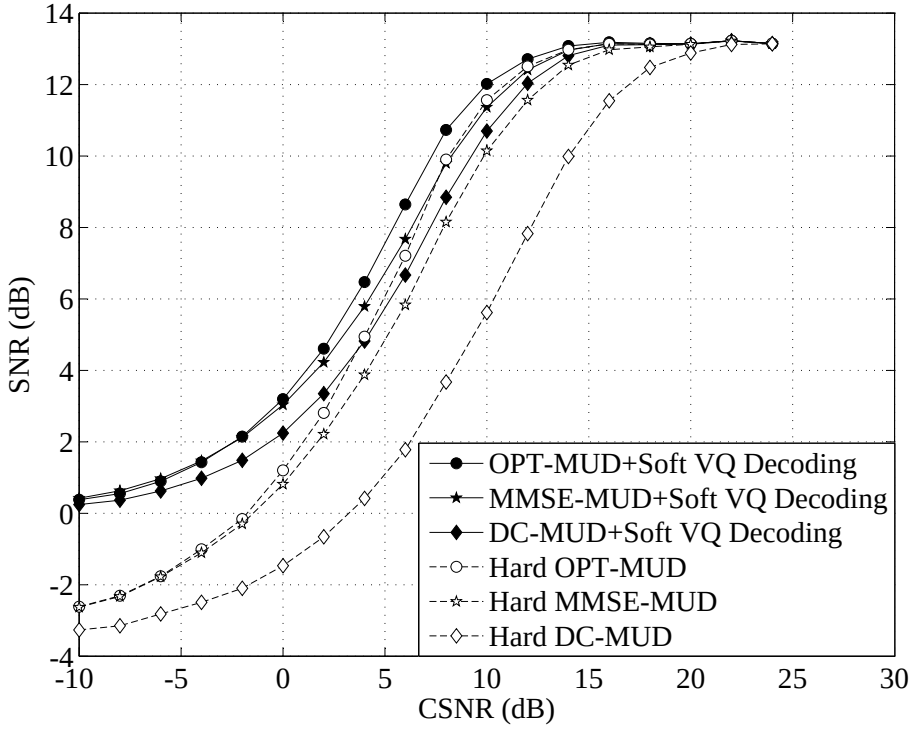

Figure 4.10 Performance comparison of different decoding schemes over a 3-path Rayleigh fading CDMA system with four users.

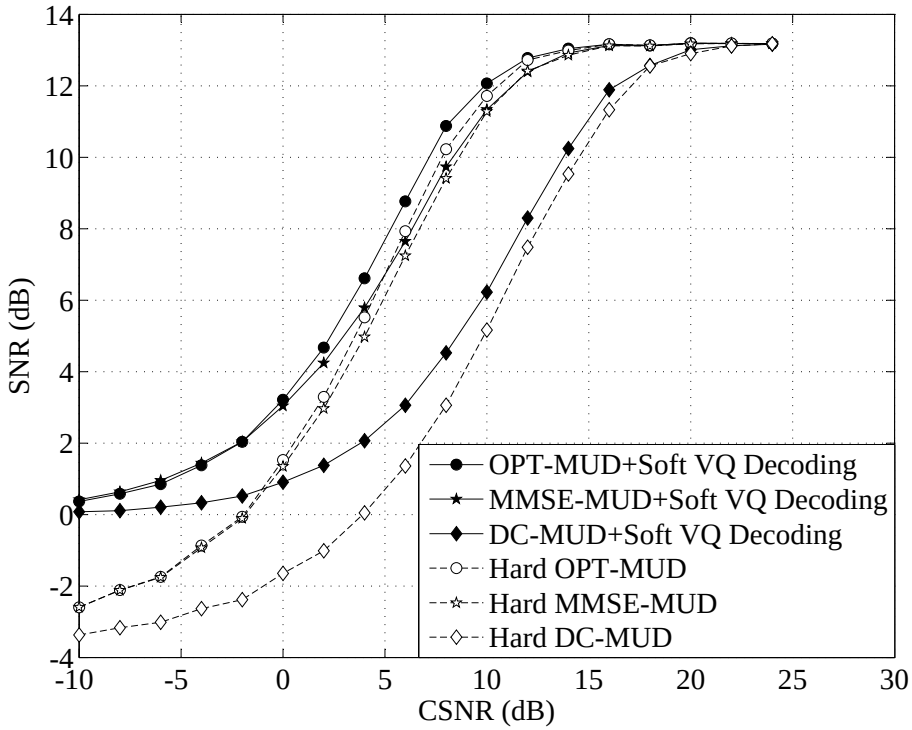

Figure 4.11 Performance comparison of different decoding schemes over a 3-path Rayleigh fading CDMA system with eight users.

4.5 Suboptimal Decoders Based on Modifications of The Optimal Multiuser Detector

The previous section presented various suboptimal decoding schemes for VQ transmitted over a frequency-selective Rayleigh fading CDMA channel. In essence, these schemes were obtained by appropriately modifying the well-known suboptimal multiuser detectors so that they can be combined with the optimal VQ decoders of individual users.

This section introduces another suboptimal decoding scheme which is resulted from a direct modification of the optimal multiuser detector. The main motivation for this suboptimal decoding is described next.

It can be seen from (4.12) that there is a summation taken over all vertices of a hypercube $\{\pm 1\}^K$ (that is, there are 2^K terms) for the suboptimal soft decoding scheme with the OPT-MUD. Since many terms of the sums in (4.12) will not contribute significantly to the result, especially at a high channel signal to noise ratio (CSNR) [7], it suggests that one can limit the summation to a subset of $\{\pm 1\}^K$ in order to reduce the computational complexity. There are a number of ways to choose this subset. This section introduces two methods to find the suitable subsets, which are based on distance measure and reliability processing.

4.5.1 The Algorithm Based on Distance Measure

As mentioned above, one is interested in reducing the number of terms in the summation in (4.12). The obvious question is how to identify a suitable subset of the vertices of a hypercube to include in the summations. Here, a suitable subset can be found based on the hard decision $\mathbf{b}^{hard}(n)$ of the transmitted information bit vector $\mathbf{b}(n)$ and its "neighbors". Such a decoder first makes the hard-bit decision and then searches the α nearest neighbors based on the smallest distances to the hard decision $\mathbf{b}^{hard}(n)$. The summation subset is then taken to include α (a positive integer less than 2^K) vectors with the nearest distances to $\mathbf{b}^{hard}(n)$. The employed

distance measure between $\mathbf{b}(n)$ and $\mathbf{b}^{hard}(n)$ is

$$l[\mathbf{b}(n), \mathbf{b}^{hard}(n)] = \|\mathbf{R}^{1/2}\mathbf{W}\mathbf{A}(n)(\mathbf{b}(n) - \mathbf{b}^{hard}(n))\|. \tag{4.35}$$

Hence, the vertices to include in the summations in (4.12), for each possible value of $\mathbf{b}^{hard}(n)$, can be computed in advance and stored. For simplicity, the suboptimal decoder with OPT-MUD, computed with α nearest neighbors, is referred to as the α-suboptimal decoder. A similar decoder is considered in [7] and [2] for AWGN and flat (single-path) Rayleigh fading channels, respectively.

4.5.2 The Algorithm Based on Reliability Processing

Instead of distance measure, an alternative algorithm to find the suitable subset based on reliability processing is investigated in this subsection. Here, the hard decision $\mathbf{b}^{hard}(n)$ is first made by using any low-comlexity linear operator, $\mathbf{L}_{K\times K}$, as follows:

$$\mathbf{b}^{hard}(n) = \text{sgn}(\mathbf{L}\mathbf{z}(n)). \tag{4.36}$$

Then, an algorithm is applied to search the subset based on the reliability measure of the initial (hard) decision.

Obviously, the performance of such an algorithm depends heavily on the reliability measurement. Here define for each hard-bit decision $\hat{b}_n(I_k)$ the corresponding soft-output $\tilde{\gamma}_k$ as follows:

$$\tilde{\gamma}_k = \mathbf{l}_k^\top \mathbf{z}(n), \qquad k = 1, 2, \ldots, K \tag{4.37}$$

where $\mathbf{l}_k^\top$ is the kth row of matrix $\mathbf{L}$. Then, the *reliability value* γ_k of the hard-bit decision $\hat{b}_n(I_k)$ is defined as the log-likelihood ratio:

$$\gamma_k \triangleq \frac{1}{2} \ln \frac{f(\tilde{\gamma}_k | b_n(I_k) = \hat{b}_n(I_k))}{f(\tilde{\gamma}_k | b_n(I_k) = -\hat{b}_n(I_k))} \tag{4.38}$$

where $f(\tilde{\gamma}_k | b_n(I_k))$ denotes the probability density function of $\tilde{\gamma}_k$ conditioned on the transmitted bit $b_n(I_k)$. For all the K users, the generated reliability vector is $\boldsymbol{\gamma} = [\gamma_1, \ldots, \gamma_K]^\top$.

Over the nth symbol duration, the detector makes the hard decision $\mathbf{b}^{hard}(n)$ for the transmitted bit sequence $\mathbf{b}(n)$. Note that, the best decision is $\hat{\mathbf{b}}_{ML}(n)$. It is expected that $\mathbf{b}^{hard}(n)$ may produce the ML decision $\hat{\mathbf{b}}_{ML}(n)$. With this motivation, a sequence of error patterns is generated as $\mathbf{e}^{(d)} \in \{0,1\}^K$, $d = 1, 2, \ldots, 2^K$, where $e_k^{(d)} = 1$ indicates an error at the bit position k. The error sequence $\mathbf{e}^{(d)}$ is applied on the vector $\mathbf{b}^{hard}(n)$ to create the bit vector $\hat{\mathbf{b}}^{(d)}$ as follows:

$$\hat{\mathbf{b}}^{(d)} = [\hat{b}_1^{(d)}, \hat{b}_2^{(d)}, \ldots, \hat{b}_K^{(d)}]^\top : \hat{b}_k^{(d)} = \hat{b}_n(I_k) \oplus e_k^{(d)}, \quad k = 1, \ldots, K \tag{4.39}$$

where $\oplus$ denotes modulo-2 addition. Naturally, the error sequence generation criterion will be the likelihood of $\hat{\mathbf{b}}(n) = \mathbf{b}^{hard}(n) \oplus \mathbf{e}^{(d)}$ based on the observation of the soft-output vector $\tilde{\boldsymbol{\gamma}}$, and its conditional density distribution $f(\tilde{\boldsymbol{\gamma}}|\mathbf{b}(n) = \hat{\mathbf{b}}(n))$. Assume that the soft-output $\tilde{\gamma}_k$ are conditionally independent random variables, then the likelihood function becomes $\prod_{k=1}^K f(\tilde{\gamma}_k|b_n(I_k) = \hat{b}_k)$ and the log-likelihood ratio (LLR) is

$$\begin{aligned}
\Lambda[\hat{\mathbf{b}}(n)] &= \frac{1}{2}\sum_{k=1}^{K} \ln \frac{f(\tilde{\gamma}_k|b_n(I_k) = \hat{b}_k)}{f(\tilde{\gamma}_k|b_n(I_k) = -\hat{b}_k)} \\
&= \frac{1}{2}\sum_{\substack{k=1 \\ \hat{b}_k = \hat{b}_n(I_k)}}^{K} \ln \frac{f(\tilde{\gamma}_k|b_n(I_k) = \hat{b}_k)}{f(\tilde{\gamma}_k|b_n(I_k) = -\hat{b}_k)} + \frac{1}{2}\sum_{\substack{k=1 \\ \hat{b}_k \neq \hat{b}_n(I_k)}}^{K} \ln \frac{f(\tilde{\gamma}_k|b_n(I_k) = \hat{b}_k)}{f(\tilde{\gamma}_k|b_n(I_k) = -\hat{b}_k)} \\
&= \frac{1}{2}\sum_{\substack{k=1 \\ \hat{b}_k = \hat{b}_n(I_k)}}^{K} \ln \frac{f(\tilde{\gamma}_k|b_n(I_k) = \hat{b}_n(I_k))}{f(\tilde{\gamma}_k|b_n(I_k) = -\hat{b}_n(I_k))} + \frac{1}{2}\sum_{\substack{k=1 \\ \hat{b}_k \neq \hat{b}_n(I_k)}}^{K} \ln \frac{f(\tilde{\gamma}_k|b_n(I_k) = -\hat{b}_n(I_k)}{f(\tilde{\gamma}_k|b_n(I_k) = \hat{b}_n(I_k))} \\
&= \frac{1}{2}\sum_{\substack{k=1 \\ \hat{b}_k = \hat{b}_n(I_k)}}^{K} \ln \frac{f(\tilde{\gamma}_k|b_n(I_k) = \hat{b}_n(I_k))}{f(\tilde{\gamma}_k|b_n(I_k) = -\hat{b}_n(I_k))} - \frac{1}{2}\sum_{\substack{k=1 \\ \hat{b}_k \neq \hat{b}_n(I_k)}}^{K} \ln \frac{f(\tilde{\gamma}_k|b_n(I_k) = \hat{b}_n(I_k)}{f(\tilde{\gamma}_k|b_n(I_k) = -\hat{b}_n(I_k))}
\end{aligned} \tag{4.40}$$

Substitute (4.38) into (4.40), the LLR is computed as

$$\begin{aligned}
\Lambda[\hat{\mathbf{b}}(n)] &= \sum_{k:\hat{b}_k=\hat{b}_n(I_k)}^{K} \gamma_k - \sum_{k:\hat{b}_k\neq\hat{b}_n(I_k)}^{K} \gamma_k \\
&= \sum_{k=1}^{K}\gamma_k - \sum_{k:\hat{b}_k\neq\hat{b}_n(I_k)}^{K} \gamma_k - \sum_{k:\hat{b}_k\neq\hat{b}_n(I_k)}^{K} \gamma_k \\
&= \sum_{k=1}^{K}\gamma_k - 2\sum_{k:\hat{b}_k\neq\hat{b}_n(I_k)}^{K} \gamma_k \\
&= \sum_{k=1}^{K}\gamma_k - 2\sum_{k:e_k=1}^{K} \gamma_k
\end{aligned} \tag{4.41}$$

Denote the second term of (4.41) as $\sum_{k:e_k=1}^{K}\gamma_k = \phi(\mathbf{e},\boldsymbol{\gamma})$. Note that, this is the only quantity of LLR effected by the choice of the error pattern $\mathbf{e}$. For our purpose of finding the subset to reduce the complexity, arrange all 2^K error patterns $\{\mathbf{e}^{(d)}\}_{k=1}^{2^K}$ in the ascending order under the following key

$$\phi(\mathbf{e}^{(d)},\boldsymbol{\gamma}) \leq \phi(\mathbf{e}^{(d+1)},\boldsymbol{\gamma}), \quad d = 1, 2, \ldots, 2^K - 1. \tag{4.42}$$

By keeping only the first β error sequences, where β is a positive integer, then the subset of β vectors is created as follows:

$$\{\hat{\mathbf{b}}^{(d)}(n)\}_{d=1}^{\beta} : \hat{\mathbf{b}}^{(d)}(n) = \mathbf{b}^{hard}(n) \oplus \mathbf{e}^{(d)} \tag{4.43}$$

With this subset, it is guaranteed that the summation in (4.12) is taken over the set of β vectors $\{\hat{\mathbf{b}}^{(d)}(n)\}_{d=1}^{\beta}$ with the biggest LLR, given $\boldsymbol{\gamma}$ at any time n.

The authors in [9] investigated an algorithm that creates the error patterns $\mathbf{e}$ given the observation $\boldsymbol{\gamma}$ under the key (4.42). However, such an algorithm must provide $\mathbf{e}$ and calculate $\phi(\cdot,\boldsymbol{\gamma})$ for every $\mathbf{e}^{(d)} \in \{\mathbf{e}^{(d)}\}_{d=1}^{\beta}$ at any bit duration n. It is recognized that the ordered error patterns under the key (4.42) are unique for all the vectors $\boldsymbol{\gamma}_s$ whose elements are also in ascending order $\gamma_1 \leq \gamma_2 \leq \ldots \leq \gamma_K$. Thus, an alternative algorithm proposed here is to obtain the subset of β vectors $\hat{\mathbf{b}}(n)$ in which the ordered sequences of β error patterns are computed only one time for all the ascending ordered vectors $\boldsymbol{\gamma}_s$. However, the subset of β elements coincides in

the ascending order of vectors $\boldsymbol{\gamma}_s$ rather than the reliability vector $\boldsymbol{\gamma}$ of $\mathbf{b}^{hard}(n)$. Therefore, the positions of bits in vector $\mathbf{b}^{hard}(n)$ are changed into $\mathbf{b}_s^{hard}(n)$ according to the index $\mathbb{I}_s$ of $\boldsymbol{\gamma}_s$'s elements so that the ordered error vectors in $\{\mathbf{e}^{(d)}\}_{d=1}^{\beta}$ can be applied on $\mathbf{b}_s^{hard}(n)$. The positions of the elements of $\mathbf{b}_s^{hard}(n)$ are finally inter-changed back to the index $\mathbb{I}$ of $\mathbf{b}^{hard}(n)$ to obtain $\hat{\mathbf{b}}^{(d)}(n)$. The set of β vectors $\{\hat{\mathbf{b}}^{(d)}(n)\}_{d=1}^{\beta}$ is the expected subset.

Starting with $\mathbf{b}^{hard}(n)$ and $\boldsymbol{\gamma}$, the outcome of the algorithm gives the set of $\{\hat{\mathbf{b}}^{(d)}(n) = \mathbf{b}^{hard}(n) \oplus \mathbf{e}^{(d)}\}_{d=1}^{\beta}$ such that $\mathbf{e}$ satisfies the key (4.42). To summarize, the detailed steps of this algorithm are presented in Appendix B.

For simplicity, the suboptimal decoder with OPT-MUD using the algorithm based on reliability processing, approximated with β vectors in the sum, is named as the β-suboptimal decoder.

4.5.3 Simulation, Results and Comparison

The two algorithms are applied for both hard and soft suboptimal decoders to reduce the computational complexity of the summations from 2^K down to a positive integer number. Simulations are run for systems that are the same as the ones in Subsection 4.4, with $K = 2, 4$ users, respectively. These two algorithms are applied for both hard and soft suboptimal decoders and the integer numbers (α, β) used for two algorithms are equal to the number of users K. For the system with $K = 2$, Figures 4.12 and 4.13 show the performance curves of the suboptimal decoders employing the two algorithms for both hard and soft decoding, respectively. Also illustrated in these two figures are the performances of the suboptimal decoders with the OPT-MUD (soft-ML), the DC-MUD and the MMSE-MUD. It is observed that the decoders with MMSE-MUD and DC-MUD perform worse than the ones using either of the two algorithms over the practical range of CSNR. Moreover, the decoders with β-algorithm performs lightly better than the ones with α-algorithm. The performance gap between the β-algorithm and the α-algorithm is at most 0.5 (dB).

Figures 4.12 and 4.13 also show that both the α-algorithm and β-algorithm cannot

approach the suboptimal decoder with the OPT-MUD at low CSNR. This is expected because both algorithms cannot pick up the suitable subsets in computing (4.12).

Similar comparisons are shown in Figures 4.14 and 4.15 for system with a larger number of users, namely $K = 4$. Observe from these two figures that the α-algorithm slightly outperforms the β-algorithm for this larger system. It should be pointed out, however, that the α-algorithm must find and store all the possible subsets of α vectors which can be excessive. The β-algorithm, on the other hand, finds the suitable subset directly from the received signal.

To summarize, at the same complexity as the decoders using either the MMSE-MUD or the DC-MUD, both α-algorithm and β-algorithm can perform very close to that of the decoder with the OPT-MUD. The use of these two algorithms offers other alternatives to the suboptimal decoding schemes in the effort of achieving complexity reduction. Basically, the computational complexities of the decoding scheme with these two algorithms increase linearly with α or β. Although the gaps between the performance curves of different decoders with and without the complexity-reduced algorithm are small over the practical range of channel signal-to-noise ratio (CSNR), the use of these two algorithms provides a complexity-controllable scheme for the decoder by simply changing the value of the parameters α and β.

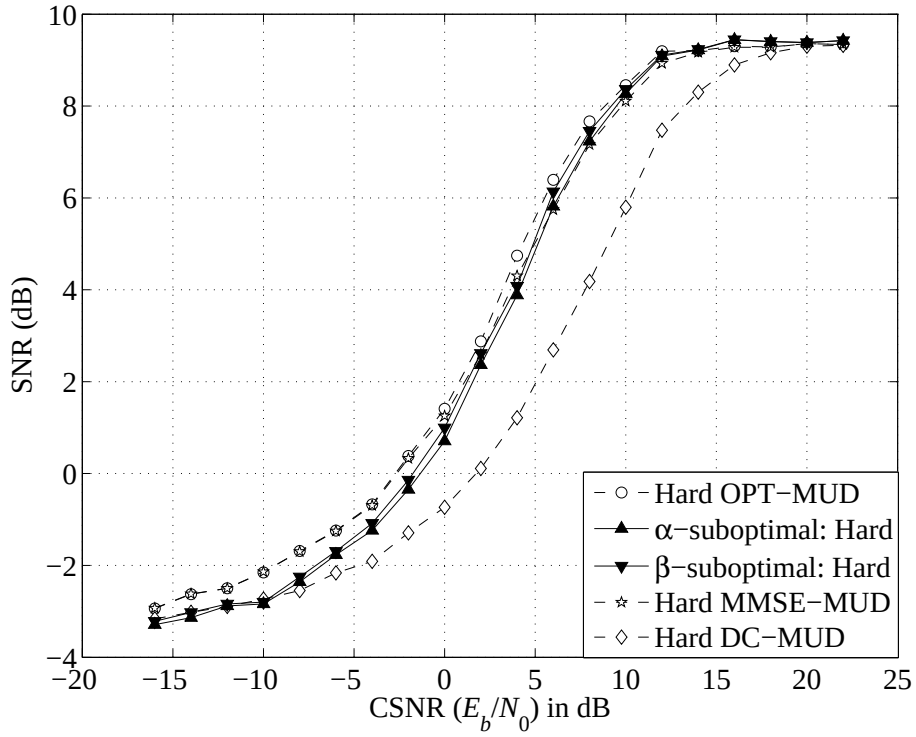

Figure 4.12 Hard decoders for the system with 2 users using random sequences of length 7, α=β=2.

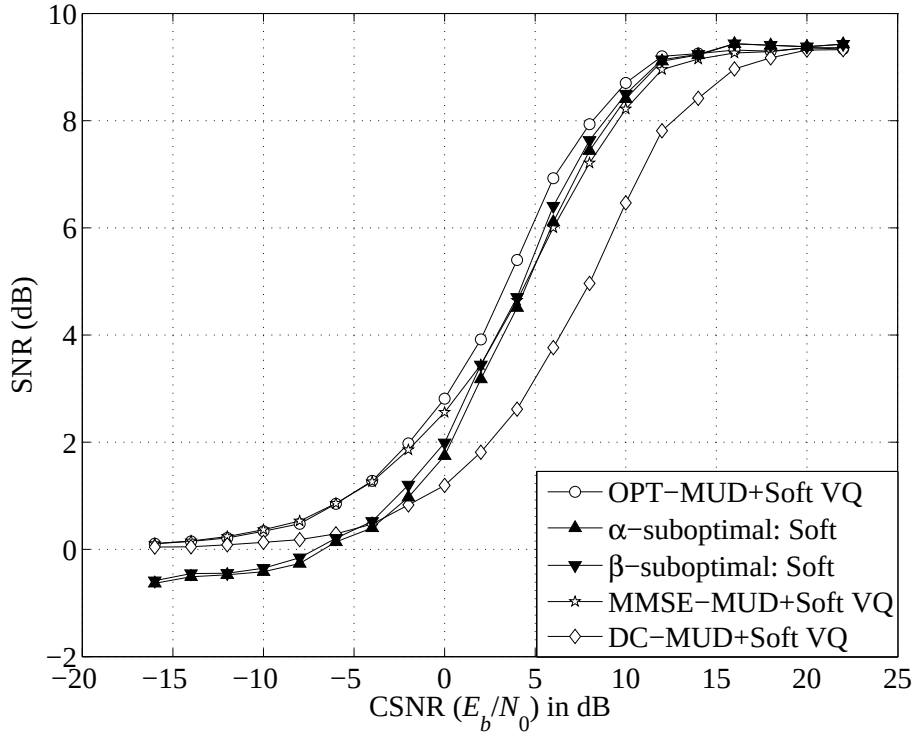

Figure 4.13 Soft decoders for the system with 2 users using random sequences of length 7, α=β=2.

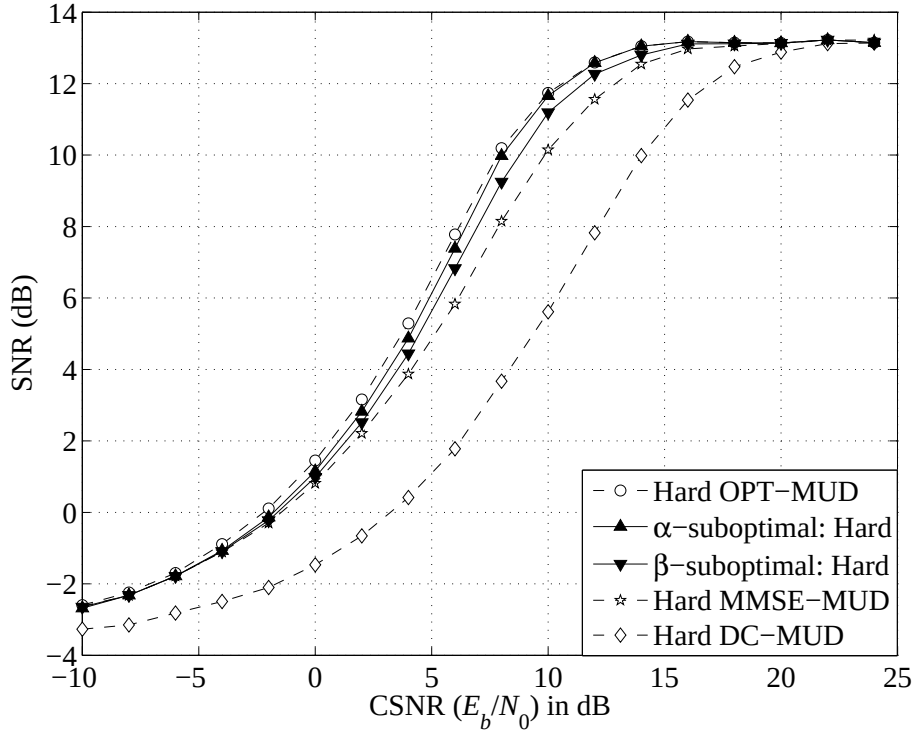

Figure 4.14 Hard decoders for the system with 4 users using random sequences of length 31, α=β=4.

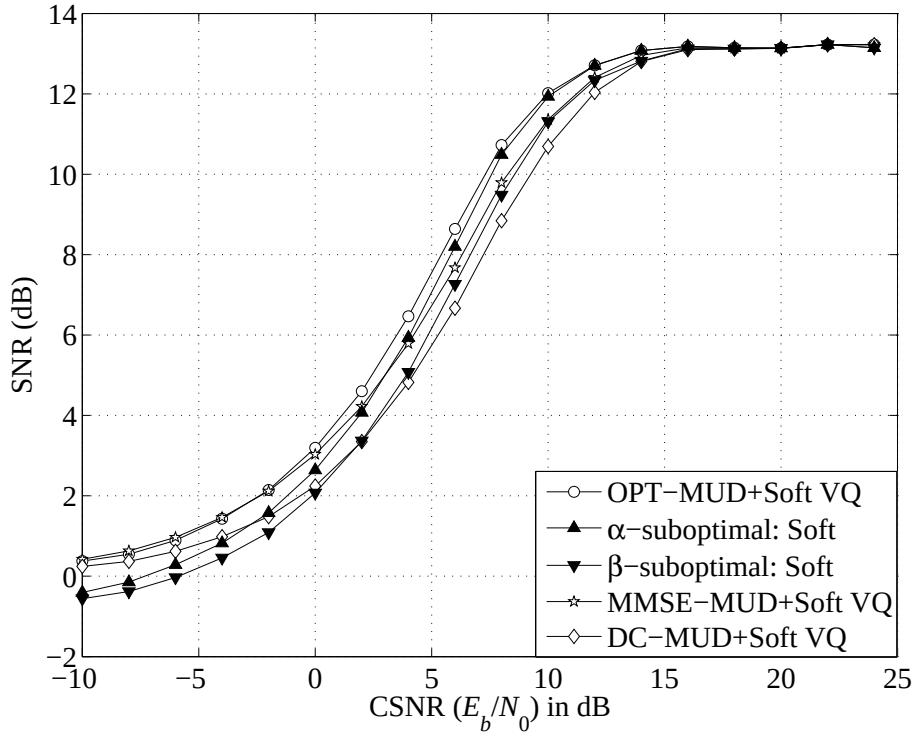

Figure 4.15 Soft decoders for the system with 4 users using random sequences of length 31, α=β=4.

5. Extensions to Systems with M-PAM Constellations

Chapter 4 considered the transmission of VQ over a frequency-selective Rayleigh fading CDMA channel. However, the system was designed only for BPSK modulation. With BPSK, the signal constellation has only two signal points. If one wants to have a better bandwidth efficiency, one must use a higher-order signal constellation. This generally makes the error performance of the system poorer because the minimum Euclidean distance between signal points in a more crowded constellation decreases for the same average energy. This chapter extends the results of the proposed decoders to systems employing M-ary pulse amplitude modulation (M-PAM) constellations. The extension is necessary to offer a flexible trade-off between complexity, spectral efficiency and performance of the system.

5.1 System Model

The system model considered in this chapter is similar to the one in Section 3.1. The only difference between these two systems at the transmitter is in the modulation scheme. The d-dimensional source vectors from K users are encoded and then transmitted over a frequency-selective Rayleigh fading CDMA channel by means of M-PAM.

Let $\{A_m = (2m - 1 - M)\frac{\Delta}{2}, 1 \leq m \leq M\}$ be the set of M possible amplitudes used to carry one of $M = 2^Q$ possible Q-bit blocks (or symbols). The value of Δ is set at $\sqrt{\frac{12}{M^2-1}}$ in order to normalize the average symbol energy to be unity, i.e., $E_s = \frac{1}{M}\sum_{m=1}^{M} A_m^2 = 1$. For the kth user, at any symbol duration n, the binary sequence of Q bits, $[b_1(I_k), \ldots, b_j(I_k), \ldots, b_Q(I_k)]$, is mapped to a symbol $p_k(n)$, taking a value from the set $\{A_m\}_{m=1}^{M}$. These symbols $p_k(n)$ are transmitted over a frequency-

selective Rayleigh fading DS-CDMA channel. The transmitter in the system under consideration is modified from the one in Subsection 3.1 and shown in Fig. 5.1.

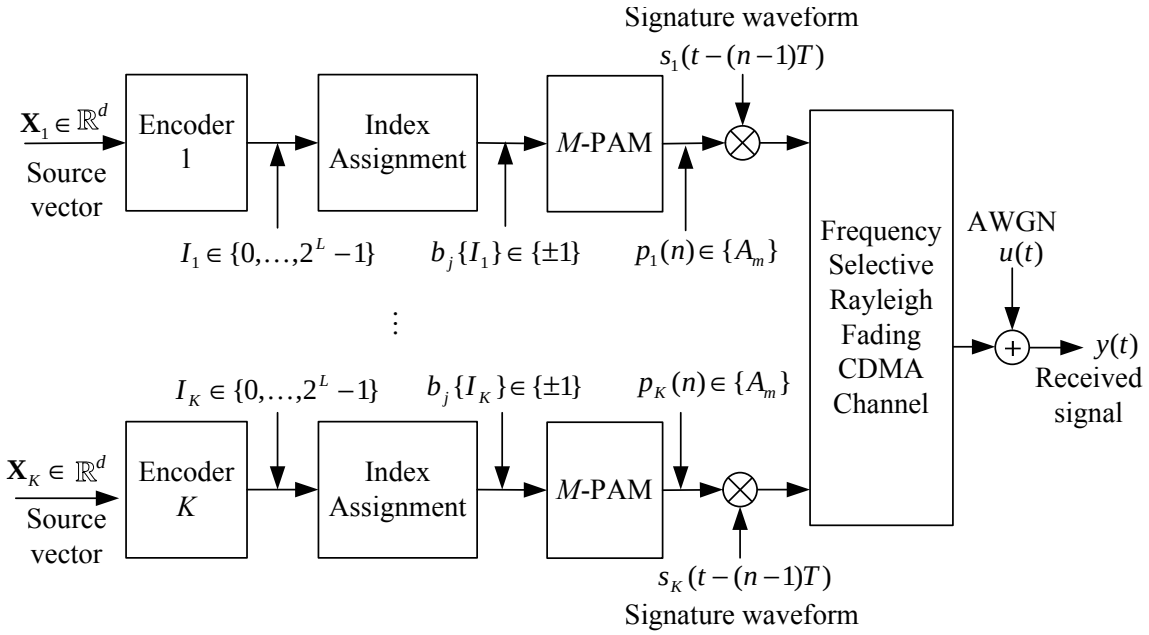

Figure 5.1 Structure of the transmitter with M-PAM.

Similarly to (3.1), the received signal component corresponding to user k in this system is given by:

$$y_k(t) \;=\; \sqrt{E_k}p_k(n)\mathbf{s}_k^\top(t-(n-1)T)\mathbf{a}_k(n), \qquad 0 \le t \le T \tag{5.1}$$

The received signal waveform $y(t)$, resulting from the transmitted signals of all the K users, is $y(t) = \sum_{k=1}^{K} y_k(t) + u(t)$. It should be pointed out that the noise $u(t)$ is the same as the one in (3.2), and instead of the transmitted bit $b_n(I_k)$, the symbol $p_k(n)$ is expressed in (5.1).

Moreover, the sufficient statistic vector $\mathbf{z}(n)$, whose components are computed from correlating the received signal waveform $y(t)$ with the delayed replicas of the signature waveforms, can be written as:

$$\mathbf{z}(n) = \mathbf{RWA}(n)\mathbf{p}(n) + \mathbf{u}(n) \tag{5.2}$$

where the vector $\mathbf{p}(n) = [p_1(n), \ldots, p_K(n)]^\top$ contains the transmitted symbols of all users at time n and all the other matrices in (5.2) are identical to the ones in (3.6).

The decoder has to make the decision for the source vectors of all the K users based on the sufficient statistic $\{\mathbf{z}(n)\}$. Similar to the case of BPSK, different processing algorithms on $\{\mathbf{z}(n)\}$ (i.e., different decoders) are discussed next.

5.2 The Suboptimal Hard Decoders

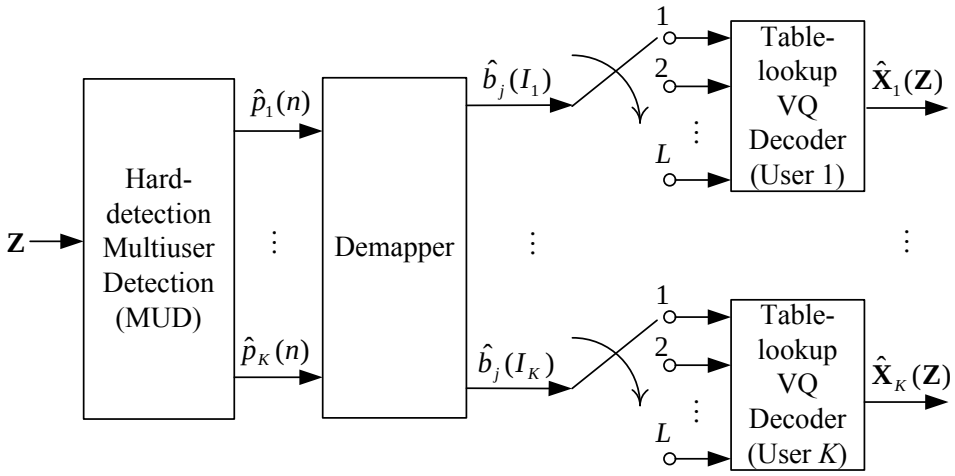

Figure 5.2 Model of the decoder based on table-lookup.

Fig. 5.2 shows the structure of the decoding approach based on a combination of separate multiuser detection (MUD) and table-lookup (or hard) VQ decoding. The sumbol $\hat{p}_k(n)$ is the hard decision made by the MUD for user k at time n. Let $\hat{\mathbf{p}}(n) = [\hat{p}_1(n), \ldots, \hat{p}_K(n)]^\top$ denote the hard decision vector for the vector of the transmitted symbols $\mathbf{p}(n)$. Three different types of the MUDs can be implemented to make the hard decision for $\mathbf{p}(n)$ as discussed in the following.

First, if the OPT-MUD is employed, its output is computed based on the maximum likelihood decision rule. From (5.2), the probability density function of $\mathbf{z}(n)$ conditioned on $\mathbf{p}(n)$ is given by

$$f(\mathbf{z}(n)) = \frac{\exp\left\{-\sigma^{-2}\left[\mathbf{z}(n) - \mathbf{RWA}(n)\mathbf{p}(n)\right]^H \mathbf{R}^{-1}\left[\mathbf{z}(n) - \mathbf{RWA}(n)\mathbf{p}(n)\right]\right\}}{(\pi\sigma^2)^{KP}|\mathbf{R}|} \quad (5.3)$$

The ML decision rule is therefore

$$\begin{aligned}\hat{\mathbf{p}}^{ML}(n) &= \arg\min_{\mathbf{p}(n)\in\{A_m\}^K}[\mathbf{p}^\top(n)\mathbf{A}^H(n)\mathbf{WRWA}(n)\mathbf{p}(n) - \mathbf{z}^H(n)\mathbf{WA}(n)\mathbf{p}(n) \\ &- \mathbf{p}^\top(n)\mathbf{A}^H(n)\mathbf{Wz}(n)] \\ &= \arg\min_{\mathbf{p}(n)\in\{A_m\}^K}\left[\mathbf{p}^\top(n)\mathbf{A}^H(n)\mathbf{WRWA}(n)\mathbf{p}(n) - 2\Re\{\mathbf{z}^H(n)\mathbf{WA}(n)\mathbf{p}(n)\}\right]\end{aligned} \tag{5.4}$$

Second, for the DC-MUD, the output of the decorrelating filter is the product of *sufficient statistic* and the inverse matrix $\mathbf{R}^{-1}$, given as follows

$$\begin{aligned}\mathbf{v}(n) &= \mathbf{R}^{-1}\mathbf{z}(n) = \mathbf{WA}(n)\mathbf{p}(n) + \mathbf{R}^{-1}\mathbf{u}(n) \\ &= \mathbf{WA}(n)\mathbf{p}(n) + \tilde{\mathbf{u}}(n)\end{aligned} \tag{5.5}$$

where $\tilde{\mathbf{u}}(n)$ is a KP-vector of complex Gaussian random variable with zero mean and covariance matrix $\sigma^2\mathbf{R}^{-1}$. The output of the DC-MUD can also be represented as the KP-vector $\mathbf{v}(n) = [\mathbf{v}_1^\top(n), \ldots, \mathbf{v}_K^\top(n)]^\top$, where $\mathbf{v}_k^\top(n)$ is the P-vector, given as

$$\mathbf{v}_k(n) = p_k(n)\sqrt{E_k}\mathbf{a}_k(n) + \tilde{\mathbf{u}}_k(n). \tag{5.6}$$

Note that the properties of vector $\tilde{\mathbf{u}}_k(n)$ have been known already from (4.29). The probability density function of $\mathbf{v}_k(n)$ is completely specified by the mean $p_k(n)\sqrt{E_k}\mathbf{a}_k(n)$ and the same covariance matrix of $\tilde{\mathbf{u}}_k(n)$. It is written as

$$\begin{aligned}f(\mathbf{v}_k(n)) &= \frac{1}{(\pi\sigma^2)^P|\mathbf{R}_{kk}^+|}\exp\left\{-\frac{1}{\sigma^2}[\mathbf{v}_k(n) - p_k(n)\sqrt{E_k}\mathbf{a}_k(n)]^H(\mathbf{R}_{kk}^+)^{-1}[\mathbf{v}_k(n)\right. \\ &- \left. p_k(n)\sqrt{E_k}\mathbf{a}_k(n)]\right\}\end{aligned} \tag{5.7}$$

With the above pdf, the decision rule for the kth user at time n is expressed as:

$$\begin{aligned}\hat{p}_k^{DC}(n) &= \arg\min_{p_k(n)\in\{A_m\}}\left[p_k^2(n)E_k\mathbf{a}_k^H(n)(\mathbf{R}_{kk}^+)^{-1}\mathbf{a}_k(n)\right. \\ &- \left. p_k(n)\sqrt{E_k}\mathbf{a}_k^H(n)(\mathbf{R}_{kk}^+)^{-1}\mathbf{v}_k(n) - p_k(n)\sqrt{E_k}\mathbf{v}_k^H(n)(\mathbf{R}_{kk}^+)^{-1}\mathbf{a}_k(n)\right] \\ &= \arg\min_{p_k(n)\in\{A_m\}}\left[p_k^2(n)E_k\mathbf{a}_k^H(n)(\mathbf{R}_{kk}^+)^{-1}\mathbf{a}_k(n)\right. \\ &- \left. 2\,\Re\left(p_k(n)\sqrt{E_k}\mathbf{a}_k^H(n)(\mathbf{R}_{kk}^+)^{-1}\mathbf{v}_k(n)\right)\right].\end{aligned} \tag{5.8}$$

Let $\alpha_0 = E_k \mathbf{a}_k^H(n)(\mathbf{R}_{kk}^+)^{-1}\mathbf{a}_k(n)$ and $\alpha_1 = 2\sqrt{E_k}\Re\left\{\mathbf{a}_k^H(n)(\mathbf{R}_{kk})^{-1}\mathbf{v}_k(n)\right\}$, the decision rule can be expressed as follows

$$\hat{p}_k^{DC}(n) = \begin{cases} \arg \min\limits_{p_k(n)\in\{A_m\}} \left| p_k(n) - \frac{\alpha_1}{2\alpha_0} \right|; \text{ if } \alpha_0 \geq 0 \\ \arg \max\limits_{p_k(n)\in\{A_m\}} \left| p_k(n) - \frac{\alpha_1}{2\alpha_0} \right|; \text{ if } \alpha_0 < 0 \end{cases} \tag{5.9}$$

Third, with the MMSE-MUD, the MMSE linear detector for user k at time n chooses the KP-vector $\mathbf{m}_k(n)$ that minimizes

$$\text{MSE}_k = E\left[\left\| p_k(n) - \mathbf{m}_k^H(n)\mathbf{z}(n)\right\|^2\right] \tag{5.10}$$

Using (5.2) and the fact that noise and data are uncorrelated, MSE_k is computed as represented in (4.17). $\mathbf{m}_k^H(n)$ is therefore exactly the same as expressed in (4.19). The output of the MMSE-MUD corresponding to the kth user can be computed as follows:

$$\begin{aligned} u_n^{(k)} &= \mathbf{m}_k^H(n)\mathbf{z}(n) \\ &= \mathbf{e}_k^\top \mathbf{A}^H(n)\mathbf{W}\mathbf{R}\left[\mathbf{R}\mathbf{W}\mathbf{A}(n)\mathbf{A}^H(n)\mathbf{W}\mathbf{R} + \sigma^2\mathbf{R}\right]^{-1}\left[\mathbf{R}\mathbf{W}\mathbf{A}(n)\mathbf{p}(n) + \mathbf{u}(n)\right] \end{aligned} \tag{5.11}$$

Similar to Section 4.2, $u_n^{(k)}$ is well approximated by a complex Gaussian distribution and it is represented as

$$u_n^{(k)} = \mu_n^{(k)} p_k(n) + \eta_n^{(k)} \tag{5.12}$$

where $\mu_n^{(k)}$ and $(\nu_n^{(k)})^2$ are computed in (4.22) and (4.25), respectively. The distribution function of $u_n^{(k)}$ is now known with $\mu_n^{(k)}$ and $\nu_n^{(k)}$, given by:

$$f(u_n^{(k)}) = \frac{1}{2\pi\nu_n^{(k)}} \exp\left\{ \frac{-\left\| u_n^{(k)} - p_k(n)\mu_n^{(k)}\right\|^2}{\left(\nu_n^{(k)}\right)^2} \right\} \tag{5.13}$$

Therefore, the decision rule for the kth user at time n can be computed as follows:

$$\hat{p}_k^{MMSE}(n) = \arg \min_{p_k(n)\in\{A_m\}} \left\| u_n^{(k)} - p_k(n)\mu_n^{(k)}\right\|^2 \tag{5.14}$$

Based on the output of the MUD, the demapper receives the sequences of $\hat{p}_k(n)$ for all the K users and then converts them into the binary sequences $[\hat{b}_1(I_k), \ldots, \hat{b}_Q(I_k)]$.

In turn, the VQ decoder of the kth user converts these bits to the estimated index $\hat{i}_k$. The table-lookup operation finds the centroid $\mathbf{c}_{\hat{i}_k}^{(k)}$ for VQ decoding, given $\hat{i}_k$. Note that, the complexity of such decoders depends on the type of the MUD. The decoding complexity is about $\mathcal{O}(PL \cdot M^K)$ operations for the OPT-MUD. On the other hand, the decoding complexity is about $\mathcal{O}(PL \cdot KM)$ computations if the other MUDs are employed.

5.3 The Suboptimal Soft Decoders

This decoding scheme has been presented in Chapter 4 and its structure is shown in Fig. 4.1. This section extends the results of such decoding approach to a system with M-PAM. To this end, the corresponding LLRs of the soft-output MUDs need to be computed accordingly for M-PAM. In particular, the soft bit estimate $\tilde{b}_j(I_k)$ is generated from soft-output MUD, and fed into the individual soft VQ decoder. An individual soft VQ decoder in turn processes the soft bit estimates and outputs the estimation of the source vector using the optimal decoding algorithm [1]. The structure and computation principles of the suboptimal soft decoding for M-PAM are basically the same as that provided in Chapter 4. The soft estimate $\tilde{b}_j(I_k)$ of the bit $b_j(I_k)$ is computed from the soft-output of the MUD as

$$\tilde{b}_j(I_k) \;=\; \tanh\left[\frac{1}{2}\lambda(b_j(I_k))\right] \tag{5.15}$$

where $\lambda(b_j(I_k))$ denotes the *a posteriori* log-likelihood ratio (LLR) of the bit $b_j(I_k)$, given by

$$\lambda(b_j(I_k)) \triangleq \log \frac{\Pr[b_j(I_k) = +1|\text{MUD}]}{\Pr[b_j(I_k) = -1|\text{MUD}]} \tag{5.16}$$

It is important to recognize that the index j in the above equations is different from the index n in (4.6) and (4.9). However, they both indicate the index of the bit duration. In the case of BPSK, n is also the symbol duration because each symbol contains only one bit. On the contrary, for M-PAM each symbol duration corresponds to a block of Q bits. In what follows, the *a posteriori* LLR is provided for each type of MUD with the assumption of equally likely transmitted bits $b_j(I_k)$.

First, substitute (5.3) into (5.16), the LLR of the soft OPT-MUD can be computed as follows:

$$\lambda^{\mathrm{OPT}}[b_j(I_k)] = \log \frac{\sum_{\mathbf{p}(n)\in\mathcal{B}_k^+} \exp\left\{-\frac{1}{\sigma^2}\left(\mathbf{z}(n)-\mathbf{RWA}(n)\mathbf{p}(n)\right)^H \mathbf{R}^{-1}\left(\mathbf{z}(n)-\mathbf{RWA}(n)\mathbf{p}(n)\right)\right\}}{\sum_{\mathbf{p}(n)\in\mathcal{B}_k^-} \exp\left\{-\frac{1}{\sigma^2}\left(\mathbf{z}(n)-\mathbf{RWA}(n)\mathbf{p}(n)\right)^H \mathbf{R}^{-1}\left(\mathbf{z}(n)-\mathbf{RWA}(n)\mathbf{p}(n)\right)\right\}}, \tag{5.17}$$

where

$$\mathcal{B}_k^+ \triangleq \{(p_1(n),\ldots,p_k^+(n),\ldots,p_K(n)) : p_r(n)\in\{A_m\}, r\neq k\} \tag{5.18}$$

$$\mathcal{B}_k^- \triangleq \{(p_1(n),\ldots,p_k^-(n),\ldots,p_K(n)) : p_r(n)\in\{A_m\}, r\neq k\}. \tag{5.19}$$

Moreover, $p_k^+(n)$ and $p_k^-(n)$ are symbols whose jth bit is $+1$ or -1, i.e., ($[b_1(I_k), \ldots, b_{j-1}(I_k), \pm 1, b_{j+1}(I_k), \ldots, b_Q(I_k)]$).

Instead of the OPT-MUD, the linear MUDs are employed to reduce the complexity that comes from the summations taken over $\mathcal{B}_k^+$ and $\mathcal{B}_k^-$. Similar to the computation of LLR from the OPT-MUD, the log-likelihood ratios of the bit $b_j(I_k)$, calculated from the soft-outputs of the DC-MUD and the MMSE-MUD in (5.7) and (5.13) respectively. They are given as follows:

$$\lambda^{\mathrm{DC}}[b_j(I_k)] = \log\frac{f[\mathbf{v}_k(n)|b_n(I_k)=+1]}{f[\mathbf{v}_k(n)|b_n(I_k)=-1]} = \log \frac{\sum_{p_k(n)\in\mathcal{P}_{k,j}^+} \exp\left\{-\frac{1}{\sigma^2}[\mathbf{v}_k(n)-p_k(n)\sqrt{E_k}\mathbf{a}_k(n)]^H(\mathbf{R}_{kk}^+)^{-1}[\mathbf{v}_k(n)-p_k(n)\sqrt{E_k}\mathbf{a}_k(n)]\right\}}{\sum_{p_k(n)\in\mathcal{P}_{k,j}^-} \exp\left\{-\frac{1}{\sigma^2}[\mathbf{v}_k(n)-p_k(n)\sqrt{E_k}\mathbf{a}_k(n)]^H(\mathbf{R}_{kk}^+)^{-1}[\mathbf{v}_k(n)-p_k(n)\sqrt{E_k}\mathbf{a}_k(n)]\right\}} \tag{5.20}$$

and

$$\begin{aligned}\lambda^{\mathrm{MMSE}}[b_j(I_k)] &= \log\frac{f[u_n^{(k)}|b_j(I_k)=+1]}{f[u_n^{(k)}|b_n(I_k)=-1]} \\ &= \log\frac{\sum_{p_k(n)\in\mathcal{P}_{k,j}^+} \exp\left\{-\left(\nu_n^{(k)}\right)^{-2}\left\|u_n^{(k)}-p_n(k)\mu_n^{(k)}\right\|^2\right\}}{\sum_{p_k(n)\in\mathcal{P}_{k,j}^-} \exp\left\{-\left(\nu_n^{(k)}\right)^{-2}\left\|u_n^{(k)}-p_n(k)\mu_n^{(k)}\right\|^2\right\}}\end{aligned} \tag{5.21}$$

where $\mathcal{P}_{k,j}^{+}$ and $\mathcal{P}_{k,j}^{-}$ are subsets of $\{A_m\}^K$ whose elements are mapped from ($[b_1(I_k)$, $\ldots$, $b_{j-1}(I_k)$, $\pm 1, b_{j+1}(I_k)$, $\ldots$, $b_Q(I_k)]$), respectively.

In summary, the LLRs of three different types of the MUDs are computed from (5.17), (5.20) and (5.21). For each type of MUD, the LLR is then used to calculate the soft-bit estimates as in (5.15). The soft-bit estimates are fed into individual soft-VQ encoders in order to make the final decisions for the source vectors.

5.4 Results and Comparison

In this section, the method used to measure the performance of systems with M-PAM is the same as in Subsection 4.4. To be precise, performance measurement is the output SNR versus the channel signal-to-noise ratio CSNR, where

$$\text{SNR}_k = \frac{E\{||\mathbf{X}_k||^2\}}{E\{||\mathbf{X}_k - \hat{\mathbf{X}}_k||^2\}}, \tag{5.22}$$

$$\text{CSNR} = \frac{E_b}{N_0}, \tag{5.23}$$

and $E_b = \frac{E_s}{Q}$ is the average transmitted energy per bit. The source of an individual user is modeled as a zero-mean, unit-variance, stationary and first order Gauss-Markov random process as described in (4.34). The parameters of the VQ used in the simulation for the system with two users are $d = 3$, $L = 3$. The number of paths and the signature waveforms are the same as used in Subsection 4.4 for the case of $K = 2$ users. Figures 5.3 and 5.4 show the performance curves of the hard and the soft suboptimal decoders for both BPSK and 4-PAM. Observe that the system with BPSK provides a better performance than that of the system with 4-PAM, especially in the medium range of CSNR. On the other hand, one can improve bandwidth efficiency from 1 to 2 (bit/second/Hz) by using 4-PAM instead of BPSK. However, the system performance loss is about 2 (dB) in the output SNR.

To obtain an even better bandwidth efficiency, a system using 8-PAM can be considered. Generally, the higher order signal constellation is used, the better bandwidth efficiency of the system is achieved. Figures 5.5 and 5.6 provide the comparisons of different suboptimal decoders for both BPSK and 8-PAM systems. The use of 8-

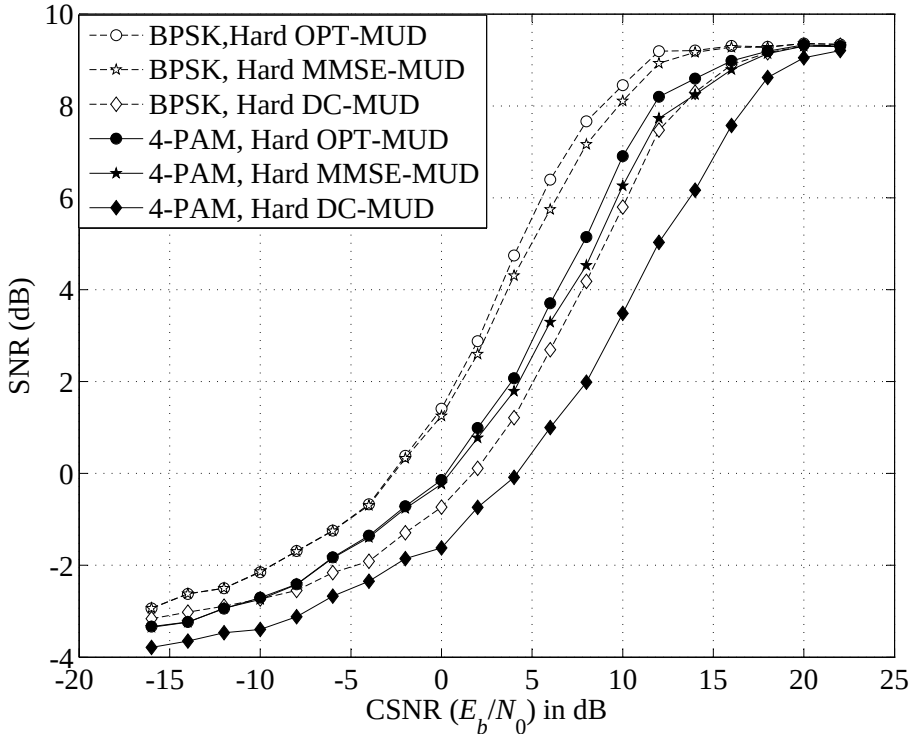

Figure 5.3 Performance of hard decoding schemes in the system employing BPSK and 4-PAM and with 2 users: Signature sequences of length 7.

PAM yields a bandwidth efficiency of 3 (bit/second/Hz). The price to pay for this higher bandwidth efficiency is the performance degradation compared to both 4-PAM and BPSK.

To provide a better insight in understanding the trade-off between spectral efficiency and performance of different modulations schemes, Figure 5.7 compares the SNR performance of three schemes for the case that the proposed soft decoding with MMSE-MUD is used. Over the medium range of CSNR that corresponds to the output SNR range between 5 to 9 dB, this figure shows that the penalty in SNR is about 3 dB, e.g., two times for every additional bit in spectral efficiency.

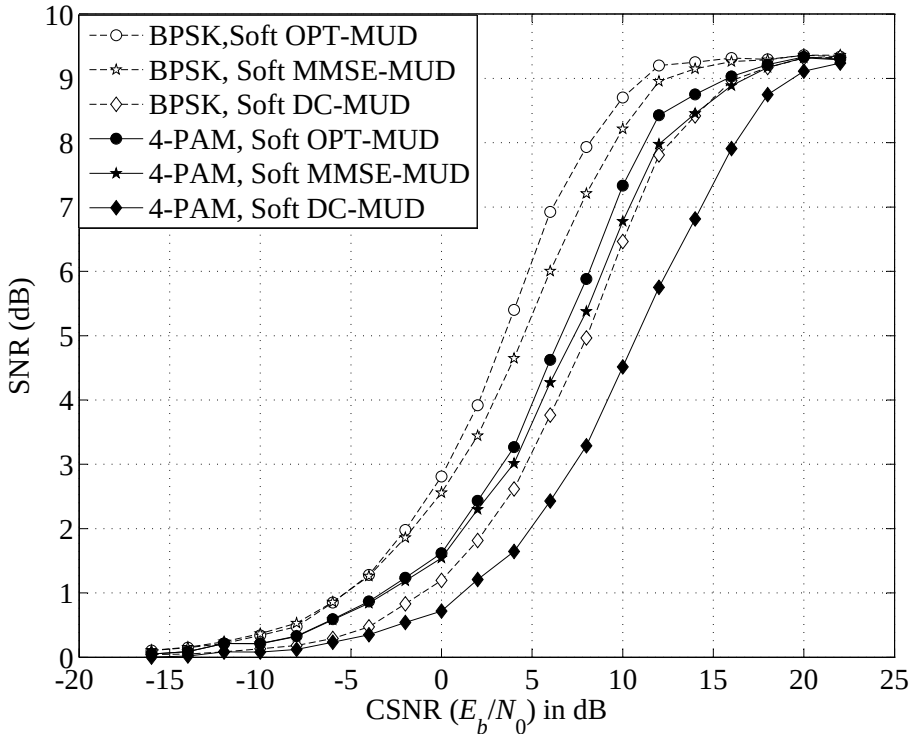

Figure 5.4 Performance of soft decoding schemes in the system employing BPSK and 4-PAM and with 2 users: Signature sequences of length 7.

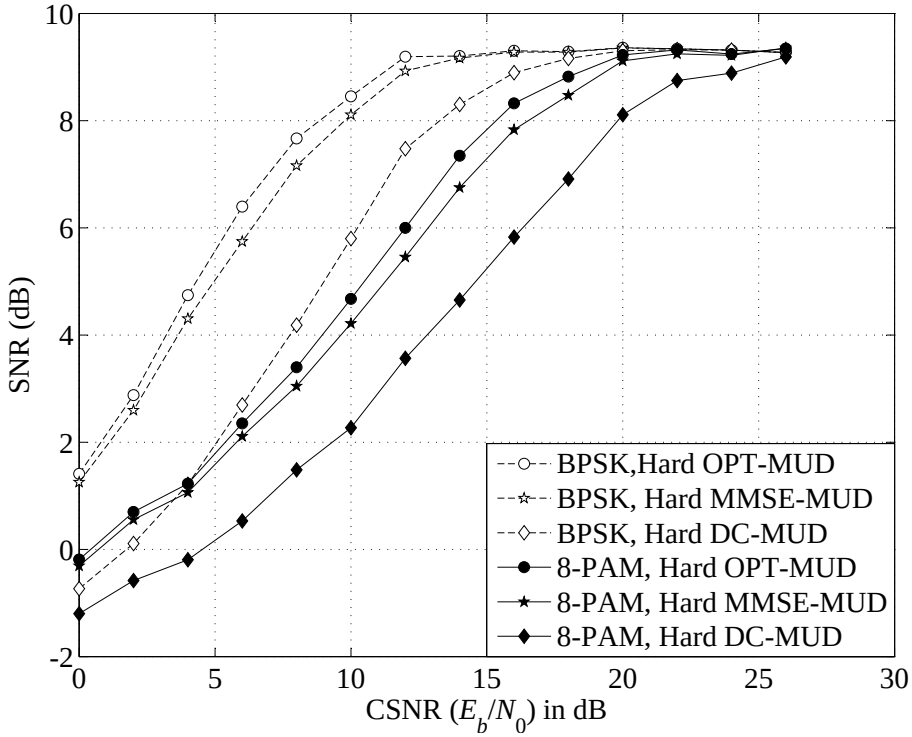

Figure 5.5 Performance of hard decoding schemes in the system employing BPSK and 8-PAM and with 2 users: Signature sequences of length 7.

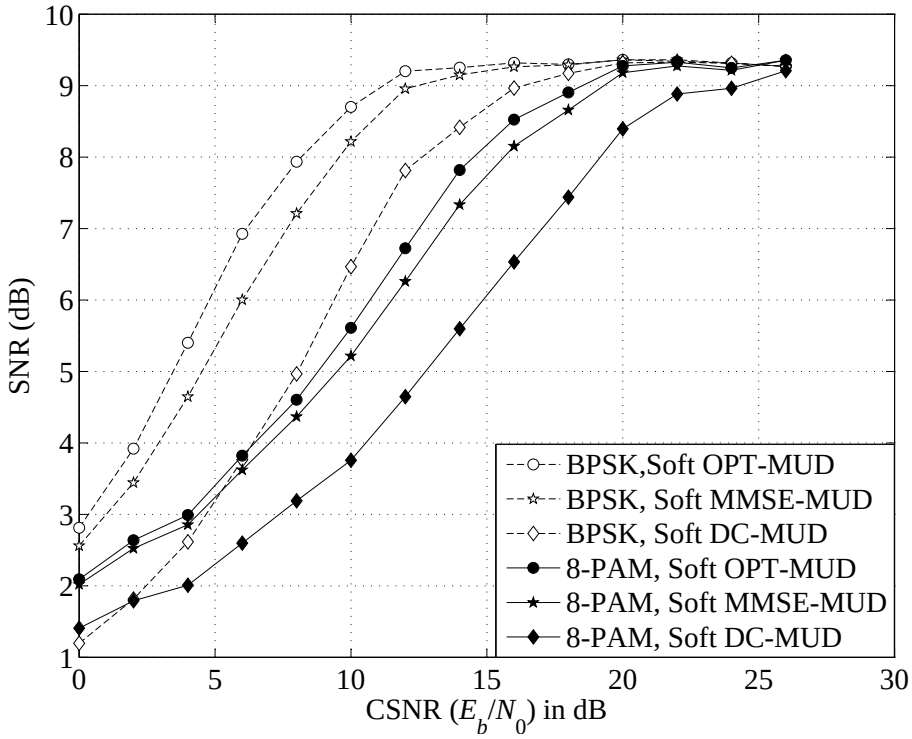

Figure 5.6 Performance of soft decoding schemes in the system employing BPSK and 8-PAM and with 2 users: Signature sequences of length 7.

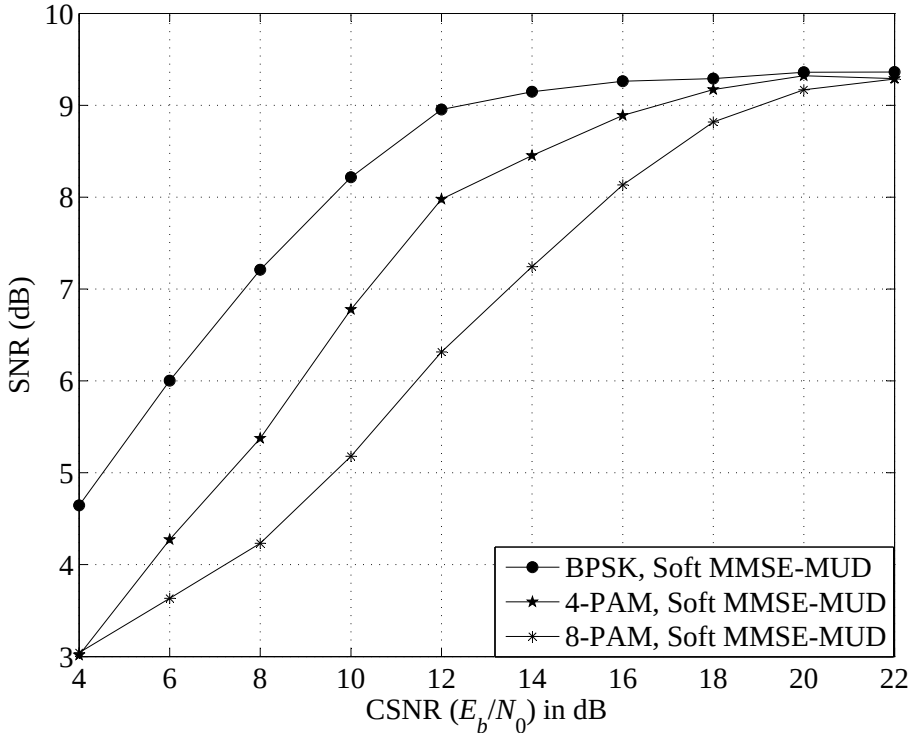

Figure 5.7 Performance curves of the suboptimal soft decoder with MMSE-MUD for the systems employing BPSK, 4-PAM and 8-PAM.

6. Conclusions and Suggestions for Further Research

6.1 Conclusions

This thesis has extended the results of the suboptimal decoding scheme, originally proposed in [1, 2] for an AWGN channel, to a frequency-selective Rayleigh fading CDMA channel. Results obtained demonstrate that such a decoding scheme also works very well in mobile wireless communications. The suboptimal soft decoder is shown to be a graceful approach to the complicated optimal decoder. The complexity of the receiver reduces from an exponential number to a linear number of K, the number of users. The use of different types of MUDs in such a suboptimal decoder also offers a great flexibility to trade the performance for complexity of the system. The results are useful in designing a practical decoder for a VQ transmission system in mobile wireless communications.

Additional algorithms were also investigated in Section 4.5 as other alternatives of the suboptimal decoder. Simulation results indicated that the decoder using both the reliability-based processing and the distance-based algorithms provide similar performance to that of the proposed suboptimal decoder in [1, 2]. In addition to good performance, the algorithms offer a decoding method whose complexities can be controlled in a very flexible manner.

The proposed decoders were also extended for systems employing M-ary PAM in order to obtain a better bandwidth efficiency. From simulation results and analysis, it can be concluded that one must suffer some performance loss to obtain a better spectral efficiency. This extension basically offers a trade-off between performance and bandwidth efficiency of the system.

6.2 Suggestions for Further Research

In this thesis, the suboptimal soft decoding scheme was studied for the transmission of VQ over a synchronous[1] uncoded system. It would be interesting and useful to extend this decoding scheme for asynchronous and coded systems. For coded systems, the BER can be reduced with the use of a good error correcting code. Therefore, the performance of the whole system will be improved. After VQ encoding, the source symbols are converted into a sequence of binary bits. It is conceivable that using an error correcting code reduces the errors in the recovery of the transmitted bits, leading to an improvement in the construction quality of the source vectors. It is interesting to design a coded system to minimize the distortion of VQ reconstruction.

The modulation schemes employed for the systems in this thesis are one-dimensional BPSK and M-PAM. When bandwidth efficiency is the primary concern, it is of interest to study signal mapping problem in multi-dimensional constellations built from other conventional higher-order constellations (such as M-PSK, M-QAM). Moreover, adaptive modulation techniques to further improve the capacity of the system would be very attractive.

[1] Actually it is symbol asynchronous, but chip synchronous system.

A. A Review of Linear Increasing Swap Algorithm (LISA)

It was shown that the channel distortion is minimized if the vector quantizer can be expressed as a linear transform of a hypercube. A linearization problem of the vector quantizer is regarded as the index assignment (IA) problem. For a vector quantizer with N cells, there are $N!$ ways to order N numbers, providing $N!$ solutions for assigning indices. In some IAs, codewords, that interchange frequently far apart in signal space, cause large contributions to the overall distortion when transmission errors occur. On the other hand, there are encoders whose careful IAs are taken mitigate the effects of channel errors. The authors in [13] proposed a powerful algorithm to find the best IA of codevectors. The encoder design includes the source-coding problem and the index-assignment problem. A coder designed in this manner is called a robust vector quantizer (RVQ).

As discussed in Section 2.1, a d-dimensional vector $\mathbf{X}$ is fed to the VQ to produce a L-bit binary codeword for transmission, $\mathbf{b}(i) = [b_L(i), b_{L-1}(i), \ldots, b_1(i)]^\top$ where i is the index of the codeword. The table-lookup decoder receives a codeword j and produces a d-dimensional reconstruction vector as output.

As the encoder is assumed to have maximum entropy, the channel distortion can be expressed [13]

$$\Phi_C = \frac{1}{N} \sum_{i=0}^{N-1} \sum_{j=0}^{N-1} \|\mathbf{c}_i - \mathbf{c}_j\|^2 \cdot p_{j/i} \tag{A.1}$$

where $p_{j/i}$ is the probability of receiving the index j given that index i was sent, and $\mathbf{c}_i$ are the centroids of the reconstruction cells. The minimization of (A.1) is precisely the problem of index assignment. There exists a class of related codebooks having the same centroids, but another order, $\mathcal{C} = [\mathbf{c}_0, \ldots, \mathbf{c}_{N-1}]$. To describe the ordering of

the VQ centroids, a row vector $\mathbf{G} = [\mathbf{b}(0), \mathbf{b}(1), \ldots, \mathbf{b}(N-1)]$ is defined as the *index assignment matrix* whose columns are the L-dimensional base-2 representations of the index integers $[0, 1, \ldots, N-1]$.

As represented in Subsection 2.1.2, an encoder centroid can be described as in (2.26), and a full codebook can be represented as

$$\mathcal{C} = \mathbf{T} \cdot \mathbf{H} \tag{A.2}$$

The $d \times N$ matrix $\mathbf{T} = [\mathbf{t}_0, \mathbf{t}_1, \ldots, \mathbf{t}_{N-1}]$ is the Hadamard transform of $\mathcal{C}$ that is divided into two parts. The linear part contains $\mathbf{t}_0, \mathbf{t}_{2^0}, \mathbf{t}_{2^1}, \mathbf{t}_{2^2}, \ldots, \mathbf{t}_{N/2}$ and the nonlinear part includes the remaining vectors. The linearity of $\mathbf{T}$ is measured by the *linearity index*

$$\ell \triangleq \frac{1}{\sigma_{VQ}^2} \sum_{j=0}^{L-1} \|\mathbf{t}_{2^j}\|^2 \tag{A.3}$$

where σ_{VQ}^2 is defined as a "variance" of the codebook, given as [13]

$$\begin{aligned} \sigma_{VQ}^2 &\triangleq \frac{1}{N} \sum_{i=0}^{N-1} \|\mathbf{c}_i\|^2 - \left\| \sum_{i=0}^{N-1} \mathbf{c}_i \right\|^2 \\ &= \sum_{i=0}^{N-1} \|\mathbf{t}_i\|^2 - \|\mathbf{t}_0\|^2 \\ &= \sum_{i=0}^{N-1} \|\mathbf{t}_i\|^2. \end{aligned} \tag{A.4}$$

It is convenient to use ℓ as a measure on how dominant the linear part of the general transform $\mathbf{T}$ is. The range of ℓ is $0 \leq \ell \leq 1$ where $\ell = 1$ denotes a purely linear transform. The relationship between the channel distortion and the linearity index is expressed with the upper bound and the lower bound as in Theorem 2 of [13], as

$$2\sigma_{VQ}^2[2q\ell + (1-(1-2q)^2)\cdot(1-\ell)] \leq \Phi_C \leq 2\sigma_{VQ}^2[2q\ell + (1-(1-2q)^L)\cdot(1-\ell)], \tag{A.5}$$

where q is the cross-over error probability of a binary symmetric channel (BSC). It can be seen from (A.5) that the larger ℓ is, the smaller Φ_C becomes. Thus, the optimal index assignment is achieved at the maximum linearity index $\ell = 1$ and the minimum channel distortion is

$$\Phi_{C\min} = 4 \cdot q \cdot \sigma_{VQ}^2. \tag{A.6}$$

The parameter ℓ is therefore an indicator of how good an index assignment is, but it gives no information on how to find the optimal index assignment.

In order to find a good index assignment, all the classes of assignments can be evaluated simultaneously. As decomposed in Theorem 3 of [13], any IA matrix, $\mathbf{G}$, can be uniquely specified through its triple as

$$\mathbf{G} = \mathbf{L}\mathbf{G}_{ez} \oplus \mathbf{w}\mathbf{1}^{\top} \tag{A.7}$$

where $\mathbf{L}$ is an invertible $L \times L$ matrix, $\mathbf{G}_{ez}$ is a reduced echelon IA matrix with an initial zero vector, $\mathbf{w}$ is a L-dimensional vector, and $\mathbf{1}$ is the column vector of N ones. With this decomposition, IAs of a cookbook can be categorized into classes. The set of IAs having the same reduced echelon matrix $\mathbf{G}_{ez}$ is called a Hadamard class. There are $\mathbb{N} = \frac{N!}{N \cdot \sum_{j=0}^{L=1} (N-2^j)}$ possible values for $\mathbf{G}_{ez}$. The *Full Linear Search Algorithm* (FLSA) presented in [13] preforms a full search among $\mathbb{N}$ Hadamard classes, which gives the same result as if an exhaustive search were performed over all index assignments.

The *Linearity Increasing Swap Algorithm* (LISA) rapidly finds a good index assignment by swapping codewords in an effective manner. With LISA, it is unnecessary to compute the complete Hadamard transform in order to calculate the linear index. The swap of two VQ centroids $\mathbf{c}_E$ and $\mathbf{c}_F$ in a codebook $\mathcal{C}$ turns $\mathbf{T}$ into the new matrix $\mathbf{T}'$ whose columns can be computed as

$$\begin{aligned} \mathbf{t'}_i &= \frac{1}{N}\left[\mathbf{c}_0 + \ldots + \mathbf{c}_F(-1)^{\mathbf{b}^{\top}(E)\mathbf{b}(i)} + \ldots + \mathbf{y}_E(-1)^{\mathbf{b}^{\top}(F)\mathbf{b}(i)} + \ldots\right] \\ &= \mathbf{t}_i - \frac{1}{N}\left[(\mathbf{c}_F - \mathbf{c}_E) \cdot ((-1)^{\mathbf{b}^{\top}(F)\mathbf{b}(i)} - (-1)^{\mathbf{b}^{\top}(E)\mathbf{b}(i)})\right] \end{aligned} \tag{A.8}$$

Thus, the new linearity becomes

$$\ell' = \ell + \frac{1}{(N \cdot \sigma_{VQ})^2} \sum_{j=0}^{L-1} \left[(\Delta b_j)^2 \|\Delta\mathbf{c}\|^2 - 2N\Delta b_j \mathbf{t}_{2^j}^{\top} \Delta\mathbf{c}\right] \tag{A.9}$$

where $\Delta\mathbf{c} = \mathbf{c}_F - \mathbf{c}_E$ and $\Delta b_j = \Delta b_j(F) - \Delta b_j(E)$. Observe that the linearity index increases if and only if the sum in (A.9) is positive. This occurs for swaps of indices with a Hamming distance of one, implying that $\Delta b_j = 0$ for all but one j value.

Therefore, $\mathbf{b}(E)$ and $\mathbf{b}(F)$ must differ only in bit j, equivalently expressed as

$$\{E, F\} \quad = \quad \begin{cases} 2m \cdot 2^j \leq E \leq (2m+1)2^j - 1, & \text{any integer } m \\ F = E + 2^j \end{cases} \tag{A.10}$$

All possible swaps of this type are depicted as a butterfly structure. For E and F matching this pattern, (A.8) and (A.9) yield the following simple expressions [13]:

$$\begin{aligned} \text{Test} \quad &: \quad \frac{1}{N} \cdot \|\Delta\mathbf{c}\|^2 + \mathbf{t}_{2^j}^{\top} \Delta\mathbf{c} > 0 \\ \text{Update } \mathbf{t}' \quad &: \quad \mathbf{t}'_{2^l} = \mathbf{t}_{2^l} + \frac{2}{N} \cdot \|\Delta\mathbf{c}\| \\ \text{Update } \ell \quad &: \quad \ell' = \ell + \frac{4}{(N \cdot \sigma_{VQ})^2} \cdot \left[\|\Delta\mathbf{c}\|^2 + N \cdot \mathbf{t}_{2^j}^{\top} \Delta\mathbf{c} \right]. \end{aligned} \tag{A.11}$$

There are totally $2^{L-1}(2^L - 1)$ possible swaps. For low computational burden, it is well worth dividing all pairwise swaps into two subsets. First, it picks out only a subset of $L \cdot 2^{L-1}$ Hamming-1 neighbors from all pairwise swaps. This swap strategy is called "Hamming-1 butterflies".

Second, the remaining $2^{L-1}(2^L - L - 1)$ pairwise swaps, having an additional increase of linearity, are invoked in a procedure named "Remaining Butterflies". The LISA presents a routine performing all pairwise swaps by first swapping the Hamming-1 neighbors and then all the others. This split is especially favorable when the total time consumption is of concern and the procedure has to be terminated before a full cycle is completed. The LISA can be described as follows

Input: An initial codebook $\mathcal{C}$.

Output: A permutation of the initial codebook with a good IA, also named $\mathcal{C}$.

Linearity Increasing Swap Algorithm (LISA):

Compute the Hadamard transform $\mathbf{T}$ of $\mathcal{C}$.

Repeat:

Hamming-1 Butterflies

For $j = 0$ to $L - 1$

For $j = 0$ to $N - 2^{j+1}$, step 2^{j+1}

For $E = i$ to $i + 2^j - 1$

$\Delta\mathbf{c} = \mathbf{c}_{E+2^j} - \mathbf{c}_E$

If $\|\Delta\mathbf{c}\|^2 + N \cdot \mathbf{t}_{2^j}^\top \Delta\mathbf{c} > 0$

Swap $\mathbf{c}_E$ and $\mathbf{c}_{E+2^j}$

$\mathbf{t}_{2^j} = \mathbf{t}_{2^j} + \dfrac{2}{N} \cdot \Delta\mathbf{c}$

Remaining Butterflies

For $j = 0$ to $L - 1$

For $v = 2^j + 1$ to $2^{j+1} - 1$

For $i = 0$ to $N - 2^{j+1}$, step 2^{j+1}

For $E = i$ to $i + 2^j - 1$

$F = E \oplus v$

$\Delta\mathbf{c} = \mathbf{c}_F - \mathbf{c}_E$

$\Delta b_r = \Delta b_r(F) - \Delta b_r(E); \quad r = 0, 1, \ldots, j$

If $\displaystyle\sum_{r=0}^{j} \left[(\Delta b_r)^2 \|\Delta\mathbf{c}\|^2 - 2N\Delta b_r \mathbf{t}_{2^r}^\top \Delta\mathbf{c}\right] > 0$

Swap $\mathbf{c}_E$ and $\mathbf{c}_F$

$\mathbf{t}_{2^r} = \mathbf{t}_{2^r} - \dfrac{\Delta b_r}{N} \cdot \Delta\mathbf{c}; \quad r = 0, 1, \ldots, j$

Until convergence.

The FLSA finds the optimal IA with the highest linearity index. It is however more theoretical than practical interest. The LISA is a significantly faster than the other algorithms tested, reaching a good, but not the best IA in the test. For large codebook, the high speed makes the LISA an attractive choice.

B. Algorithm Based on Reliability Processing

1) Sort $\boldsymbol{\gamma} = \{\gamma_k\}_{k=1}^{K}$ in increasing order such that $\gamma_{h_1} \leq \ldots \leq \gamma_{h_K}$. This gives $\boldsymbol{\gamma}_s = [\gamma_{h_1}, \ldots, \gamma_{h_K}]^\top$ with index $\mathbb{I}_s = [h_1, \ldots, h_K]^\top$.

2) Exchange the positions of bits in $\mathbf{b}^{hard}(n)$ from index $\mathbb{I}$ to index $\mathbb{I}_s$ to obtain $\mathbf{b}_s^{hard}(n)$.

3) Define the error pattern sequences $\varepsilon_p \triangleq \{\mathbf{e}^{(p_t)}\}, p = 0, \ldots, K, t = 1, \ldots, 2^p$ where $\{\mathbf{e}^{(p_t)}\}$ are ordered under the key $\phi(\cdot, \boldsymbol{\gamma})$:

$$\phi(\mathbf{e}^{(p_t)}, \boldsymbol{\gamma}) \leq \phi(\mathbf{e}^{(p_{t+1})}, \boldsymbol{\gamma}), t = 1, 2, \ldots, 2^p - 1 \tag{B.1}$$

and satisfies

$$\mathbf{e}_h^{(p_t)} = 0 \text{ for every } h \in \{h_{p+1}, h_{p+2}, \ldots, h_K\} \text{ and } 1 \leq t \leq 2^p. \tag{B.2}$$

Here, $e_h^{(\cdot)}$ is the hth position in the error pattern $\mathbf{e}^{(\cdot)}$ and (B.2) states that $\mathbf{e}^{(p_t)}$ introduce errors only in the p lowest reliability positions of the initial bit decision vector $\mathbf{b}^{hard}(n)$. The implementation starts with $\varepsilon_0 = \{\mathbf{e}^{(1)} = [0, 0, \ldots, 0]^\top\}$. Define also the error pattern sequences $\varepsilon'_p \triangleq \{\mathbf{e}'^{(p_t)}\}, p = 0, 1, \ldots, K-1, t = 1, 2, \ldots, 2^p$, where $\{\mathbf{e}'^{(p_t)}\}$ is such that

$$e_h'^{(p_t)} = \begin{cases} 1, & \text{if } h = h_{p+1} \\ e_h^{(p_t)}, & \text{otherwise} \end{cases} \tag{B.3}$$

Therefore, each $\{\mathbf{e}'^{(p_t)}\}$ contains exactly one more error in bit position h_{p+1} than the corresponding error pattern $\{\mathbf{e}^{(p_t)}\}$. It follows that $\phi(\mathbf{e}'^{(p_t)}, \boldsymbol{\gamma}) = \phi(\mathbf{e}^{(p_t)}, \boldsymbol{\gamma}) + \gamma_{h_{p+1}}$ and $\{\mathbf{e}'^{(p_t)}\}$ is also ordered under the key (4.42).

At this point, it is important to observe the following. If the two ordered sequences $\varepsilon_p = \{\mathbf{e}^{(\cdot)}\}$ and $\varepsilon'_p = \{\mathbf{e}'^{(\cdot)}\}$ are merged together, one obtains $\varepsilon_{p+1} =$

$[\{\mathbf{e}^{(\cdot)}\}, \{\mathbf{e}'^{(\cdot)}\}]$ in increasing order of the same key (4.42). Therefore, the iterative generation of ε'_p from ε_p and the mergence of two sequences to form ε_{p+1} for $p = 0, 1, \ldots, K-1$ will lead to ε_K of all 2^K error patterns under the key $\phi(\cdot, \boldsymbol{\gamma})$. Since only the first β error patterns in ε_K are needed, this process can be simplified greatly. For this purpose, the operation of the algorithm can be stopped when the length of ε_p is β. This set is exactly the same to the set of the first β elements in ε_K.

4) Apply β elements of ε_K on $\mathbf{b}_s^{hard}(n)$ to create $\{\hat{\mathbf{b}}_s^{(d)}(n) = \mathbf{b}_s^{hard}(n) \oplus \mathbf{e}^{(d)}\}_{d=1}^{\beta}$.

5) Return the positions of all the elements in $\{\hat{\mathbf{b}}_s(n)\}$ to the original index $\mathbb{I}$ to obtain the expected set $\{\hat{\mathbf{b}}^{(d)}(n)\}_{d=1}^{\beta}$.

References

[1] H. H. Nguyen, "A soft decoding scheme for vector quantization over a CDMA channel," in *Proc. IASTED International Conference on Communications Systems and Applications (CSA)*, (Banff, Canada), pp. 328–333, July 2004.

[2] H. H. Nguyen, "A soft decoding scheme for vector quantization over a CDMA channel," *IEEE Trans. Commun.*, vol. 53, pp. 1603–1608, Oct. 2005.

[3] J. G. Proakis, *Digital Communications*. New York: McGraw-Hill, 4th ed., 2001.

[4] H. Abut, *Vector Quantization*. The Institute of Electrical and Electronics Engineers, Inc., New York, 1990.

[5] L. Rabiner and B. H. Juang, *Fundamentals of Speech Recognition*. Prentice Hall, Englewood Cliffs, N.J., 1993.

[6] H. H. Nguyen, "Notes in informations and communications theories," *Department of Electrical Engineering, University of Saskatchewan, Saskatoon, Canada.*

[7] M. Skoglund and T. Ottosson, "Soft multiuser decoding for vector quantization over a CDMA channel," *IEEE Trans. Commun.*, pp. 327–337, Mar. 1998.

[8] T. Ottosson and M. Skoglund, "Joint source-channel multiuser decoding for Rayleigh fading CDMA channels," *IEEE Trans. Commun.*, vol. 48, pp. 13–16, Jan. 2000.

[9] Z. Liu and D. A. Pados, "Near-ML multiuser detection with linear filters and reliability-based processing," *IEEE Trans. Commun.*, vol. 51, pp. 1446–1450, Sept. 2003.

[10] Y. Linde, A. Buzo, and R. Gray, "An algorithm for vector quantizer design," *IEEE Trans. Commun.*, vol. 28, pp. 84–95, Jan. 1980.

[11] P. Hedelin, P. Knagenhjelm, and M. Skoglund, "Vector quantization for speech transmission," in *Speech Coding and Synthesis*, K.K. Paliwal and W.B. Kleijn, Eds. Amsterdam, The Netherlands: Elsevier, 1995.

[12] M. Skoglund, "On channel-constrained vector quantization and index assignment for discrete memoryless channels," *IEEE Trans. Inform. Theory*, vol. 45, pp. 2615–2622, Nov. 1999.

[13] P. Knagenhjelm and E. Agrell, "The Hadamard transform–a tool for index assignment," *IEEE Trans. Inform. Theory*, vol. 42, pp. 1139–1151, July 1996.

[14] M. Skoglund and P. Hedelin, "Hadamard-based soft decoding for vector quantization over noisy channels," *IEEE Trans. Inform. Theory*, vol. 45, pp. 515–532, Mar. 1999.

[15] F. J. MacWilliams and N. J. A. Sloane, *The Theory of Error-Correcting Codes*. Amsterdam, the Netherlands: North Holland, 1977.

[16] P. Hedelin, P. Knagenhjelm, and M. Skoglund, "Theory for transmission of vector quantization data," in *Speech Coding and Synthesis*, K.K. Paliwal and W.B. Kleijn, Eds. Amsterdam, The Netherlands: Elsevier, 1995.

[17] S. Verdú, *Multiuser Detection*. Cambridge University Press, 1998.

[18] H. V. Poor and S. Verdú, "Probability of error in MMSE multiuser detection," *IEEE Trans. Inform. Theory*, vol. 43, pp. 858–871, May 1997.

[19] G. Moustakides and H. Poor, "On the relative error probabilities of linear multiuser detectors," *IEEE Trans. Inform. Theory*, vol. 47, pp. 450–456, Jan. 2001.

[20] H. Nguyen and E. Shwedyk, "On a unified linear multiuser receiver," in *Proc. IEEE Int. Symp. Inform. Theory.*, (Lausanne, Switzerland), p. 494, 2002.

[21] H. H. Nguyen, "A unified linear multiuser receiver for CDMA systems," *IEICE Trans. Commun.*, pp. 2792–2794, Sept. 2003.

[22] S. X. Nguyen and H. H. Nguyen, "Suboptimal decoding scheme for vector quantization over a frequency-selective Rayleigh fading CDMA channel," in *Proc. IEEE Canadian Conference on Electrical and Computer Engineering (CCECE).*, (Saskatoon, Canada), pp. 2086–2089, May 2005.

[23] Q. Zhao, "http://code.ucsd.edu/ qizhao/seqs.html," in *Electrical and Computer Engineering, University of California, San Diego.*